

(0-4 d), exposure to corticosteroids, or days of alcohol fixation (1-53 d). The alcohol fixed cases with the longest fixation times (41-53 d) showed variable degeneration of the RC. Immunostains for androgens stained Leydig cells, but not the RC.

Conclusions: RC are very common, probably ubiquitous in normal testicles, but their number is variable. They show amphiphilic properties, dissolving rapidly in aqueous solutions (10% formalin). RC are not common in cytologic preparations from normal testes, and their presence suggests the presence of a LCT. Immunostains for androgens stain specifically the Leydig cells, but not RC.

29 Age-Related EBV-Associated Lymphoproliferative Disorder With Widespread Gastrointestinal Involvement and Subsequent Development of T-Cell Lymphoma

Guldeep Uppal, Alaina Chodoff, Zi-Xuan Wang, Jeffrey Baliff, Jerald Gong. Thomas Jefferson University Hospital, Philadelphia, PA.

Background: Age-Related EBV-associated Lymphoproliferative Disorder (AR-EBVLPD) has emerged as a new subset of B-cell lymphoproliferative disorders. AR-EBVLPD is associated with a wide clinicopathologic spectrum, ranging from a benign nodal reactive hyperplasia to aggressive EBV+ diffuse large B-cell lymphoma. Here, we report a unique case of AR-EBVLPD that deviates from the characteristic progression of this disease with persistent, wide-spread gastrointestinal disease, and subsequent development of peripheral T-cell lymphoma, not otherwise specified (PTCL, NOS). This is the first reported case of PTCL, NOS associated with AR-EBVLPD.

Design: A 70 year old female presented with failure to thrive and weight loss. Her clinical history was negative for any known cause of endogenous or iatrogenic immune suppression. Initial gastric and small bowel biopsies revealed severe chronic inflammation. She later presented with gastric outlet obstruction and a distal gastrectomy was performed. Histopathological examination revealed persistent chronic gastritis with a focal EBV positivity by in situ hybridization. Molecular studies revealed clonal immunoglobulin heavy (IgH) chain gene rearrangement. Over the next year, patient's clinical condition deteriorated. Repeat upper gastrointestinal biopsies were performed along with excision biopsy of a cervical lymph node. The gastrointestinal biopsies showed persistent EBV-associated LPD, polymorphic type along with appearance of atypical T-cell infiltrate. The lymph node biopsy showed features were most consistent with diagnosis of PTCL, NOS. Esophageal and lymph node biopsies showed a clonal T-cell receptor rearrangement (TCR) with identical clonal peaks. IgH rearrangement was not detected. Patient succumbed to the illness and an autopsy was performed. No palpable lymphadenopathy was detected at the time of autopsy. Examination of the visceral organs showed extensive superficial ulceration of the small bowel, distal stomach and esophagus. Esophageal and gastric biopsies revealed sheets of atypical T cells which were strongly positive for EBV.

Results: We presume that the patient's progressive clinical deterioration coincided with an increasing burden of EBV infected tumor cells. This led to altered T-cell repertoire, and the development of a malignant clonal T-cell population.

Conclusions: This is a novel case of peripheral T-cell lymphoma arising in association with an EBV-driven B cell proliferation.

30 Spectrum of Significant Liver Diseases at Autopsy in Children in a Tertiary Care Institute

Rakesh Vasishtha, Pooja Murgai, Nandita Kakkar, Ashim Das, Babu Thapa. Postgraduate Institute of Medical Education and Research, Chandigarh, India; PGIMER, Chandigarh, India.

Background: To study the etiology of hepatic diseases in children at autopsy in North India.

Design: One hundred and eighty one pediatric autopsy cases, (age range 0-14 years) who presented with signs and symptoms of hepatic diseases were analyzed.

Results: Of these 66.9% were males. Metabolic disorders (38.7%) were the commonest followed by hepatitis (viral, autoimmune and others) (19.9%), infiltration by leukaemia /lymphoma (11.0%), infections (6.1%), histiocytic disorders (5.5%), vascular disorders (2.2%), extra hepatic biliary atresia- EHBA (2.2%), congenital hepatic fibrosis (1.1%), progressive familial intrahepatic cholestasis (0.6%), benign recurrent intrahepatic cholestasis (0.6%), tumors (0.6%), and other causes (12.2%).

Conclusions: Liver diseases are common in children with a male dominance. Amongst the metabolic disorders, cystic fibrosis (CF), Reye syndrome, Indian childhood cirrhosis (ICC), Galactosemia and Wilson disease were the commonest. In CF, cholestasis was seen in 6 and invasive fungal infection in 5 cases. Both classical and atypical types of ICC were noted. Predominant macrovesicular steatosis was present in 2 cases of Reye syndrome. In galactosemia, steatosis was absent in 3 cases wherein frank micronodular cirrhosis was present. Acute hepatitis was commoner than chronic. It being an autopsy study, incidence of EHBA was low.

31 Maternal Death Analysis in Japan: An Autopsy-Based Study (2011-2013)

Tomoko Wakasa, Tomoaki Ikeda, Makoto Takeuchi, Hatsue Ishibashi-Ueda, Naohiro Kanayama, Naoaki Tamura, Yoshio Matsuda, Jun Yoshimatsu. Nara Hospital, Kindai Hospital, Faculty of Medicine, Ikoma, Japan; Mie University School of Medicine, Tsu, Japan; Osaka Medical Center for Maternal and Child Health, Izumi, Japan; National Cerebral and Cardiovascular Center, Suita, Japan; Hamamatsu University School of Medicine, Hamamatsu, Japan; International University of Health and Welfare Hospital, Nasushiobara, Japan.

Background: To determine the cause of maternal death, an autopsy is essential. At autopsy, the diagnosis of amniotic fluid embolism (AFE) and pulmonary thromboembolism (PT) particularly requires careful examination. The causes of maternal death are assessed by the Maternal Mortality Evaluation Committee supported

by the Ministry of Health, Labour and Welfare ever since the initiation of registration of all maternal deaths to the Japan Association of Obstetricians and Gynecologists in 2010. There were 147 cases of maternal death registered in Japan (2011-2013), with the maternal mortality rate being 3.9 per 100,000 live births as the average annual live birth count was 1039279. Of the 147 cases, 59 autopsies were performed (Autopsy rate: 40.1%); in 51 of the 59 autopsies, assessment by the Committee was completed. In this study, we analyzed all 51 registered autopsy cases (2011-2013) and classified the causes of maternal death.

Design: We analyzed all autopsy reports and medical records in the 51 cases. In suspected cases of AFE, we measured the serum levels of zinc-coproporphyrin-1 and sialyl-Tn to detect substances specific to amniotic fluid in maternal blood.

Results: In the 51 maternal deaths we analyzed, the age ranged from 23 to 42 years, with a median of 36 years. We identified 32 and 19 maternal deaths, respectively, due to direct and indirect obstetric causes. The direct causes included: AFE, 17 (33.3%); PT, 4 (8%); uterine rupture, 2 (4%); injury to birth canal, 1 (2%); atonic bleeding or DIC of unknown causes, 4 (8%); pregnancy-induced hypertension, 2 (4%); other 2 causes, 1 (2%) each. The indirect obstetric causes were: sepsis, 6 (12%); malignant lymphoma, subarachnoid hemorrhage, dissecting aneurysm of the aorta, and neurofibromatosis type I (NF-1), 2 (4%) each; other 3 causes, 1 (1%) each; and unknown causes, 2 (4%). Among the AFE cases, 13 and 4, respectively, started with atonic bleeding and cardiopulmonary collapse. Five of the 6 sepsis patients died of invasive group A *Streptococcus* (GAS) infection.

Conclusions: AFE, PT, and GAS infection were the main causes of maternal death.

Bone and Soft Tissue Pathology

32 Angiosarcoma Arising in Association With Dacron Grafts and Orthopedic Joint Prostheses: Clinicopathologic, Immunohistochemical and Molecular Analysis

Abbas Agaimy, Ofer Ben-Izhak, Thomas Lorey, Marcus Scharpf, Brian Rubin. University Hospital of Erlangen, Erlangen, Bavaria, Germany; Rambam Health Care Campus, Haifa, Israel; Caritas-Krankenhaus, Bad Mergentheim, Germany; University Hospital Tübingen, Tübingen, Germany; Cleveland Clinic, Cleveland, OH.

Background: Angiosarcoma has been rarely reported to arise in close proximity to implanted foreign material such as Dacron vascular grafts and orthopedic metal prostheses used for bone fixation or joint replacement with less than 20 cases reported to date.

Design: In this study, we provide detailed clinical and histological descriptions of 5 cases (2 new cases and 3 previously reported cases) and perform immunohistochemical and molecular analyses of all cases.

Results: All patients were males aged 50-84 (median, 71). Three received Dacron grafts and two received total hip prostheses. Angiosarcoma was closely associated with the implanted foreign material in all cases and arose within 4.6- 17 years (mean 9 years) after implantation of foreign material. Clinical symptoms were unexplained recurrent bleeding and suspected infection in the joint prosthesis cases and fatigue, weight loss and abdominal pain/symptoms in patients with Dacron graft-associated angiosarcomas. Four patients received surgical and/or palliative radio-chemotherapy. Four died of disease (range 1-24 months; mean 8 months). One patient was alive after surgery, radiochemotherapy and embolization of pulmonary metastases (last follow-up 17 months). Histologically, all tumors were high-grade with predominant solid epithelioid morphology and variable vasoformative component. All tumors expressed CD31, ERG and FLI-1, but not D2-40. Pancytokeratin expression was seen in 3 cases. TP53 was expressed in <10% of tumor cells and SMARCB1 was intact in all cases. There were no copy number alterations of *MDM2*, *CDK4* or *c-MYC*.

Conclusions: Prosthesis-associated angiosarcomas are characterized by high-grade nuclear features, predominance of solid epithelioid cytology and lack of lymphatic endothelial differentiation. Absence of *c-MYC* amplification indicates a different pathogenesis compared to histologically similar secondary (radiation-associated) angiosarcomas. Likewise, absence of *MDM2* amplification in the 3 Dacron-associated cases argues against pathogenesis similar to intimal sarcoma.

33 Genomic Characterization of PEComas: Dichotomy of Genetic Abnormalities With Therapeutic Implications

Narasimhan P Agaram, Yun-Shao Sung, Lei Zhang, Chun-Liang Chen, Hsiao-Wei Chen, Michael Berger, Cristina Antonescu. Memorial Sloan Kettering Cancer Center, New York, NY.

Background: Perivascular epithelioid cell neoplasms (PEComa) are a family of mesenchymal tumors with hybrid myo-melanocytic differentiation. Although most PEComas harbor loss of function *TSC1/TSC2* mutations, a small subset were reported to carry *TFE3* gene rearrangements. As no comprehensive genomic study has addressed the molecular classification of PEComa, we sought to investigate by multiple methodologies the incidence and spectrum of genetic abnormalities and their potential genotype-phenotype correlations in a large group of 37 PEComas.

Design: RNA sequencing and Fusion seq analysis was performed on eleven tumors. RT-PCR, DNA-PCR and Fluorescence In Situ Hybridization (FISH) methodology was used to validate the gene fusions. Targeted exome sequencing using the IMPACT assay was performed on twelve tumors. Mutations were validated using Sanger sequencing.

Results: The tumors were located in soft tissue (9 cases) and visceral sites (28) including uterus, kidney, liver, lung and urinary bladder. Combined RNA sequencing and FISH analysis identified 8 (22%) *TFE3* gene rearranged tumors, with 3 cases showing *SFPQ/PSF-TFE3* fusions and one case a novel *DVL2-TFE3* fusion. The *TFE3*-positive lesions showed distinctive nested/alveolar morphology and were equally distributed between soft tissue and visceral sites. Additionally, novel *RAD51B* gene rearrangements were

identified in 3 (8%) uterine PEComas, which showed a complex fusion pattern with *RRAGB/OPHN1* genes in 2 cases. Other, non-recurrent gene fusions, *HTR4-ST3GAL1* and *RASSF1-PDZRN3*, were identified in 2 cases. Targeted exome sequencing using the IMPACT assay was used to address if the presence of gene fusions are mutually exclusive from *TSC* gene abnormalities. *TSC2* mutations were identified in 80% of the *TFE3* fusion-negative cases tested. Co-existent *TP53* mutations were identified in 63% of the *TSC2* mutated PEComas. Our results showed that *TFE3*-rearranged PEComas lacked co-existing *TSC2* mutations, indicating alternative pathways of tumorigenesis. **Conclusions:** This comprehensive genetic analysis significantly expands our understanding of molecular alterations in PEComas and brings forth the genetic heterogeneity of these tumors. *TFE3*-rearranged tumors have a different pathogenesis and most likely represent a separate entity from fusion-negative, *TSC2*-mutated PEComas, a finding that significantly impacts the therapeutic management of these tumors.

34 Myocardin (MYOCD) Gene Is Amplified in a Minor Subset of Leiomyosarcoma: A Targeted Exome-Sequencing Study of 35 Cases

Narasimhan P Agaram, Tarik Silk, Lei Zhang, Francois Le Loarer, Sasinya Scott, Michael Berger, Cristina Antonescu, Samuel Singer. Memorial Sloan Kettering Cancer Center, New York, NY.

Background: Leiomyosarcomas (LMS) are one of the most common histologic subtypes, comprising about 24% of all sarcomas. LMS belong to the class of sarcomas with complex genetic alterations with numerous, often non-recurrent chromosomal imbalances and aberrations. We investigated a group of LMS using next-generation sequencing platform to identify recurrent genetic abnormalities and possible therapeutic targets.

Design: Targeted exome sequencing of 275 cancer associated genes was performed using the IMPACT assay on 35 cases of primary soft tissue and visceral (extra-uterine) LMS with matched normal tissue. The assay utilizes solution phase hybridization-based exon capture and deep-coverage massively parallel DNA sequencing. Sequence data were analyzed to identify three classes of somatic alterations: single-nucleotide variants, small insertions/deletions (indels), and copy number alterations. Key genetic alterations were further investigated using FISH assay.

Results: The study group included patients with equal gender distribution and a mean age of 61 years (range: 37 – 84). The primary sites included retroperitoneal/intra-abdominal, extremity, truncal and visceral, with a mean size of 10 cm. Histologically, 31 tumors were classified as high grade, while 4 were low grade LMS showing mild atypia, low mitotic activity and no necrosis. The most common single abnormality identified was *TP53* mutations in 16 of 35 (46%) cases. Losses of chromosome regions 10q21-23 (*PTEN*), 13q12-14.2 (*RBI*), 16q22.1 and 17p13.1 (*TP53*), involving key tumor suppressor genes, were also highly frequent events. Gains mainly involved chromosome regions 17p11.2 (*MYOCD*) and 15q25-26 (*IGF1R*). Validating sequencing results, FISH analysis showed amplification of the myocardin (*MYOCD*) gene in 6 of 25 (24%) cases analyzed, seen in 3 abdominal and 3 extremity high grade tumors. *IGF1R* amplification was identified in 2 cases from back and perineum. None of the 4 low grade LMS showed losses or mutations of *PTEN* or *TP53* tumor suppressor genes.

Conclusions: Genetic complexity is the hallmark of LMS with chromosome losses of important tumor suppressor genes (*PTEN*, *RBI* and *TP53*) being a common feature. *MYOCD*, a key gene associated with smooth muscle differentiation, is amplified in a subset of both retroperitoneal and extremity high grade LMS. Further studies are necessary to investigate the significance of gains / amplifications in the development of these tumors.

35 The Accuracy of Soft Tissue Fine Needle Aspiration Cytology: A Single Institution Experience

Omar Ahmed, Jihan Abdusattar, Ziyen Salih, Shadi Qasem. Wake Forest School of Medicine, Winston-Salem, NC.

Background: The diagnosis of soft tissue lesions or neoplasms by fine needle aspiration (FNA) has always been a challenge. Some reports claim high accuracy and diagnostic specificity, while others observe different results in practice. Our goal is to analyze our institutional experience with soft tissue cytology with regards to accuracy and specificity of the diagnosis.

Design: The cytology reports of 602 cases of soft tissue FNA (ST-FNA) biopsies with subsequent excision or surgical biopsy, in the last 10 years, were reviewed. The FNA diagnoses were classified into 4 categories: Diagnostic specific (DS), when the diagnosis was helpful in guiding therapy; Diagnostic Non-specific (DNS), when the diagnosis was vague and did not help guide therapy; Insufficient for diagnosis (IS), when the material was not satisfactory; and Discrepant diagnosis (DC), when there was a major discrepancy in diagnosis (e.g. benign vs malignant). In addition, a cohort of 200 consecutive breast FNA (BR-FNA) cases were reviewed for comparison, in a similar fashion.

Results: In ST-FNA, 54% of the cases were found to be DS, 25% DNS, 5% DC and 16% IS. In comparison, 69% of BR-FNA were DS, 14% DNS, 3% DC, and 15% IS [Table 1] 64 (11%) ST cases had an associated core biopsy in comparison to 12 (6%) BR cases. ST cases with core biopsies showed 55% DS rate, 8% DC, 27% DNS and 11% IS. Reactive, myxoid and lipomatous lesions encompassed 52% of the DC diagnoses.

Results	ST-FNA	BR-FNA
DS	324 (53.8%)	138 (69%)
DNS	151 (25.1%)	28 (14%)
DC	29 (4.8%)	5 (2.5%)
IS	98 (16.3%)	29 (14.5%)
Total	602	200

Conclusions: Our results show that ST-FNA is less likely to be specific and more likely to be discrepant than BR-FNA, and this is not related to the adequacy of the material. The presence of a needle core biopsy with the FNA did not improve the diagnostic specificity overall. ST-FNA is helpful but has its limitations, especially in reactive, myxoid and lipomatous lesions.

36 ETV6-NTRK3 Is Expressed in a Subset of ALK-Negative Inflammatory Myofibroblastic Tumors: Case Series of 20 Patients

Ali Alassiri, Rola Ali, Amy Lum, Angela Goytain, Yaoqing Shen, Poul Sorensen, Caron Strahlendorf, Janessa Laskin, Marco Marra, Torsten Nielsen, Stephen Yip, Cheng-Han Lee, Tony Ng. Vancouver General Hospital, Vancouver, BC, Canada; University of British Columbia, Vancouver, BC, Canada; Kuwait University, Kuwait, Kuwait; British Columbia Cancer Agency, Vancouver, BC, Canada; British Columbia Children's and Women's Hospital, Vancouver, BC, Canada; University of Alberta, Edmonton, AB, Canada.

Background: Inflammatory myofibroblastic tumor is a genetically heterogenous tumor of viscera and soft tissues. About 50% of cases harbor the anaplastic lymphoma kinase (*ALK*) gene rearrangement, and recent studies have described novel fusions involving *ROS1* and *PDGFRB* genes in a small subset of ALK-negative cases. However, the molecular features of the remaining cases are not yet defined.

Design: We report, as an index case, a large, highly aggressive inflammatory myofibroblastic tumor of lung in a 17-year-old female. Frozen tumor tissue samples (obtained from both before and after chemotherapy treatment) were molecularly characterized through whole genome and transcriptome sequencing, along with peripheral blood. Subsequently, we investigated a cohort of 19 ALK-negative inflammatory myofibroblastic tumors of various anatomic sites. All cases were screened by FISH for rearrangement of the *ETV6* locus, and by RT-PCR for the *ETV6-NTRK3* fusion transcript.

Results: Whole genome and transcriptome sequencing revealed an *ETV6-NTRK3* fusion transcript in the index case. This was confirmed by FISH studies for *ETV6* gene rearrangement, as well as by RT-PCR. In addition, two additional cases in our cohort demonstrated *ETV6* rearrangement by FISH. The presence of *ETV6-NTRK3* fusion transcript was confirmed by RT-PCR in one case, after assaying for multiple known fusion transcript variants. All remaining cases were negative for known variants of *ETV6-NTRK3* by RT-PCR.

Conclusions: We demonstrate the expression of the *ETV6-NTRK3* fusion oncogene in a subset of inflammatory myofibroblastic tumors, lending further support to the role of oncogenic tyrosine kinases in the pathophysiology of this tumor type. Our data also further expands the growing spectrum of tumor types expressing the *ETV6-NTRK3* fusion.

37 Pecomats Harbor Heterogeneity of Genomic Alterations Within the PI3K/mTOR Pathway as Demonstrated By Comprehensive Genomic Profiling

Siraj Ali, Kai Wang, Mark Rosenzweig, Roman Yelensky, Julia Elvin, Juliann Chmielecki, Rachel Erlich, Doron Lipson, David Stockman, Daniela Katz, Vincent Miller, Philip Stephens, Jeffrey Ross. Foundation Medicine Inc, Cambridge, MA; University of South Carolina School of Medicine, Greenville, SC; Hadassah-Hebrew University Medical Center, Jerusalem, Israel.

Background: The Perivascular Epithelioid Cell tumor (PEComa) family is a group of hamartoma-like tumors with variable malignant potential. Loss of function alterations of *TSC2* and subsequent hyperactivation of the PI3K/mTOR pathway have been linked to these neoplasms, although empirically not all PEComas respond to rapamycin analogs. We performed a comprehensive genomic profiling (CGP) study of PEComas to predict potential correlates to mTOR-targeted therapy.

Design: DNA was extracted from 40 microns of FFPE sections from 10 PEComas. Comprehensive genomic profiling (CGP) was performed on hybridization-captured, adaptor ligation based libraries to a mean coverage depth of >750X for 3,769 exons of 236 cancer-related genes plus 47 introns from 19 genes frequently rearranged in cancer. The results were evaluated for all classes of genomic alterations (GA). CRGA were defined as GA linked to drugs on the market or under evaluation in mechanism driven clinical trials.

Results: All ten patients were female, with a median age of 52 years (range 19-92). Six PEComas had immunohistochemical (IHC) characterization available: two cases had SMA-/HMB45 focally positive, one case had SMA-/HMB45 focally positive, two cases had SMA+/HMB45- and one case had SMA focally positive/HMB45 strong positive staining. For four cases, no IHC characterization was available. CGP revealed 38 GAs in the 10 tumors (3.8 per tumor), with all tumors containing at least one GA. There were 19 clinically relevant GAs (CRGA) (1.9 per tumor) involving 12 different genes with all 10 (100%) of PEComas featuring at least 1 CRGA: *TSC2* (50%); *CDKN2A* (20%); *NF2*, *PTEN*, *PDK1*, *NOTCH1*, *GNAQ*, *FGFR3*, *CDK4*, *ATRX*, and *ATK1/3* (each at 10%). Five of 10 (50%) PEComas harbored *TSC2* alterations, and the remaining cases harbored other GA within the PI3K/mTOR pathway. One PEComa harbored a *RPTOR* amplification and loss of heterozygosity (LOH) of *AKT1* and another case harbored LOH of *AKT3* and *FGFR3*. The remaining 3 PEComas harbored either *NF2* truncation, *PTEN* deletion, or *PDK1* amplification.

Conclusions: Fifty percent of PEComas were wild type for *TSC2*, but harbored other GA consistent with hyperactivation of the PI3K/mTOR pathway, without IHC correlation to genomic profiles. The sensitivity of other PI3K/mTOR pathway GA to rapamycin analogs is unknown, and CGP may provide insight into correlating which PEComas benefit from treatment from mTOR inhibitors.

38 Histopathologic Features of Chronic Nonbacterial Sclerosing Osteomyelitis: A Retrospective Review

Alyaa Al-Ibraheemi, Kyle Kurek, Kelley Dentino, Bonnie Padwa, Sook Woo. Boston Children's Hospital, Boston, MA; Mass General Hospital, Boston, MA; Brigham & Women's Hospital, Boston, MA.

Background: Chronic nonbacterial sclerosing osteomyelitis (CNSO) is a variant of chronic osteomyelitis and is commonly seen in the children or young adult in the jaw bones. To date, the histopathologic features have not been well-described. The purpose of our study is to delineate the histopathology of CNSO.

Design: An IRB-approved retrospective review of medical records, imaging and histopathology of patients with CNSO was performed. Demographic data, clinical symptoms, and radiographic findings were recorded. Biopsy specimens were evaluated for the architecture of the bone, presence of atypical osteoid, osteoblastic rimming, osteoclastic activity, medullary fibrosis, and inflammation.

Results: There were 23 patients, 14 females and 9 males with disease onset at a mean age of 10.4 years. All cases involved the mandible and all reported pain and recurrent swelling; 43% had trismus. All patients had clinical features of chronic resolving-relapsing multifocal disease. 15 patients had biopsies with an average of 2.4 biopsies (range 2-10). Parallel and interconnecting thin trabeculae of woven bone with thin and thick seams were observed in 13 patients. The bone exhibited osteoblastic rimming and pockets of chronic inflammation in all patients and osteoclastic activity was observed in 12 patients. Atypical osteoid was noted in 15 patients while necrotic bone was noted in 5 patients. Delicate, curvilinear trabeculae of woven bone in a hypocellular fibroblastic stroma resembling fibrous dysplasia were seen in 6 patients. Medullary patchy nodular fibrosis seen in 10 patients. Focal abscesses were observed in 3 patients.

Conclusions: CNSO is a distinct entity with unique clinical, radiological and pathological features. In our study, four distinct histological features were noted including parallel and interconnected osteoid seams, atypical osteoid, fibrous dysplasia-like areas and patchy nodular fibrosis. The differential diagnoses may suggest osteosarcoma or fibrous dysplasia. Clinical and radiological correlation is essential for accurate diagnosis.

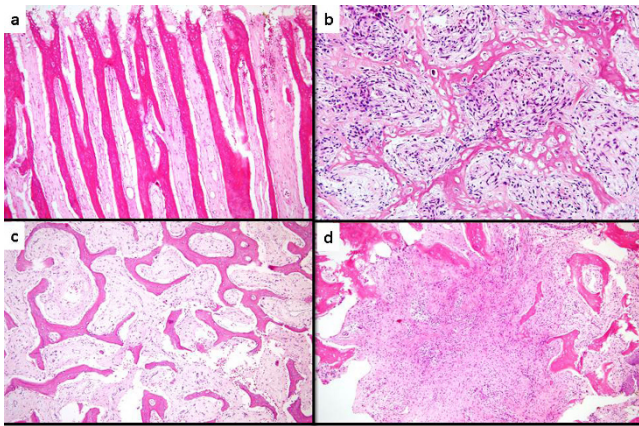


Fig 1: four distinct histological features: a) striking parallel osteoid seams, b) atypical osteoid, c) fibrous dysplasia-like areas and d) patchy nodular fibrosis

39 Molecular Characterization of Inflammatory Myofibroblastic Tumors With Frequent ALK and ROS1 Rearrangements and Rare Novel RET Gene Fusions

Cristina Antonescu, Albert Suurmeijer, Lei Zhang, Yun-Shao Sung, Achim Jungbluth, William Travis, Hikmat Al-Ahmadie, Christopher Fletcher, Rita Alaggio. Memorial Sloan Kettering Cancer Center, New York, NY; University Medical Center of Groningen, Groningen, Netherlands; Brigham & Women's Hospital, Boston, MA; University of Padova, Padova, Italy.

Background: Approximately 50% of conventional IMTs harbor *ALK* gene rearrangement and overexpress ALK. Recently gene fusions involving other kinases have been implicated in the pathogenesis of IMT, including *ROS1* and in 1 patient *PDGFRB*. However, it remains uncertain if the emerging genotypes correlate with clinicopathologic characteristics of IMT. In this study we expand the molecular investigation of IMT in a large cohort of different clinical presentations and analyze for potential genotype-phenotype associations.

Design: Criteria for inclusion in the study were a typical morphology and tissue availability for molecular studies. The lack of ALK immunoreactivity was not an excluding factor. As overlapping gene fusions involving actionable kinases are emerging in both IMT and lung cancer, we set out to evaluate abnormalities in *ALK*, *ROS1*, *PDGFRB*, *NTRK1* and *RET* by FISH. Additionally, next generation paired-end RNA sequencing and FusionSeq algorithm was applied in 4 cases, which identified *EML4-ALK* fusions in 2 cases.

Results: Of the 62 IMTs (from 24 children, 38 adults), 34 (55%) showed *ALK* gene rearrangement. Of note *EML4-ALK* inversion was noted in 6 (18%) cases, seen mainly in the lung and soft tissue of young children including 2 lesions from newborns. There were 6 *ROS1* rearranged IMTs, all except one presenting in children, mainly in the lung and intra-abdominally and showed a distinctive fascicular growth of spindle cells with long cell processes, often positive for ROS1 IHC. Two of the cases showed *TFG-ROS1* fusions. Interestingly, 2 adult IMTs revealed *RET* rearrangement, a previously unreported finding. No gene abnormalities were identified in the remaining kinases tested by FISH.

Conclusions: Our results show that 42/62 (68%) of IMTs are characterized by kinase fusions, offering rationale for targeted therapeutic strategies. Interestingly 90% of fusion negative IMT were seen in adults, while >50% of pediatric IMT showed gene rearrangements. *EML4-ALK* inversion and *ROS1* fusions emerge as common fusion abnormalities in IMT, closely recapitulating the pattern seen in lung cancer.

40 A Broad Survey of Neural Crest Transcription Factor Sox10 in Benign and Neoplastic Tissues

Rebecca Asch-Kendrick, Robert Anders, Pedram Argani, Jonathan Epstein, Peter Illei, Elizabeth Montgomery, George Netto, Rajni Sharma, Ie-Ming Shih, Matthew Tilson, Gang Zheng, Ashley Cimino-Mathews. Johns Hopkins Hospital, Baltimore, MD.

Background: Immunohistochemistry (IHC) for the neural crest transcription factor Sox10 is used in surgical pathology primarily to support the diagnosis of nerve-sheath tumors and melanoma. In addition, Sox10 is also known to label salivary gland neoplasms including adenoid cystic carcinomas (ACC), benign breast lobules, and a subset of breast carcinomas including 66% of triple negative breast carcinomas (Human Pathol 2013;44:959-65). However, a broad survey of Sox10 labeling in human neoplasms has not been performed. Here, we evaluated Sox10 expression in 927 epithelial, mesenchymal or neuroectodermal tumors and 20 benign tissues.

Design: 31 tissue microarrays (TMAs) containing benign and malignant neoplasms, reactive lesions and control tissue were labeled with Sox10 IHC. Nuclear labeling >1% was considered positive. TMAs contained 518 non-neuroendocrine carcinomas (adrenal, bladder, endometrial, gastric, esophageal, liver, lung, kidney, ovarian, prostate), 161 sarcomas (including 4 clear cell sarcoma [CCS] and 2 malignant peripheral nerve sheath tumor [MPNST]), 149 benign neoplasms and lesions, 67 neuroendocrine neoplasms, 15 granular cell tumors (GCT) and 10 melanomas. Benign control tissue included lung, breast, prostate, placenta, myometrium, stomach, tonsil, pancreas, liver, skin, bone, thyroid, esophagus, smooth muscle, gallbladder, bowel, brain, thymus, kidney and nerve. In addition, 10 whole sections of primary breast ACC were evaluated.

Results: Among the neoplasms, Sox10 labeling was seen in 100% breast ACC, 100% melanomas, 100% GCT, 75% CCS, and 47% paragangliomas (PG). No Sox10 labeling was seen in the remaining tumors, including MPNST. Among control tissues, Sox10 labeling was seen in breast lobules, epidermal melanocytes, nerve, ganglia, and scattered neural-crest derived cells in gastric and intestinal mucosa.

Conclusions: In addition to melanoma, nerve sheath tumors, salivary gland neoplasms, and breast carcinomas, nuclear Sox10 immunolabeling is seen in PG, GCT and CCS. Melanoma and PG could be histologically confused with each other, as both have a nested morphology, are cytokeratin negative, and can be S100 positive, such that Sox10 positivity is a potential pitfall in this differential. Among the carcinomas studied here, nuclear Sox10 labeling is specific for breast carcinoma and is not seen in carcinomas of other visceral sites.

41 Dentine Matrix Protein (DMP-1): A Marker of Bone Formation and Mineralization in Soft Tissue Tumours

Nicholas Athanasou, Yusuke Inagaki, Takeshi Kashima, Edward Hookway, Yasuhito Tanaka, Andrew Hassan, Udo Oppermann. Nuffield Orthopaedic Centre – Oxford University, Oxford, United Kingdom; Nara Medical University, Kashihara, Japan.

Background: Dentine matrix protein 1 (DMP-1) is a non-collagenous matrix protein found in dentine and bone. It is highly expressed by osteocytes and has been identified in primary benign and malignant osteogenic bone tumours. Bone formation and matrix mineralization are seen in a variety of benign and malignant soft tissue tumours and tumour-like lesions.

Design: In this study we analyzed immunohistochemically DMP-1 expression in a wide range of soft tissue lesions (n=254) in order to assess whether DMP-1 expression is useful in the histological diagnosis of soft tissue tumours.

Results: Matrix staining of DMP-1 was seen in all cases of myositis ossificans, fibrous tumour of the digits, extraskeletal soft tissue osteosarcoma and in most cases of ossifying fibromyxoid tumour. DMP-1 was also noted in dense collagenous connective tissue of mineralizing soft tissue lesions such as tumoral calcinosis, dermatomyositis and calcific tendinitis. DMP-1 was expressed in areas of focal ossification and calcification in synovial sarcoma and other soft tissue tumours. With few exceptions, DMP-1 was not expressed in other benign and malignant soft tissue tumours.

Conclusions: Our findings indicate that DMP-1 is a matrix marker of bone formation and mineralization in soft tissue tumours. DMP-1 expression should be particularly useful in distinguishing extraskeletal osteosarcoma and ossifying fibromyxoid tumour from other soft tissue sarcomas and in identifying areas of osteoid/bone formation and mineralization in soft tissue tumours.

42 Whole Exome Sequencing of Benign and Malignant Granular Cell Tumors

Prashant Bavi, Andrew Rosenberg, Feisal Yamani, Natalie Stickle, Carl Virtanen, Neil Winegarden, Julia Wang, Michael Roehrl. University Health Network, Toronto, ON, Canada; Miller School of Medicine, University of Miami, Miami, FL.

Background: Granular cell tumor (GCT) is a neoplasm of purported Schwann cell differentiation that arises in a variety of anatomic sites. Histologically it is classified into benign and malignant variants, the latter are most uncommon. Since the mutational landscape of benign and malignant GCT is largely unknown, we deciphered the molecular signature of GCT by whole exome sequencing (WES).

Design: Benign GCTs (n=8) and malignant GCTs (n=2) with matched tumour and normal FFPE tissues were sequenced using whole exome capture and HiSeq 2000 sequencers. Average exome coverage was deep at 212x (range, 165-248x). Using MuTect software, this data was filtered for germline SNPs based on the variant caller looking for somatic calls. Functional variant significance was classified on the basis of reports in publicly available databases.

Results: The study population was composed of predominantly females (75%) with a median age of 46.5 years. Distribution of the 8 benign GCTs tumors according to site was pharynx (n=1), tongue (n=1), esophagus (n=2), breast (n=1) and subcutaneous soft tissues (n=3). Both malignant GCTs occurred in subcutaneous soft tissue sites (flank and axilla). WES of patients with normal/tumor paired samples showed from 6 to 23 exonic mutations (4-16 non-synonymous), with no apparent difference in exonic mutation load between benign and malignant GCT. Mutated genes in benign GCT include PTCHD2, LAD1, PPP4R2, ZNF717, ORA11, SETD1B, CENPJ, MYO5C, RABEP1, TRPM4, EIF4ENIF1, STARD8, and CENPI. Mutated genes in malignant GCT include INTS7, RAB1A, PIK3CA, TGFBI, MDN1, OPRM1, TP53, IRS4, SLC6A1, SWI5, MED13, and CILP2. Interestingly, only malignant GCT showed alterations in key known driver oncogenes such as TP53 and PIK3CA. In addition, both malignant but none of the benign GCTs had MUC3A gene copy number gains. Further analysis of indels, CNVs, and exonic translocations is ongoing.

Conclusions: Identification of genetic alterations specific to GCT using WES even from archival FFPE material is feasible. These findings may provide the pathway for investigations aimed at determining the usefulness of a novel strategy for treating malignant PIK3CA-mutated GCT with targeted inhibitors (such as PI3K/AKT/mTOR inhibitors), either alone or in combination with other agents.

43 Loss of p16 Expression and 18q23 Deletions as Potential Negative Prognostic Factors in Osteosarcoma

Dariusz Borys, Lukas Nystrom, Robert Canter, Andrew Horvai, Roger Schultz. Loyola University, Chicago, IL; University of California, San Francisco, CA; UCD, Sacramento, CA.

Background: Osteosarcoma (OS) is a malignant primary tumor of bone affecting adolescent and young adults. There are few if any molecular markers to predict behavior and prognosis of OS. Our previous studies showed role of p16 as prognostic marker in OS. In the current study we used IHC for p16 and tumor necrosis studies to determine which other factors correlate with poorest chemotherapy response.

Design: Genomic DNA was extracted from FFPE OS specimens obtained prior to initiation of chemotherapy. Microarray analysis was performed using a Roche® NimbleGen® array [OncoChip®(v2)] with whole genome oligonucleotide coverage designed to reduce coverage in benign variable regions and enhance coverage in >2400 cancer features (i.e., genes known or suspected to be important in neoplasia). The microarray platform includes coverage of 67K SNPs with an average spacing of 40kb, affording the detection of genome-wide AOH, including copy-neutral events. p16 expression was determined by IHC staining.

Results: Microarray results were obtained on 46/59 DNAs extracted from OS FFPE samples. Data on both p16 expression and pathologic tumor response to chemotherapy were available on 25/46 samples. Summarizing, deletion of RB1 (72%), gain of RUNX2 (68%), deletion of TP53 (52%), deletion 18q23 (48%) and p16- by IHC (28%) were common findings. Most abnormalities, particularly RB1 and TP53 deletion and RUNX2 gain did not correlate with chemotherapy response. IHC p16- status correlated strongly with failed chemotherapy response (6/10). Alterations of 18q correlated slightly with poor response (p=0.0796). Poor response cases included 3 cases with deletion of 18q23, 3 cases with LOH for 18q23, 1 case with copy gain (trisomy 18). Comparison of 18q genomic abnormalities in cases with a favorable versus poor response suggested a smallest region of overlap for a negative factor at 18q23 that includes the *SALL3* [ital] gene.

Conclusions: We identified complex genotypes in the OS samples with frequent occurrence of previously identified biomarkers such as deletion *RBI* [ital], deletion *TP53* [ital], deletion 18q23 and gain of *RUNX2* [ital]. Comparison of genomic findings to p16- status and chemotherapy response revealed p16- status to be the best overall indicator of a poor chemotherapy response, with the poorest responders being both p16- and altered for 18q23 including *SALL3* gene. Additional studies are warranted to validate these findings and further characterize the role of *CDKN2A* [ital], *SALL3* [ital] and other factors that influence response to therapy in osteosarcoma patients.

44 Osteosarcoma: Is Post Chemotherapy Necrosis an Overvalued Prognostic Marker?

Christalle Katte Carreon, Andrew Doan, Carolyn Fein Levy, Arlene Redner, Morris Edelman. Hofstra North Shore Long Island Jewish School of Medicine and Cohen Children's Medical Center of New York, New Hyde Park, NY.

Background: Evaluation of resected post treatment osteosarcoma (OS) specimens is critical for therapeutic decision making and prognostic assessment. As per the Huvos grading system, ≥90% tumor necrosis (TN) following chemotherapy is considered a favorable response. Our study compared recurrence and survival rates between OS patients with ≥90% TN and <90% TN.

Design: Patients diagnosed with high grade OS at Cohen Children's Medical Center from 1996 to 2011 were selected if they had undergone wide local resection after chemotherapy. Pathology reports and medical records were reviewed. Craniofacial osteosarcomas were excluded. This study was approved by the institutional IRB.

Results: There were 23 subjects (52% male, 48% female, 44% African-American, 26% Caucasian, 30% Asian, Hispanic or other ethnicity). Age at diagnosis ranged from 4 to 29 years (mean = 14.61 +/- 4.58 years, median = 15). Primary sites included distal femur (13 cases), proximal tibia (5 cases), proximal humerus (3 cases), distal ulna (1 case) and rib (1 case). Diagnoses included conventional OS (21 cases), telangiectatic OS (1 case), small cell OS (1 case). Nine patients died due to disease. The 1-year, 2-year, and 5-year survival rates were 90.91%, 86.36%, and 63.94%, respectively. Seven patients had either local or distant recurrence. The 1-year, 2-year, and 5-year progression free rates were 100%, 85.21%, and 67.70% respectively. The percentage chemotherapy-induced TN in the resection specimens ranged from 10% to 100% (mean:

63.61%, median: 70%). Six cases showed ≥90% TN. The median follow-up time was 7.14 years (95% CI: 6.3-9.2 years). There were no statistically significant differences between the high percentage TN group (≥90%) and low percentage TN group (<90%) with respect to overall survival, age at diagnosis, gender, ethnicity, tumor stage, and presence/absence of metastasis at time of diagnosis. There was also no difference if the necrosis cut points were set at 70% or 80%. There was a significant association between age at diagnosis and time-to-recurrence (p<0.039; Hazard ratio=1.157; 95% CI: 1.008 to 1.328). For every year increase in age, the risk of recurrence increased by 16%.

Conclusions: At our institution, post chemotherapy percentage TN did not correlate with overall survival or recurrence. Older subjects were at higher risk of recurrence than younger subjects.

45 CTNNB1 Mutations and Estrogen Receptor Beta Expression in Neuromuscular Choristoma and Associated Fibromatosis

Jodi Carter, Robert Spinner, John Hawse, Caterina Giannini, Karen Fritchie. Mayo Clinic, Rochester, MN.

Background: Neuromuscular choristoma (NMC) is a rare, malformative lesion composed of admixed nerve fibers and mature skeletal muscle, typically arising within the nerve fascicles of major nerve roots or trunks. Interestingly, desmoid-type fibromatosis often develops following biopsy or surgical intervention for NMC. To date, little is known about the pathogenesis of NMC or its association with fibromatosis (NMC-Fi). Desmoid-type fibromatosis is associated with CTNNB1 (beta-catenin) mutations, and the canonical Wnt signaling pathway, involving beta-catenin, has been implicated in development of the neuromuscular junction. Thus, we hypothesized that NMC and NMC-Fi may also harbor CTNNB1 mutations. In addition, desmoid-type fibromatosis expresses estrogen receptor beta (ER beta) and anti-estrogenic strategies are a therapeutic mainstay in unresectable cases. Therefore, we also characterized the ER isoform expression profile in NMC and NMC-Fi.

Design: Cases of NMC with or without NMC-Fi were retrieved from our institutional archives. Clinico-radiologic and histologic features were re-evaluated to confirm the previous diagnoses. All NMC and NMC-Fi cases with available material underwent mutation analysis for CTNNB1 T41A, S45F and S45P by pyrosequencing. All cases were also tested for beta-catenin, ER alpha and ER beta protein expression using isoform-specific antibodies.

Results: NMC occurred in 2 females and 3 males (mean age 14 years, range <1 to 51 y), as masses involving the sciatic nerve (N=4) or brachial plexus (N=1). In 4 of 5 cases, biopsy-confirmed NMC-Fi developed following biopsy or surgical intervention for the NMC. Three (of 5) (60%) NMC had CTNNB1 mutations (2:S45F; 1:T41A), including one case without NMC-Fi and two cases with subsequent NMC-Fi. In the latter group, the NMC-Fi had identical CTNNB1 mutations to those detected in the NMC. In 2 cases, CTNNB1 mutation was present in the NMC-Fi, but not in the original NMC. All NMC and NMC-Fi showed aberrant nuclear beta-catenin localization, strong and diffuse nuclear ER beta expression and lacked ER alpha expression.

Conclusions: To our knowledge, we report for the first time that CTNNB1 mutations occur in NMC and NMC-Fi with high frequency. Furthermore, NMC and NMC-Fi express ER beta, and may respond to therapeutic estrogen antagonism.

46 Diagnostic Utility of Periostin To Distinguish Low Grade Chondrosarcoma From Enchondroma

Shaoyong Chen, Xianyin Lai. Indiana University, Indianapolis, IN.

Background: Differentiation of low-grade chondrosarcoma from enchondroma can be very challenging histologically. To search for new protein biomarker candidates, a liquid chromatography - tandem mass spectrometry (LC-MS/MS) approach was carried out. One of top biomarker candidates, periostin, was identified and validated immunohistochemically. Periostin, also called osteoblast-specific factor 2, is an extracellular matrix protein and plays an important role in tumor progression in various types of cancer.

Design: Formalin-fixed paraffin-embedded tissue blocks of low grade chondrosarcoma (5 cases) and enchondroma (5 cases) were obtained from the IU Health Pathology Laboratory and were used for protein extraction, respectively. Then protein reduction, alkylation, and digestion were performed using a previously published protocol. The digested protein specimens were analyzed using LC-MS/MS. Periostin immunostaining was performed in 23 low grade CHS and 31 enchondroma. The periostin immunostaining was scored according to staining extent (percentage of staining in the whole tumor tissue section); 0, <1%; 1+, 1-25%; 2+, 26-50%; 3+, 51-100% and intensity (weak, moderate, or strong). Only extracellular matrix staining is considered to be positive.

Results: Among the 23 low grade chondrosarcoma, 16 cases were positively stained (3+ in 2 cases, 1+ in 14 cases), while only 4 out of the 31 enchondroma tissue samples were positively stained (1+ in 4 cases). Among all positive staining cases, 90% (18/20) cases show strong focal staining (1+).

Conclusions: Immunohistochemical staining of periostin in 23 low-grade chondrosarcoma and 31 enchondroma tissue specimens disclosed the specificity of 87% and the sensitivity of 70%. The main limitation of periostin staining is focal pattern, instead of diffuse pattern.

47 IDH1/2 Mutational Testing for the Diagnosis of Conventional and Dedifferentiated Chondrosarcoma

Shaoyong Chen, Shi Wei, Kristin Post, Kendra Curless, Eyas Hattab, Liang Cheng. Indiana University, Indianapolis, IN; University of Alabama, Birmingham, AL.

Background: There is a growing trend to combine molecular testing with routine histologic examination for rendering a specific diagnosis. It has been reported in two previous studies that the metabolic enzymes isocitrate dehydrogenase 1 (*IDH1*) and *IDH2* mutations are detected frequently (56% to 61%) in cartilaginous tumors but not

in other mesenchymal tumors. In this study, we characterize the *IDH1/2* mutations in conventional and dedifferentiated chondrosarcoma (CHS) collected at our institution. **Design:** A computerized search of the laboratory information system was performed for the 9-year period from 2005 through 2014 to identify CHS cases. Thirty cases (19 without decalcification and 11 with decalcification) were collected. The H&E slides from all cases were re-examined and diagnoses confirmed. DNA was extracted from formalin-fixed, paraffin-embedded tissues. *IDH* mutation analysis was performed using the Qiagen *IDH1/2* RGQ PCR Kit, which detected mutations in codons 132 and 100 of the *IDH1* gene and codon 172 of the *IDH2* gene, respectively.

Results: The age of the patients ranged from 27 to 95 years with a mean of 60. The male to female ratio was 1.5:1. The tumor size ranged from 2.5 cm to 47 cm. Among 19 specimens without decalcification, seventeen cases (13 conventional CHS and 4 dedifferentiated CHS) tested well for mutational analysis. One conventional CHS and one dedifferentiated CHS failed the test due to insufficient DNA quantity and unknown reason, respectively. All 11 conventional CHS with decalcification failed the test. A somatic mutation in either *IDH1* or *IDH2* was detected in 4 conventional CHS and 4 dedifferentiated CHS. Specifically, they were 2 R132H, 1 R132C, and 1 R132 mutations in *IDH1* gene and 4 R172 mutations in *IDH2* gene. The remaining 9 cases showed wild type *IDH1* and *IDH2*.

Conclusions: Overall, 8/17 (47%) chondrosarcoma cases harbored a mutation in either *IDH1* or *IDH2* genes. DNA extracted from decalcified specimens is not suitable for mutational analysis due to severe damage by hydrochloric acid. Identification of *IDH1/IDH2* mutations may be useful in confirming the diagnosis of chondrosarcoma, especially among dedifferentiated examples.

48 Prevalence of MiTF and Other Melanocytic Markers in Undifferentiated Pleomorphic Sarcoma: Caution Is Advised

Bonnie Choy, Peter Pytel, Rex Haydon, Anthony Montag, Nicole Cipriani. University of Chicago Medicine, Chicago, IL.

Background: Undifferentiated pleomorphic sarcoma (UPS) is a soft tissue sarcoma that does not demonstrate a specific lineage of differentiation. Diagnosis of UPS may be challenging, as other lesions with undifferentiated spindle cell morphology must first be excluded, including melanoma. Microphthalmia-associated transcription factor (MiTF), a DNA-binding protein that plays a role in melanocyte development, was originally reported as a highly specific nuclear marker for benign cutaneous nevi and epithelioid melanoma. A later study reported MiTF expression in a number of spindle cell lesions, including fibrous histiocytoma and fibrosarcoma. Our aim was to evaluate the prevalence of MiTF and other melanocytic markers (SOX10, Melan-A, HMB45, and S100) in UPS.

Design: MiTF, SOX10, Melan-A, HMB45, and S100 immunohistochemical stains were performed on formalin-fixed paraffin-embedded resection specimens from 19 adult patients (age 41-83) with UPS of the deep soft tissue of the extremities or trunk. Neoadjuvant chemo- or radiotherapy was given in 5 patients. No patient had a known history of melanoma.

Results: In 17 of 19 UPS (89%), tumor cells showed nuclear positivity for MiTF, ranging from very focal to diffuse. 4 cases had been previously treated. In 3 cases (all MiTF-positive, 1 previously treated), focal nuclear staining for HMB45 was seen. In 1 case (MiTF-positive, untreated), focal nuclear staining for S100 was seen. None of the UPS showed expression of SOX10 or Melan-A.

Conclusions: There is a high prevalence (89%) of nuclear MiTF expression in UPS. Additionally, 16% and 5% of cases showed nuclear HMB45 and S100 staining, respectively. This finding urges against using MiTF in isolation to differentiate between UPS and melanoma, as well as caution in using focal staining for a single additional melanocytic marker. MiTF may be used to support a diagnosis of melanoma *only* if multiple other melanocytic markers are positive.

49 Molecular Detection of Solitary Fibrous Tumors Shows Distinctive Site- and Age-Related Variability in NAB2-STAT6 Fusion Types: Clinicopathological, Immunohistochemical, and Genetic Analysis in 90 Cases

I-Chieh Chuang, Tse-Ching Chen, Hui-Chun Tai, Shih-Chiang Huang, Chien-Feng Li, Yu-Chien Kao, Jen-Wei Tsai, Hsuan-Ying Huang. Kaohsiung Chang Gung Memorial Hospital, Kaohsiung, Taiwan; Chang Gung Memorial Hospital, Taoyuan, Taiwan; Changhua Christian Hospital, Changhua, Taiwan; Chi Mei Medical Center, Tainan, Taiwan; Wan Fang Hospital, Taipei, Taiwan; E-Da Hospital, Kaohsiung, Taiwan.

Background: Solitary fibrous tumor (SFT) harbors the *NAB2-STAT6* gene fusion with complex exon composition but consistent STAT6 nuclear expression. Previously, RT-PCR was performed mainly on fresh tissues, since FISH is technically demanding to detect the two rearranged, juxtaposed genes.

Design: We investigated the associations between clinicopathological features and this pathogenic hallmark by analyzing STAT6 immunostain in 28 intrathoracic, 38 extrathoracic, and 24 meningeal SFTs, histologically classified as 1 dedifferentiated, 13 malignant, 12 atypical, and 64 typical cases. RT-PCR was performed on assessable RNAs from 80 formalin-fixed and 2 fresh samples.

Results: RT-PCR revealed 11 exon composition types of *NAB2-STAT6* fusion in 74 cases and negative results in 8. Among 3 common types collectively accounting for 86.5% of fusion-positive cases, *NAB2ex6-STAT6ex16* (n=16) exhibited highly variable breakpoints and occasional incorporation with sequences of *NAB2* and/or *STAT6* introns, unlike the predominant *NAB2ex4-STAT6ex2* (n=33) and nearly frequent *NAB2ex6-STAT6ex17* (n=15). Being diffuse and intense in 86(95.6%) cases, STAT6 nuclear immunopositivity was observed in 89(98.9%) SFTs, including all 74 fusion-positive tumors, with focal cytoplasmic staining in few histological mimics. Notably, 7 of 8 fusion-negative cases still exhibited STAT6 nuclear expression, suggesting rare fusion variants beyond the detection by RT-PCR. Regardless of histological classification, the

NAB2ex4-STAT6ex2 was related to older age (p=0.007) and preferentially occurred in the intrathoracic SFTs, compared with the meningeal (p<0.001) or extrathoracic counterparts (p=0.003) that more frequently harbor *NAB2ex6-STAT6ex16*, *NAB2ex6-STAT6ex17*, or other miscellaneous variants.

Conclusions: Most SFTs strongly and diffusely express STAT6 in the nuclei, representing a robust diagnostics and corresponding to 90.2% of cases detectable for *NAB2-STAT6* transcripts. The determination of *NAB2-STAT6* fusion variants may be clinically and biologically relevant, given the site- and age-dependent differences in the preponderant fusion variants.

50 MDM2 Amplification in Problematic Lipomatous Tumors: Analysis of FISH Testing Criteria

Michael Clay, Anthony Martinez, Sharon Weiss, Mark Edgar. Emory University Hospital, Atlanta, GA.

Background: To differentiate lipoma and its variants (L/V) from well-differentiated liposarcoma (ALN/WDL), we perform fluorescent in-situ hybridization (FISH) for *MDM2* amplification in the following situations: 1. Deep “lipomas” that are greater than 10 cm, 2. Superficial or deep “lipomas” with an ambiguous level of atypia or atypia of uncertain significance, 3. Recurrent deep “lipomas,” and 4. All retroperitoneal/abdominal “lipomas”. We have analyzed our experience to determine the situations in which testing is most informative.

Design: All differentiated lipomatous tumors on which FISH for *MDM2* amplification was performed using above criteria since 2010 were reviewed (n=298; consultation cases= 226; institutional cases =72). Final classification was based on the *MDM2* amplification status. No cases were included if the diagnosis could be made on the basis of the hematoxylin-eosin slides. Statistical analysis was performed in each category.

Results: FISH was most often performed for “lipomas” greater than 10 cm (n=126), followed by superficial or deep lesions with equivocal atypia (n=96; 44 superficial, 52 deep), retroperitoneal “lipoma” (n=63), and recurrent deep lipomas (n=32). Of the deep tumors >10 cm, 56 tumors proved to be ALN/WDL, and 70 L/V; the two did not differ statistically in size (p=0.58). For lesions with equivocal atypia, 52 lesions were deep (21 ALN/WDL, 31 L/V), and 44 lesions were superficial (1 ALN/WDL; 43 L/V). Among recurrent deep “lipomas,” ALN/WDL (n=17) and L/V (n=15) were represented nearly equally, but among retroperitoneal tumors L/V (n=40) were represented more frequently than ALN/WDL (n=23). No ALN/WDL occurred in superficial/deep tissues of the hands and feet. Overall, testing identified 118 ALN/WDLs (40% of cases tested).

Conclusions: FISH for *MDM2* amplification is invaluable for deep lesions that are >10 cm, recurrent or have ambiguous atypia as well as for abdominal/retroperitoneal lesions, as it identifies a significant subset of patients that would otherwise be considered to have lipomas and would receive different therapy. Testing is less valuable for superficial lesions with ambiguous atypia because they rarely prove to be ALN/WDL and would not require therapy beyond conservative excision given their location. The unexpectedly high percentage of lipomas among retroperitoneal lesions probably reflects both the bias of our consultation practice and refinement of our diagnostic accuracy.

51 SATB2 Expression Is Sensitive But Not Specific for Osteosarcoma Compared To Other High-Grade Primary Bone Sarcomas

Jessica Davis, Andrew Horvai. University of California, San Francisco, CA.

Background: Osteosarcoma (OS) is defined by the presence of osteoid or bone production by malignant cells. However, osteoid can be focal. Thus not all biopsies demonstrate this diagnostic feature making the distinction between OS and other poorly differentiated bone tumors, including fibrosarcoma (FS) and undifferentiated pleomorphic sarcoma (UPS) is challenging. Yet, treatment and enrollment in clinical trials depends on accurate pathologic diagnosis. The special AT-rich sequence-binding protein 2 (SATB2) is a nuclear matrix protein that regulates osteoblast differentiation. SATB2 shows promise as a diagnostic adjunct for OS insofar as SATB2 immunostaining is highly sensitive for osteoblasts. However, the specificity of SATB2 to discriminate OS from other high-grade bone sarcomas, where SATB2 might be most useful, is not well characterized. This study sought to determine if SATB2 can distinguish OS from other bone sarcomas, even when osteoid is absent on a biopsy.

Design: Forty bone biopsies of high-grade sarcomas lacking tumor-produced osteoid or bone were identified in departmental archives. Seven tumors could be classified as OS because osteoid production by viable malignant cells was present on resection specimens. The remaining 33 tumors (22 UPS and 11 FS) lacked osteoid production on the biopsies and on subsequent resection specimens and lacked definitive radiographic features of OS. Clinicopathological features were recorded. Using standard immunohistochemistry on whole sections, SATB2 nuclear expression was measured for staining extent (0, no staining; 1+, <5%; 2+, 5-25%; 3+, 26-50%; 4+, 51-75%; 5+, 76-100%) and intensity (weak, moderate, strong).

Results: All OS (7/7, 100%) were positive for SATB2 and 4/7 (57%) showed strong staining. SATB2 was positive in 11/22 (50%) UPS and 5/11 (45%) FS. Together, 8/33 (24%) non-OS tumors displayed strong staining. Sensitivity and specificity of SATB2 for OS were 100% and 51%, respectively. Tissue decalcification status, patient age and gender did not correlate with SATB2 staining (p>0.99, p=0.19 and p>0.99, respectively).

Type of sarcoma	Extent of staining						# with strong staining
	0	1+	2+	3+	4+	5+	
UPS (n=22)	11	1	2	2	2	4	5 (23%)
Fibrosarcoma (n=11)	6	3	0	0	1	1	3 (21%)
Osteosarcoma (n=7)	0	1	3	1	1	1	4 (57%)

Conclusions: These results support that SATB2 is a highly sensitive marker OS even in the absence of osteoid. However, a positive SATB2 result lacks sufficient specificity to reliably distinguish OS from other high grade bone sarcomas.

52 Clinicopathologic Correlates of NAB2-STAT6 Fusion Transcript Types in Solitary Fibrous Tumor

Elizabeth Demicco, Khalida Wani, Wei-lien Wang. Mount Sinai Health System, New York, NY; University of Texas MD Anderson Cancer Center, Houston, TX.

Background: Recurrent *NAB2-STAT6* fusion drives tumorigenesis of solitary fibrous tumor (SFT). Different fusion transcript types have been reported to be associated with distinct clinicopathologic subsets of tumors, and with clinical outcomes.¹ We investigated the frequency of several common and uncommon fusion variants in a subset of SFT with clinicopathologic correlation.

Design: RNA was extracted from 31 formalin-fixed, paraffin embedded (FFPE) primary pleural SFTs and subjected to multiplexed QRT-PCR for 3 of the most frequently reported fusion transcript types (*NAB2-STAT6* exons 4-2; 6-16; and 6-17, as well as 7-2, an unusual fusion variant), using previously published primer sequences.¹ Results were correlated with STAT6 immunohistochemistry, clinicopathologic features and patient outcomes.

Results: All 31 cases were strongly positive for nuclear STAT6 (C-terminal) by immunohistochemistry. QRT-PCR was successful in 29 cases. 17/29 (59%) cases had a 4-2 fusion type in multiplexed reactions. Twelve cases were negative for all 4 tested fusion types. Tumors with 4-2 fusion trended to be larger at diagnosis (median 9 cm (range 3.0-23.0 cm)) than cases with unknown fusion ((median 5 cm (1.0-12.4 cm)) (p=0.072). There were no statistically significant differences in patient age, mitotic activity, race, or sex between cases with 4-2 fusion type and cases with unknown fusion type. Using our previously published risk stratification system,² only 29% of patients with 4-2 fusion type would be considered low-risk of metastasis in contrast to 83% of patients with unknown-fusion variants (p=0.004).

Clinical follow-up was available in 17 cases (12 with 4-2 fusion type, and 5 unknown fusion), and ranged from < 1 month to 13 years (median 44 months). One patient with 4-2 fusion developed metastases at 37 months, while 16 patients were disease-free at last follow-up.

Conclusions: Our findings confirm a relatively high frequency of the 4-2 *NAB2-STAT6* fusion type in pleural SFT. However, a higher proportion of our cases than expected were negative for this type, likely due to differences in patient population. Testing is underway on an additional 175 cases of pleural, meningeal and soft tissue SFT.

References:

1. Bartholomeß S et al. Am J Pathol 2014; 184(4):1209-18.
2. Demicco EG et al. Mod Pathol 2012; 25(9):1298-306.

53 Subcutaneous Minimally Atypical Lipomatous Tumors With Variable Fat Cell Size – A Study of 13 Cases

Harry Evans. University of Texas MD Anderson Cancer Center, Houston, TX.

Background: Over the years I have observed in consultation subcutaneous fatty tumors that exhibit notable variation in fat cell size but not more than slight nuclear enlargement and atypia. Being uncertain of their proper classification and behavior, I decided to undertake a review.

Design: Consultation cases in our files diagnosed before 2008 and described in the reports as showing the abovementioned features were reviewed. Inclusion criteria were that there be adequate pathologic material demonstrating the appropriate histologic characteristics and at least some follow-up information.

Results: The study group consisted of 12 men and 1 woman aged 36 to 79 yrs (median 57 yrs). The most common tumor locations were the neck and back (3 each; 1 man had 2 separate tumors involving the neck and back). Other sites included the chest wall (2), breast (1-the woman), breast and axilla (1-a man), arm (1), shoulder (1), scrotum (1), and pubic area (1). All the tumors were subcutaneous. Excision (sometimes in fragments) was the initial treatment in all cases. This was followed by re-excision in 3 cases (shoulder, breast, and scrotum), with all re-excision specimens being negative for tumor. Tumor size (which was estimated from aggregate or largest fragment dimensions in the instances of fragmented specimens) ranged from 4.1 to 9.1 cm (median 6 cm). Histologically, all the tumors demonstrated variable fat cell size, sometimes strikingly so. In contrast to this, nuclear enlargement and atypia ranged from inapparent to slight. Microscopic foci of fat necrosis, which varied from occasional to plentiful, were a consistent finding. Some tumors had an intermixed fibrous or fibromyxoid component, but this never dominated and always lacked nuclear atypia (which was instead confined to fat cells). On follow-up of 4 to 11 yrs (median 9 yrs), 10 patients had no recurrence of the tumor. 2 had local recurrences excised, 1 at 6 yrs (neck) and 1 at 9 mos (the patient with neck and back tumors, both of which recurred); additional follow-up could not be obtained on either patient. A third patient (breast and axilla) had a local recurrence that had not been excised at the latest follow-up of 9 yrs.

Conclusions: The tumors reported on here form a group distinct from both atypical lipomatous tumors and ordinary lipomas by virtue of their combination of preponderant occurrence in men, exclusively subcutaneous location, significant variability of fat cell size coupled with unnoticeable to minor nuclear atypia, and appreciable but relatively low rate of local recurrence.

54 Frequency and Clinicopathologic Profile of PIK3CA Mutant GISTs

Anna Felisiak-Golabek, Bartosz Wasag, Tiffany Coates, Jerzy P Lasota, Markku Miettinen. National Cancer Institute, Bethesda, MD; Medical University, Gdansk, Poland.

Background: GIST, the most common mesenchymal tumors of GI tract is driven by oncogenic activation of receptor tyrosine kinases, *KIT* or *PDGFRA*. Recently, gain-of-function mutations in *PIK3CA*, a gene that encodes the 110 α catalytic subunit of PI3K, were reported in GIST. Previously, mutational activation of PI3K/AKT signaling pathway has been identified in human cancer. In GIST, *PIK3CA* mutations were found in 2 gastric tumors (in one concurrent to *KIT* mutation) and in treatment resistant metastatic lesion of BRAF-mutant GIST. It seems that mutational activation of PI3K/AKT signaling pathway may play a role in both GIST pathogenesis and tumor progression. The aim of this study was to define frequency of *PIK3CA* and *AKT1* mutations in imatinib-naïve GISTs.

Design: Cohort of well characterized, CD117 and DOG1 positive GISTs was evaluated for *PIK3CA* exon 9 and 20 and c.49G>A (p.E17K) *AKT1* mutation. DNA was extracted from FFPE tumor samples. *PIK3CA* exon 20 and *AKT1* exon 3 PCR amplification products were analyzed by Sanger sequencing, while *PIK3CA* exon 9 were evaluated by high resolution melting analysis.

Results: Seven *PIK3CA* mutations were identified in 6 of 415 (1.5%) analyzed GISTs, although they account for 2.5% of malignant tumors. Following substitutions were identified: c.3140A>G, c.3140A>T, c.3103G>A, c.3127A>G, c.3137C>T, c.3143A>G, c.3158C>T. At the protein level, these substitutions would lead to p.A1035T, p.M1043V, p.A1046V, p.H1047R, p.H1047L, p.H1048R, p.T1053I mutations, respectively. In one tumor two substitutions c.3103G>A and c.3158C>T were detected. Three *PIK3CA* mutants were previously evaluated for *KIT*, *PDGFRA*, *BRAF* and *RAS* mutations and turned to be *KIT* exon 11 mutants. There were 2 gastric and 4 retroperitoneal tumors. These 6 patients included 3 men and 3 female (mean age, 51 years). Five tumors were > 10cm with the mitotic activity 3 to 72 mitosis/50HPF. The follow-up showed short, < 35 months, survival (n=5). No *PIK3CA* exon 9 or *AKT1* mutants were identified in 100 GISTs analyzed.

Conclusions: *PIK3CA* mutations were identified in a subset of imatinib-naïve, highly advance, malignant GISTs. This could suggest that *PIK3CA* mutant clones may have proliferative advantage over other clones without the pressure imposed by targeted therapies. Because presence of *PIK3CA* mutation may have significant implications on the selection of the targeted therapy, screening for such mutations should be considered in primary highly advance and metastatic GISTs.

55 Composite Hemangioendothelioma: A Clinicopathologic Study of Nine Cases

Masaharu Fukunaga. Jikei University Daisan Hospital, Tokyo, Japan.

Background: Composite hemangioendothelioma (HE) is a low-grade malignant vascular tumor showing varying combinations of benign, low-grade malignant, and malignant vascular components. The predominant histologic components are histologically identical to epithelioid HE and retiform HE. There have been only 28 cases of composite HE reported in the English literature, and its nature and biological behavior remain unknown.

Design: The clinicopathologic and immunohistochemical features of nine cases of composite HE including a case with associated Maffucci syndrome are described.

Results: The patients were seven females and two males with a median age of 36.0 years (range, 8-75 years). All tumors occurred in the dermis and/or subcutis. The tumors arose in the foot or lower leg in 6 patients, in the face in two patients, and as multiple tumors in the left upper extremity in one patient. Two patients had congenital tumors, in the lower thigh and foot, or upper extremity. The lesions were usually of several years duration. The size of individual tumors ranged from 1.0 to 30 cm. The tumors were composed of a complex admixture of histologic components resembling various vascular lesions. The predominant components, present in all cases, resembled retiform HE and epithelioid HE. Angiosarcoma-like areas were observed in three cases. Lymphangioma-like areas were found in two cases. Areas of spindle cell hemangioma, cavernous hemangioma or arteriovenous malformation were identified in two cases each. The two congenital cases exhibiting multiple lesions had angiosarcoma-like components and an angiomatosis-like growth pattern. One patient each was associated with Kasabach-Merritt or Maffucci syndrome. Immunohistochemically, all tumors showed expression of at least two endothelial markers (CD31, CD34, factor VIII-related antigen and/or D2-40). Of eight cases that were followed up (median duration, 8.2 years), one tumor recurred locally. One was a recent case. To date, none of the patients have developed metastases. There was no difference in biologic behavior among cases with various combinations of histology in this study.

Conclusions: The findings expand the clinical and histologic spectrum of this tumor. There was no difference in biologic behavior among cases showing various combinations of histology in this study and previously reported cases. Composite HE should continue to be regarded as a low-grade malignant vascular tumor (hemangioendothelioma), with significant potential for local recurrence, but little if any potential for distant metastasis.

56 Primary Ewing Sarcoma of the Gastrointestinal Tract: A Clinicopathologic and Molecular Study of 28 Cases

Rondell Graham, Michael Torbenson, Alaa Salim, Long Jin, Margaret Chou, Andre Oliveira, David Stockman. Mayo Clinic, Rochester, MN; University of Texas MD Anderson Cancer Center, Houston, TX; Children's Hospital of Philadelphia, University of Pennsylvania, Philadelphia, PA; University of South Carolina School of Medicine, Greenville, SC.

Background: The presentation of Ewing sarcoma(ES) in the gastrointestinal(GI) tract is rare and can be confused with other tumors bearing overlapping histologic features.

Design: Tumors with diagnoses of ES involving the GI tract were retrieved from the institutional archives from 1991 to 2014. The diagnosis of ES was confirmed by histologic review together with immunohistochemistry and molecular testing on paraffin embedded sections. Tumors were assessed by fluorescence in situ hybridization (FISH) for rearrangement of *EWSR1* locus and RT-PCR for *EWSR1-FLI1* and *EWSR1-ERG* fusion transcripts. A control group of 20 randomly selected cases of ES of bone were selected for comparison.

Results: Ewing sarcoma(n=28) occurred in 17M/11F (median 35 yrs, range 3-79) and varied in size from 3.5-17.0 cm (median 8.5). Tumors involved the small intestine(n=9), colon(n=7), pancreas(n=7) and stomach(n=5). In 13 cases, tumor extension into the mesentery and omentum was noted. Original referring diagnoses included desmoplastic small round cell tumor and lymphoma. In 8 cases, the patients presented with metastases to liver, lung and/or regional lymph nodes. Tumors featured highly cellular sheets of small round cells which expressed CD99(100%), FLI1(75%), chromogranin(15%), and synaptophysin(39%). Desmin, CD117, and S-100 protein were negative in all cases. Rearrangement of *EWSR1* locus by FISH was present in 16/16 cases, with *EWSR1-FLI1* in 9/14 cases(64%) and *EWSR1-erg* in 3/14(21%) cases; no fusion transcript was identified in 2 cases, consistent with alternate fusions. Nine patients died of disease after 3 to 85mo (median, 23mo); 8 patients were alive with disease and 2 without evidence of disease (median, 7mo). Metastases developed in 17 patients after periods of up to 81mo. ES of the GI tract had inferior five-year survival rates(27%) when compared to osseous ES(56%).

Conclusions: Primary ES of the GI tract is rare and can be distinguished from other small round cell tumors by careful integration of histologic and molecular data. When compared to historical controls of osseous ES, primary ES of the GI tract appears to present at a more advanced age and follow a more aggressive clinical course.

57 Next-Generation Sequencing of Follicular Dendritic Cell Sarcomas Reveals Recurrent Alterations in the Retinoblastoma and Hedgehog Signaling Pathways

Gabriel Griffin, Lynette Sholl, Neal Lindeman, Jason Hornick. Brigham & Women's Hospital, Boston, MA.

Background: Follicular dendritic cell (FDC) sarcoma is a rare mesenchymal neoplasm that usually arises at lymphoid tissue-rich sites. Extranodal tumors often pursue an aggressive clinical course; however, effective systemic therapies are lacking. The genetic basis for FDC sarcoma is unknown. The purpose of this study was to search for recurrent genomic alterations in FDC sarcoma by next-generation sequencing (NGS).

Design: DNA was extracted from formalin-fixed paraffin-embedded tissue sections from 7 cases of FDC sarcoma (6 M, 1 F; age range: 22-60 yrs; 2 neck lymph nodes, 2 abdominal cavity, 1 tonsil, 1 liver, 1 chest wall). Samples were analyzed by targeted exon hybrid capture (Agilent) and NGS using the Illumina HiSeq 2500, interrogating exonic sequences of 300 cancer-associated genes for mutations and copy number variants (CNV), as well as 113 introns across 35 genes for rearrangements. Mutation calls were generated using MuTect and GATK, copy number calls using VisCap Cancer, and large structural variants using BreakMer. Based on the NGS results, immunohistochemistry (IHC) for RB1 was performed.

Results: CNV were uninterpretable in 2 samples due to poor coverage. All 5 other samples showed frequent genetic losses across multiple chromosomes and a lack of amplification events, suggestive of tumor suppressor gene-driven biology. *CDKN2A* deletions were observed in 3 of 5 (60%) tumors (2 homozygous; 1 with 1-2 copy deletion), and 3 of 5 (60%) showed *RB1* alterations (1 homozygous deletion; 1 truncating mutation; 1 heterozygous deletion accompanied by *RBL2* heterozygous deletion). Loss of *RB1* expression in the former 2 cases was confirmed by IHC. Homozygous deletion of *CYLD* was identified in 2 of 5 (40%) cases, both with RB pathway alterations. Of note, no *BRAF* mutations were identified.

Conclusions: FDC sarcoma harbors recurrent alterations in the retinoblastoma (*RB1*, *CDKN2A*) and hedgehog (*CYLD*) signaling pathways. These pathways have been shown to cooperate in the tumorigenesis of other types of malignant neoplasms, including retinoblastoma and small cell carcinoma. Loss of *CYLD* suggests possible opportunities for targeted therapy (currently in clinical trials for other tumor types), at least in a subset of cases.

58 ERG Expression in Low Grade Hyaline Cartilage Neoplasms: A Potential Diagnostic Tool in the Evaluation of Enchondromas and Low-Grade Chondrosarcomas

Sounak Gupta, Wonwoo Shon, Karen Fritchie. Mayo Clinic, Rochester, MN; University of Florida College of Medicine, Gainesville, FL.

Background: Enchondromas are benign cartilaginous neoplasms which rarely recur and can be managed conservatively. In contrast, low grade chondrosarcomas are locally aggressive tumors with potential for recurrence and rare metastasis. Despite differences in clinical behavior, distinguishing enchondroma from low grade chondrosarcoma on morphologic features alone is extremely difficult with high interobserver variability. Experimental studies have shown that the *ets* transcription factor ERG is involved in cartilage tissue development and maintenance of chondrocytes in a differentiated state. ERG has also been reported to be preferentially expressed in embryonic and

growth plate cartilage. Prompted by our recent finding of ERG protein expression in selected chondrogenic mesenchymal tumors, we sought to explore the utility of ERG as an immunohistochemical marker in differentiating enchondromas from low grade chondrosarcomas.

Design: A total of 29 enchondromas (14 involving small bones of the hands and feet and 15 affecting long bones) and 16 cases of axial low grade (grade 1 (of 3)) chondrosarcomas (skull base, vertebral body, rib, sternum, pelvis) were retrieved from the Mayo Clinic surgical pathology archives. Clinical and radiologic findings were reviewed and correlated with histologic features to confirm the diagnoses. A representative tissue block from each case was selected and immunostained with anti-ERG monoclonal antibody to the N-terminus (9FY, 1:50-1:100, BioCare). Nuclear localized ERG expression was graded as 0 (no staining), 1+ (<5%), 2+ (5-50%) and 3+ (>50%). Cases with 2+ or 3+ scores were considered positive. ERG expression in vascular endothelial cells was utilized as a positive internal control.

Results: All but 1 enchondroma (28/29, 97%) were negative for ERG expression (0 or 1+), while 69% (11/16) of low grade chondrosarcomas were positive for ERG (2+ or 3+) with 6 cases showing 2+ staining and 5 cases showing 3+ staining.

Conclusions: ERG seems to be preferentially expressed in low grade chondrosarcomas compared to enchondromas ($p<0.05$) and may be a potential diagnostic aid in the histopathologic classification of low grade hyaline cartilage neoplasms.

59 Mammary-Type Myofibroblastoma: Clinicopathologic Characterization in a Series of 140 Cases

Brooke Howitt, Christopher Fletcher. Brigham & Women's Hospital and Harvard Medical School, Boston, MA.

Background: Mammary-type myofibroblastoma (MTMF) is an uncommon benign neoplasm initially described in the breast; however, it is now recognized to occur in a wider anatomic distribution. MTMF is associated with cytogenetic abnormalities in 13q, and frequently shows loss of Rb by immunohistochemistry (IHC).

Design: Archival cases were retrieved and the diagnosis of MTMF was confirmed. Hematoxylin and eosin (H&E) stained slides and IHC stained slides were reviewed when available (CD34, desmin, and Rb). Patient age, gender, anatomic location of tumor, type and duration of preceding symptoms, tumor size, and type of sampling (biopsy vs excision) was recorded. For excisions, margin status was recorded when possible. Clinical data were requested for recurrent tumor, metastasis, and patient status at last followup.

Results: 140 cases of MTMF comprised this study, consisting of 92 (66%) males and 48 (34%) females with a mean age of 54.5 years (range 4-96 years). The mean tumor size was 6.9 cm (range 1-22 cm). Anatomic location included breast (14; 10%), chest wall/axilla (8; 6%), inguinal/groin/vulva/scrotal/paratesticular (61; 44%), trunk (19; 14%), extremities (18, 13% lower; 2, 1% upper), head/neck (3; 2%), vaginal (2; 1%), or visceral (mostly retroperitoneal or pelvic, 13; 9%). Most cases showed typical morphologic features of MTMF. Cytologic atypia or epithelioid morphology was present in 10 (7%) and 6 (2%) cases, respectively. CD34 and desmin were positive in 90% and 89%, respectively. Both CD34 and desmin were negative in 3%. Rb was lost by IHC in 57/62 (92%) with 17 cases showing only a subset of tumor cells losing Rb expression. Rb was intact in 2 (3%) and equivocal in 3 (5%). No cases with followup data available thus far (n=31) had tumor recurrence (mean 15.5 months, median 11 months).

Conclusions: Even when allowing for consult bias, MTMF appear to be more common at extra-mammary sites than in the breast, and can cause diagnostic difficulty when atypia or epithelioid morphology is present, or when located at an unusual anatomic site. Immunophenotypically, MTMF usually shows loss of Rb expression (92%), and is frequently positive for CD34 and desmin; however rare cases (3%) are negative for both. Recurrence seems to be rare, even in the presence of positive resection margins.

60 Frequent FOS Gene Rearrangements in Epithelioid Hemangioma

Shih-Chiang Huang, Hsiao-Wei Chen, Lei Zhang, Yun-Shao Sung, Brendan Dickson, Thomas Krausz, Christopher Fletcher, Cristina Antonescu. Chang Gung Memorial Hospital, Taoyuan, Taiwan; Memorial Sloan Kettering Cancer Center, New York, NY; Mount Sinai Hospital, Toronto, Canada; University of Chicago, Chicago, IL; Brigham & Women's Hospital, Boston, MA.

Background: Epithelioid hemangioma (EH) is a benign vasoformative tumor with distinctive epithelioid cytology and ubiquitous clinical presentation. Despite a small subset of atypical EHs bearing *ZFP36-FOSB* fusions, no additional genetic abnormality has been disclosed in conventional EH lesions.

Design: We applied next generation paired-end RNA sequencing and FusionSeq algorithm to a typical EH occurring in the rib of a 45 year-old man. A novel *LMNA-FOS* gene fusion was identified, which was then confirmed by reverse transcription polymerase chain reaction and fluorescence in situ hybridization. Break-apart *FOS* probes were then used to screen 34 cases of EH without *FOSB* alterations. The clinical and pathological features of *FOS*-rearranged EH were investigated.

Results: There were 14 cases (41%) with *FOS* gene rearrangements, including 10 males and 4 females, with a mean age of 45 years (range 15-67). Most of the *FOS*-rearranged EH were intra-osseous (7/14, 50%) and soft tissue (5/14, 36%), while 2 occurred in the skin. The predominant anatomic site affected was within extremities (10/14, 71%), with rare examples in the head and neck, trunk and penis. Histologically, all tumors were composed of an intimate mixture of lumen-forming vascular structures and strands of epithelioid endothelial cells, with variable amount of inflammatory infiltrate. Three cases had increased cellularity with solid growth pattern and focal spindling. Only one case demonstrated moderate nuclear pleomorphism and increased mitotic activity (5/10 HPF).

Conclusions: *FOS* rearrangement was present in 41% of EHs with classic morphology and emerges as the most frequent genetic abnormality in this disease, which can be used as a reliable molecular marker in the work-up of challenging epithelioid vascular tumors. The oncogenic activation of *FOS* and *FOSB*, members of the Fos gene family

that dimerize with JUN proteins forming the transcription factor complex AP-1, is emerging as a key event in the tumorigenesis of benign and intermediate groups of vascular tumors.

61 Novel FUS-KLF17 and EWSR1-KLF17 Fusions in Myoepithelial Tumors

Shih-Chiang Huang, Hsiao-Wei Chen, Lei Zhang, Narasimhan Agaram, Mary Davis, Morris Edelman, Christopher Fletcher, Cristina Antonescu. Chang Gung Memorial Hospital, Taoyuan, Taiwan; Memorial Sloan Kettering Cancer Center, New York, NY; Spectrum Health System, Grand Rapids, MI; North Shore-LIJ Health System, Manhasset, NY; Brigham & Women's Hospital, Boston, MA.

Background: Myoepithelial (ME) tumors of soft tissue and bone have diverse morphologic appearances and genetic alterations, with about half harbouring *EWSR1* gene rearrangements. Although documented as isolated case reports, the prevalence of *FUS* gene abnormalities and any related fusion partners remains undetermined among the ME spectrum.

Design: Fluorescence in situ hybridization (FISH) was used to screen 62 *EWSR1*-negative soft tissue, bone and visceral ME tumors for *FUS* abnormalities. In an index *FUS*-rearranged case with available frozen tissue, 3'-Rapid Amplification of cDNA Ends (RACE) was applied to identify the fusion partner. Results were further confirmed by RT-PCR, followed by FISH screening the entire cohort of *FUS*-rearranged cases. As the fusion partner proved to be a recurrent event, 16 additional bone and soft tissue *EWSR1*-positive ME lesions lacking a known fusion partner were tested for this abnormality. The correlation between genotype and clinicopathologic features was also investigated.

Results: Five (8.1%) *FUS*-rearranged cases were identified, spanning divergent age groups, tumor locations, morphological characteristics and behavior. A novel *FUS-KLF17* fusion was identified by 3'RACE in an 11 year-old girl with a foot lesion, metastatic to ipsilateral thigh. Two additional cases with *FUS-KLF17* fusions were identified in the lung of a 30 year-old man and tibial periosteum of an 8 year-old boy. Additionally, one *KLF17* rearrangement (6.3%) was found in a foot soft tissue lesion among the 16 *EWSR1*-positive ME tumors. The *KLF17*-rearranged ME tumors had a predilection for children and exhibited trabecular growth in a myxohyaline stroma, but did not correlate with a malignant phenotype. *KLF17* (Krueppel-like factor 17), a member of KLF transcription factor family, has not been previously implicated in gene fusions, but was shown to regulate epithelial-mesenchymal transition and metastasis in other cancers.

Conclusions: This is the largest series assessing *FUS* gene abnormalities in a broad spectrum of ME lesions. A small subset of ME tumors harbor *FUS* rearrangements, most of them (60%) being associated with *KLF17* fusion. *FUS* FISH analysis is recommended in *EWSR1*-negative lesions in which a ME diagnosis is suspected. *KLF17* is also a rare gene fusion partner to *EWSR1* in ME tumors.

62 Diagnostic and Prognostic Value of CTNNB1 Mutation Testing in Sporadic Fibromatosis

Soo Hyun Hwang, Taeun Kim, Boram Lee, Yoon-La Choi. Samsung Medical Center, Seoul, Republic of Korea.

Background: Fibromatoses are benign fibroblastic or myofibroblastic tumors that are locally aggressive and recur frequently. Although no reliable markers for tumor recurrence risk have been identified, point mutations in the *CTNNB1* gene are consistently observed in sporadic fibromatoses. The aim of this study was to investigate the frequencies of *CTNNB1* genotypes in these tumors and to correlate specific genotypes with clinicopathologic parameters, including propensity for recurrence.

Design: The tumor population included 95 desmoid-type fibromatoses. *CTNNB1* genotyping was performed on all 95 tumors and β -catenin immunohistochemical staining was performed on tissue microarray blocks. We analyzed relationships between recurrence and variables such as *CTNNB1* mutation, β -catenin immunostaining, and clinical parameters.

Results: *CTNNB1* mutations were found in 71/95 tumors (75%). Of these, an ACC to GCC transition in codon 41 (T41A) was identified in 40 cases (42%), TCT to TTT in codon 45 (S45F) was identified in 27 cases (28%), and TCT to CCT in codon 45 (S45P) was identified in 4 cases (4%). Nuclear β -catenin expression was found in 82/94 tumors (87%). In the follow-up of 91 patients, 31/91 patients (34%) developed tumor progression. On multivariate analysis in desmoid tumors, age younger than 30 years and tumor size ≥ 10 cm were significantly associated with tumor recurrence (age: $p=0.026$, odds ratio 0.320, 95% CI 0.117-0.875; and size: $p=0.017$, odds ratio 5.467, 95% CI 1.361-21.965). The other variables, including gender, tumor location, *CTNNB1* mutation, margin status and immunostaining for β -catenin, were not significantly associated with recurrence.

Conclusions: *CTNNB1* mutation testing may potentially be used to improve the accuracy of diagnosis but not be demonstrated tumor recurrence alone in sporadic fibromatoses.

63 Explanted Surgical Meshes: What Pathologists Are Missing?

Vladimir Iakovlev, Gaiane Iakovleva, Robert Bendavid. St. Michael's Hospital, University of Toronto, Toronto, ON, Canada; Markham Stouffville Hospital, Markham, ON, Canada; Shouldice Hospital, Richmond Hill, ON, Canada.

Background: Polypropylene meshes, introduced in the late 50's, are presently used in millions of surgeries worldwide. Up to 10% are excised for complications or recurrence generating a large, but underutilized body of study material. Paradoxically, most conclusions of mesh-body interactions are based on animal studies while countless specimens pass through pathology departments.

Design: 32 excised hernia meshes from 12 female and 20 male patients with age range 24-82 years were reviewed. Of 13 ventral hernias 2 were removed for migration into the urinary bladder and fallopian tube, 4 for infection and 7 for recurrence. Of 19

groin meshes 7 were excised for pain and 12 for recurrence. The following parameters were scored independently by two pathologists: mesh deformation, extent of fibrous encapsulation, nerve density and ingrowth, degree of inflammation, edema, vascular thrombosis, fat necrosis, muscle involvement, polypropylene degradation.

Results: All meshes showed folds and scar encapsulation bridging >90% of mesh pores. Density of nerve branches ingrown into the meshes was higher in the specimens excised for pain ($p<0.001$). Involvement of striated muscle showed less pronounced, but significant association with pain ($p=0.05$). Meshes removed for pain also showed trends of more pronounced foreign body reaction and edema in the scar inhabiting the mesh. The amount of scarring with bridging fibrosis and the degree of foreign body reaction tended to be reduced over time, but appeared patient dependent. Polypropylene material showed a degradation layer forming a sheath around the filaments. The layer was detectable by its ability to trap dyes, however it retained birefringence of polypropylene in polarized light.

Conclusions: Tissue ingrown into the mesh is innervated and exposed to all regular pain mechanisms. Mechanical nerve irritation of entrapped nerves is likely the leading mechanism of pain while connection to striated muscle, edema and foreign body reaction appear to contribute into the development of pain. Polypropylene used in mesh manufacturing degrades while exposed to the body environment and the clinical impact of polypropylene degradation needs to be studied further. Overall, the explant specimens, mostly neglected over the decades contain primary information of the mesh-body interactions. A systematic examination revealed previously unreported findings which can help understanding of the mechanisms of complications and guide technical and treatment strategies.

64 Primary Pseudomyogenic Hemangioendothelioma of Bone

Alero Inyang, Carrie Inwards, Andrew Folpe, G Petur Nielsen, Andrew Rosenberg. University of Miami, Miami, FL; Mayo Clinic, Rochester, MN; Massachusetts General Hospital, Boston, MA.

Background: Pseudomyogenic hemangioendothelioma (PMH) also known as "epithelioid-sarcoma-like hemangioendothelioma", is a well-recognized neoplasm that usually arises in the soft tissue; concurrent bone involvement occurs in approximately 24% of cases. PMH of bone without soft tissue involvement is rare. We describe the clinicopathologic findings of 6 such cases; the largest series reported to date.

Design: Cases were identified from the authors' institutions. Clinical history, imaging studies, histology, and immunohistochemistry were reviewed. Microscopically, the tumors were analyzed for growth pattern, nuclear atypia, mitoses, necrosis, and inflammatory cells.

Results: The patients included 5 males and 1 female; age ranging from 14 to 74 (mean 40.5 years). Five patients had numerous multifocal lesions; 3 had disease in bones of the distal lower extremity, 1 had lesions in bones of the distal upper extremity, and 1 had tumor in the spine, ribs, scapula, pelvis, and proximal femur. The 6th patient had a solitary pelvic lesion. On X-ray and CT the tumors were well circumscribed and lytic, and some had a sclerotic rim. On MR the lesions were T2 hyper-intense. The tumors were intracortical and intramedullary cavity and limited to the skeletal system. Histologically, 5 of 6 tumors were composed predominantly of spindle cells arranged in intersecting fascicles with scattered epithelioid cells. In the sixth case the cells were mainly epithelioid. The neoplastic cells contained abundant densely eosinophilic cytoplasm, and oval to elongate vesicular nuclei, with variably distinct nucleoli. There was limited cytologic atypia, no necrosis, and few mitoses (0-2/10HPF). Tumor associated inflammation included lymphocytes, neutrophils, eosinophils, and hemosiderin-laden macrophages. The stroma was inconspicuous. Unique findings included abundant intratumoral reactive woven bone and hemorrhage with numerous osteoclast-like giant cells. Immunohistochemically the tumor cells were positive for keratin in all cases, ERG and CD31 in 5 of 6 cases, and FLI-1 in 2 of 3 cases; CD34 was negative. Follow-up is limited but no patient has developed metastases; and all have stable osseous disease.

Conclusions: PMH exclusively involving bone is rare. It tends to be multicentric, involve the distal lower extremity, has relatively indolent radiologic features, and infrequently metastasizes or rapidly enlarges. Because of its rarity, unusual presentation, and morphology, accurate diagnosis can be challenging.

65 Genetics of Extraskelatal Osteosarcoma: A Clinicopathological and Molecular Study

George Jour, Lu Wang, Wen Chen, John Healey, Lisa Choi, Khedoudja Nafa, Meera Hameed. Memorial Sloan Kettering Cancer Center, New York, NY.

Background: Extraskelatal osteosarcoma (ESOSA) is a rare soft tissue neoplasm representing < 5% of osteosarcomas and <1% of all soft-tissue sarcomas. These tumors show osteoid and/or chondroid matrix and overlapping features with their skeletal osteosarcomas. Herein, we investigate the clinicopathological and molecular features of ESOSA in a series of cases and explore potential morphological and molecular parameters that may affect outcome.

Design: 27 cases were retrieved and reviewed. Clinical history and followup were obtained through electronic record review. DNA from FFPE tissue was extracted and processed from 9 cases. DNA copy number alterations (CNA) and allelic imbalances (AI) were analyzed by SNP-array using Affymetrix OncoScan FFPE Assay using OncoScan Console (Affymetrix) and OncoScan Nexus Express software (BioDiscovery). Log rank and Cox proportional hazards models were used for statistical analysis.

Results: Our series includes 27 patients [male =9, female =18] with an average age of 63 years (19-93) and a median follow up of 24 months (6-120 months). Tumor morphology included giant cell rich (n=7), undifferentiated pleomorphic sarcoma with osteoid (n=9), osteoblastic and/or chondroblastic (n=10) and telangiectatic (n=1). Tumor sites included (trunk) (n=10) and extremities (n=17). Ten patients (37%) died of their disease. Twelve (44%) showed no evidence of disease while 5 (19%) showed

local recurrence and/or metastasis at last follow up. Patients with tumor size > 5 cm and non-giant cell histology had a worse disease free survival (DFS) by univariate analysis ($p=0.05$ and $p=0.03$, respectively). Multivariate analysis including age, sex, site, tumor size, resection margin status, treatment modality and histological subtype didn't reveal any independent prognostic variable for DFS or local recurrence. Frequent genomic alterations included copy number losses in 3p (67%), 9p (78%), 10q (67%), 13q (78%) and 17p (78%). Homozygous deletions of *CDKN2A*, *RBI* and *TP53* were noted in 33%, 22% and 11%, respectively. No CNA or AI were detected in genes implicated in skeletal osteosarcoma such as *EGFR*, *MDM2*, *HER2*, *CDK4*, and *MYC*. No association was found between molecular events and clinical outcome.

Conclusions: Our findings suggest that there are genetic differences between ESOSA and skeletal osteosarcomas. In this small group of tested cases, inactivation of tumor suppressor genes rather than activation of oncogenes seem to drive tumorigenesis. Additional cases are being analyzed.

66 Expressions of Core Subunits of SWI/SNF Chromatin Remodeling Complex in SMARCB1/INI1-Deficient Tumors

Kenichi Kohashi, Hidetaka Yamamoto, Yuichi Yamada, Yoshino Oda. Graduate School of Medical Sciences, Kyushu University, Fukuoka, Japan.

Background: SWI/SNF chromatin remodeling complex utilizes the energy of ATP hydrolysis to remodel nucleosomes and to modulate transcription. This complex is composed of evolutionarily conserved core subunits: SMARCB1 (INI1), SMARCA4 (BRG1), SMARCC1 (BAF155) and SMARCA2 (BAF170). These genes have the potential of tumor suppressors and these alterations have been identified in various neoplasms. Malignant rhabdoid tumor (MRT) and epithelioid sarcoma (ES) are classified as tumor of uncertain differentiation, and they show a complete loss of INI1 protein expression as well as very aggressive biological behavior. The histological features of ES, especially proximal-type ES (P-ES) resemble those of MRT. Some data regarding the histologic and immunohistochemical differences between P-ES and MRT exist, but such findings are not yet conclusive. To date, there has been no investigation focused on SWI/SNF chromatin remodeling complex in INI1-deficient tumor series.

Design: We analyzed the BRG1, BAF155 and BAF170 protein expression in 34 MRTs, 20 P-ES and 28 conventional-type ES (C-ES), and these mRNA expressions in 18 MRTs (including 3 cell lines), 3 P-ESs (including 2 cell lines) and 1 C-ES cell line. A total immunostaining score was calculated as the product of a proportion score and an intensity score. The proportion score described the estimated fraction of positive-stained tumor cells (0, none; 1, < 1%; 2, 1%–10%; 3, 10%–33.3%; 4, 33.3–66.7%; 5, > 66.7%). The intensity score represented the estimated staining intensity (0, no staining; 1, weak; 2, moderate; 3, strong).

Results: Total immunostaining median scores in MRT, C-ES or P-ES are as follows: BRG1 (MRT, 4.5; P-ES, 3; C-ES, 5), BAF155 (MRT, 4; P-ES, 0; C-ES, 0) and BAF170 (MRT, 3; P-ES, 5.5; C-ES, 6). Statistically significant differences are also found [BRG1, $P=0.046$ (C-ES vs P-ES); BAF155, $P=0.002$ (MRT vs P-ES, $P=0.032$ (MRT vs C-ES)); BAF170, $P=0.004$ (MRT vs C-ES)]. Median values of mRNA are as follows: BRG1 (MRT, 46.6; P-ES, 24.9; C-ES, 105.4), BAF155 (MRT, 43.3; P-ES, 22.4; C-ES, 61.9) and BAF170 (MRT, 52.3; P-ES, 38.7; C-ES, 167.2).

Conclusions: In MRT and ES, expressions of some core subunits of SWI/SNF chromatin remodeling complex are reduced. Therefore, combined reduced expressions of these proteins may have an important role in tumorigenesis in these tumors. In addition, evaluation of BAF155 immunorexpression may be a useful diagnostic tool to distinguish MRT from P-ES.

67 Clinicopathological Prognostic Factors of Primary Central Chondrosarcoma: Analysis of 182 Cases By Numerical Score on Histology

Eiichi Konishi, Yasuaki Nakashima, Masayuki Mano, Yasuhiko Tomita, Akio Yanagisawa. Kyoto Prefectural University of Medicine, Kyoto, Japan; Kyoto University Hospital, Kyoto, Japan; Osaka National Hospital, Osaka, Japan; Osaka Medical Center for Cancer and Cardiovascular Disease, Osaka, Japan.

Background: Histological diagnosis of primary central chondrosarcoma (pcCHS) is still challenging because it is unclear which features are important as objective prognostic indicators. In this study, we analyzed clinicopathological features of pcCHS, using numerical score on histology, in order to elucidate the features predicting prognosis. Clinicopathological characteristics of pcCHS were also shown.

Design: PcCHSs were collected within the Kansai Musculoskeletal Oncology Group, Japan. Histology of all cases were reviewed and given the numerical score on 17 pathological findings. With data of age, sex, location, follow-up period and outcome, statistical analysis was performed.

Results: 182 pcCHSs were reviewed (male:female=84:98). All patients are Japanese. The average age at the presentation was 50.9 years (15–83 years). The average follow-up period was 65.4 months (1–258 months). 106 cases (58.2%) were of long bones, 38 (20.9%) of the bones of the limb girdles, and 6 (3.3%) of small bones of hands and feet. 30 cases (16.5%) were of the bones of the trunk and 2 (1.1%) from the skull. 21 patients died of disease. Histologically, 91 cases (50.0%) were grade 1, 71 (39.0%) were grade 2, and 20 (11.0%) were grade 3, respectively. The 5-year and 10-year disease specific survival rates were 98.7:95.1% (grade 1), 84.5:71.7% (grade 2), and 33.1:33.1% (grade 3). Survival curves of each grade were statistically different each other ($p<0.05$). Cox hazards analysis on the score of clinicopathological findings showed that grade, calcification and age were significant factors ($p<0.05$), predicting prognosis. The hazard ratios of age, grade 1 vs 2, and grade 1 vs 3 were 1.040, 5.118 and 17.914, respectively. But that of calcification was 0.176.

Conclusions: By analysis of 184 pcCHSs, age and histological grade were significant predictive factors for poor prognosis (patient's death) but calcification was that for good prognosis. Calcification has been regarded as a sign of enchondroma, but it will be a

simple maker for good prognosis. In Japan, there was a mild female preponderance for pcCHS. Long bones were more frequently involved than the previous results. But the prognosis was basically similar.

68 P16 Expression Predicts Necrotic Response After Neoadjuvant Chemotherapy in Osteosarcomas: Reappraisal With a Larger Series Using Whole Sections

Kemal Kosemehmetoglu, Fisun Ardic, Yildirim Karslioglu, Olcay Kandemir, Ayhan Ozcan. Hacettepe University, Ankara, Turkey; Abdurrahman Yurtaslan Ankara Oncology Education and Research Hospital, Ankara, Turkey; Gulhane Military Medical Academy, Ankara, Turkey.

Background: Over 90% necrosis after neoadjuvant chemotherapy is a good prognostic factor in osteosarcomas. In a recent study using tissue microarrays of 40 conventional osteosarcomas, P16 expression is shown to independently predict the necrotic response to neoadjuvant chemotherapy. In this study, we aimed to investigate this recent finding using whole sections in a larger group of osteosarcomas.

Design: Eighty four cases having both pretreatment biopsies and resection specimens after neoadjuvant chemotherapy were collected from the archives of 3 reference hospitals. Age, sex, tumor size, tumor subtype, and location were recorded. Percentage of pathologic tumor necrosis was reevaluated. Four mm-thick slides of pretreatment biopsies were immunostained for P16 (BD Pharmingen, G175-405, 1:25) using Leica Bond Autostainer. Over %30 strong nuclear staining is regarded as positive.

Results: Median age of the patients was 17 (range 5–68), and male to female ratio was 2.23. Mean tumor diameter was 9.9 cm (range, 2–30 cm). Tumors were most commonly of osteoblastic type (60%), followed by chondroblastic (19%) and fibroblastic (15%) subtypes. The most common locations were femur (46%), tibia (27%), and humerus (7%). P16 positivity was seen in 55% of the patients. Median percentage of pathologic necrosis was 65%; 38% of the patients gave favourable ($\geq 90\%$) response to neoadjuvant therapy. In univariate analysis, P16 expression was significantly correlated with presence of $\geq 90\%$ necrotic response to neoadjuvant chemotherapy ($p=0.043$). P16 expression was also associated with tumor size (correlation coefficient: 0.27, $p=0.020$), whereas patient age showed an indirect correlation with necrotic response (correlation coefficient: -0.27, $p=0.013$). On multivariate logistic regression analysis including age, sex, tumor subtype, location, size, and P16 expression, P16 expression (odds: 4.69, $p=0.015$), female sex (odds: 6.29, $p=0.008$) and tumor size (odds: 0.85, $p=0.018$) were found to be independently associated with chemotherapy response.

Conclusions: With a larger series using whole sections, P16 expression, female sex, and tumor size were found to be independent predictors of response to neoadjuvant chemotherapy in osteosarcomas.

69 Angiosarcomas of the Breast: Clinicopathologic Analysis and Prognostic Features

Lik Hang Lee, Doha Itani, Laura Chin-Lenn, Ashwini Yenamandra, Tori Leftwich, Hua Yang. University of Calgary, Calgary, AB, Canada; Vanderbilt University, Nashville, TN.

Background: Breast angiosarcoma is a rare condition arising de novo or secondary to breast carcinoma radiation therapy. We attempt to identify prognostic elements of breast angiosarcoma and assess MYC amplification status.

Design: Cases of breast angiosarcoma diagnosed between 1997 and 2014 in our metropolitan region were selected for histopathological review and clinical data collection. A tissue microarray was established to assess MYC amplification by FISH.

Results: Sixteen patients (two primary, patients 1 and 2, and fourteen secondary) were identified (Table 1). Primary angiosarcoma occurred at a younger age (44±17 years) than secondary (69±11 years, $p=0.01$). Perineural invasion predicted poor disease-specific survival (DSS, $p=0.03$) but not disease-free survival (DFS, $p=0.09$). Other variables that adversely affected DSS and DFS, but showed no statistical significance, included high grade cytology, high FNCLCC grade, epithelioid/poorly differentiated growth pattern, necrosis, hemorrhage, lymphovascular invasion, and breast parenchymal involvement. All secondary angiosarcoma showed MYC amplification while primary angiosarcomas did not. Patient 1 developed a second angiosarcoma with higher grade in the opposite breast after 55 months.

Table 1: Selected Clinicopathologic Features

Patient	Age at Diagnosis	Disease-Free Survival (Months)	Survival (Months)	FNCLCC Grade	Growth Pattern	Perineural Invasion
1	32	55	Alive	1	Conventional	No
2	56	Disease-Free	Alive	2	Conventional	No
3	75	Unknown	Unknown	3	Epithelioid	No
4	70	11	23	3	Epithelioid	Yes
5	79	1	5	3	Epithelioid	No
6	66	25	28	3	Poorly Differentiated	No
7	76	2	8	3	Epithelioid	Yes
8	50	Disease-Free	Alive	2	Epithelioid	Yes
9	73	Disease-Free	Alive	1	Conventional	No
10	86	1	4	2	Epithelioid	No
11	62	Disease-Free	Alive	3	Epithelioid	No
12	70	8	Alive	3	Epithelioid	No
13	50	Disease-Free	Alive	2	Epithelioid	No
14	77	8	14	2	Epithelioid	No
15	74	3	8	3	Epithelioid	Yes
16	58	10	16	3	Epithelioid	Yes

Conclusions: Several clinicopathologic factors appear to be relevant to patient prognosis, particularly perineural invasion. Because of the rarity of breast angiosarcomas, this case series may contribute to the knowledge on this disease.

70 Multi-Platform Mutation Analysis of Gastrointestinal Stromal Tumor and Histologic-Clinical Correlation

Jacqueline Lekostaj, Sarah Hornberg, Mohammed Milhem, Aaron Bossler, Deqin Ma. University of Iowa Hospitals and Clinics, Iowa City, IA.

Background: *KIT* and *PDGFRA* are the most commonly mutated genes in gastrointestinal stromal tumor (GIST). Mutations in these two genes are mutually exclusive and correlate with tumor location, aggressiveness and response to targeted therapy. We analyzed GISTs through traditional Sanger and next generation sequencing (NGS), with a focus on the clinicopathologic correlation of tumors with *KIT* double mutations or *PDGFRA* mutations.

Design: Twenty-one GISTs were selected from archives. DNA sequencing of *KIT* and *PDGFRA* was performed through a combination of NGS using the Ion PGM and the AmpliSeq™ Cancer Hotspot Panel v2 (Life Technologies, Carlsbad, CA), a laboratory developed NGS panel, and Sanger sequencing (*KIT* exons 8, 9, 11, 13, 15, 17). All NGS positive findings were confirmed by Sanger. The clinical course was retrieved from chart review.

Results: 81% (17/21) of cases contained *KIT* (14) or *PDGFRA* (3) mutation and 2 wildtype patients carried a clinical diagnosis of neurofibromatosis 1. *KIT* mutations were most frequent in exon 11 (9) followed by double mutations (3) and exon 9 (2). All *PDGFRA* mutations were in exon 18. All patients with single *KIT* mutation, except 1 with W557_K558del, responded well to tyrosine kinase inhibitors (TKI). One patient with double primary *KIT* exon 11 and 13 mutations showed stable disease; the other had unknown mutation chronology and progressed despite multiple TKIs. The third double-mutant tumor developed a secondary mutation in exon 14 rendering it resistant to TKI. One patient with *PDGFRA* point mutation progressed on TKI; the other had a low-risk tumor, successfully treated with surgery. The patient with *PDGFRA* deletion received TKI with good outcome.

Gene	Mutation	Size (cm)/mitosis per 50HPF	Treatment	Response to TKI
KIT	c.1703 A>C (Y568S), c.1924A>G (K642E)	18/33	imatinib	stable
	c.1669_1674del (W557_K558del), c.1961T>C (V654A)	4/30	imatinib + sunitinib + sorafenib	progression
	c.1674_1676del (K558_V559delinsN), c.2008_9AC>GA (T670E)	6/29	imatinib	partial
PDGFRA	c.2525A>T (D842V)	14/22	imatinib + sunitinib	recurrence
	c.2525A>T (D842V)	3/3	resection	NA
	c.2528_2539del (I843_S847del)	5/0	imatinib	shrinkage

Conclusions: *KIT* double mutations and *PDGFRA* mutations are common in our cohort of patients and can be reliably detected by NGS. Response to TKI therapy corresponded to histology, tumor stage, and the type of mutation present.

71 Impact of Tissue Decalcification on Immunohistochemical Detection of Select Sarcoma Markers

Haiyan Liu, Jianhui Shi, Vivian Xu, Fan Lin. Geisinger Medical Center, Danville, PA.

Background: Application of an immunohistochemical (IHC) assay on decalcified tissues is frequently performed in an anatomic pathology laboratory. It has been documented that tissue decalcification (decal) may have a negative impact on an assay for certain antigens. In this study, we investigated the impact of decal on the detection of frequently used sarcoma markers using sarcoma cell lines.

Design: Three sarcoma cell lines were obtained from the American Type Culture Collection. A set of IHC markers as listed in the Table were tested on each cell line on a cell block. No single cell line expressed all markers. Three cell lines collectively expressed all target markers. The cell pellets containing a mixture of the 3 cell lines were first fixed in 10% neutral buffered formalin for 8 hours (h) and then decalcified in Decalcifier B (Fisher Healthcare, item #23245683) for the following durations: 0 minutes (min) (no decal), 30 min, 60 min, 3 h, 6 h, 1 day, 3 days and 1 week. A tissue microarray (TMA) block containing these tissue/cell line cores with the different decal times was constructed. The aforementioned IHC markers were applied to the TMA sections using the Ventana Ultra staining platform. The staining intensity was recorded as strong (S), intermediate (I), or weak (W). The percentage of cells stained was recorded as 0, 1+, 2+, 3+, or 4+ and compared to the sample with no decal.

Results: The results are summarized in the Table.

Markers/0 min	30 min	60 min	3 hours	6 hours	1 day	3 days	1 week
Desmin/3+,S	3+,S	3+,S	3+,S	3+,S	3+,S	3+,S	2+,S
Myogenin/2+,S	2+,S	2+,I	1+,W	0	0	0	0
MyoD1/3+,S	3+,S	3+,S	2+,I	1+,I	1+,I	1+,I	1+,I
CD99/4+,S	4+,S	4+,S	4+,S	4+,S	4+,S	4+,S	4+,S
NKX2.2/3+,S	3+,S	2+,S	2+,I	1+,W	1+,W	0	0
Fli-1/2+,S	2+,S	2+,I	1+,I	1+,I	1+,I	1+,I	1+,I
SMA/1+,I	2+,I	2+,I	2+,I	0	0	0	0
ERG/2+,S	2+,S	1+,I	1+,W	0	0	0	0

Conclusions: These data demonstrate that tissue decal has 1) a significant negative impact on ERG detection; on myogenin, MyoD1, NKX2.2, and Fli-1 detection; and on SMA detection after 30 min, 60 min, and 3 h of decal, respectively; 2) has a limited impact on the detection of desmin and CD99 following 1 week's decal.

72 Histologic and Immunohistochemical Analysis of Cases of Synovial Chondromatosis With Pre-Operative Concern for Malignancy Based on Radiologic Evidence of Extra-Articular Disease

Seth Lummus, Jeffrey Schowinsky. University of Colorado School of Medicine, Aurora, CO.

Background: Primary synovial chondromatosis (SC) is an uncommon condition involving a proliferation of cartilage within synovium and articular spaces. While SC is regarded as a benign condition, it is reported to rarely transform to chondrosarcoma, with a recent publication suggesting such transformation may occur in up to 6% of cases. SC is usually limited to the joint space, but extra-articular spread of SC can occur, and radiologic detection of such spread is clinically worrisome for transformation to sarcoma. Recent literature suggests that 50–70% of central chondrosarcomas and enchondromas harbor mutations of *IDH1* encoding isocitrate dehydrogenase 1, with R132C, R132G, and R132H mutations being most frequent. Such mutations have not previously been detected in SC.

Design: A database search identified pathology cases at our hospital from 2000-2014 with a diagnosis of 'synovial chondromatosis.' Chart review was performed to identify cases with a pre-operative concern for malignancy based on extra-articular spread of disease. These cases were pulled for histologic review, and blocks selected for immunohistochemistry (IHC) with a monoclonal antibody directed against the R132H mutant form of *IDH1* (Dianova, Hamburg).

Results: 15 cases of synovial chondromatosis were identified, with pre-operative concern for malignancy due to extra-articular disease in 5 cases (representing 3 patients). Review of all 5 cases showed benign appearing histology, characterized by numerous, well-separated nodules of cartilage with no significant atypia, no necrosis, and no significant mitotic activity. SC was present within the extra-synovial fibroadipose tissue in all 3 patients, and was present involving the marrow space in 1 patient. IHC showed expression of mutated *IDH1* in 1 of 3 patients.

Conclusions: Distinguishing between SC and chondrosarcoma in cases of locally aggressive SC poses a diagnostic difficulty for the pathologist. The literature is inconsistent in providing guidance on this subject, with some authors requiring malignant histologic features for a diagnosis of sarcoma but others not. Despite the small sample size, this study shows that locally aggressive cases of SC with entirely benign histology may express mutated *IDH1* protein, which has not been reported in previous studies, further confusing the diagnostic picture. Adoption of a diagnostic categorization that recognizes this degree of diagnostic uncertainty may be prudent until more definitive diagnostic criteria are available to the pathologist.

73 Assessment for Risk Factors Associated With Local Recurrence in Chordoma

Stacey Mardekian, Bryan Hozack, John Abraham, Brian O'Hara, Atrayee BasuMallick, Wei Jiang. Thomas Jefferson University, Philadelphia, PA.

Background: Chordoma is a rare but locally aggressive malignancy. We aimed to identify risk factors associated with local recurrence, which may help guide clinical surveillance and treatment decisions.

Design: We performed a retrospective study of 60 patients diagnosed with chordoma between 1990 and 2014, who underwent surgery in our institution. Medical charts and all available pathology cases (n=94) were reviewed. Clinical and histologic variables were recorded. Descriptive statistic analyses (Student *t* tests, Fisher exact probability tests, and Mann-Whitney's U tests) were performed (2-tailed for all). *p* values <0.05 were considered statistically significant.

Results: In the entire cohort (n=60), the mean age at presentation was 56.4 yrs (19-83); M:F=1.3:1, and 89% were Caucasians (Black 7%, Asian 4%). Tumor size averaged 5.2 cm (range 1.6-15.0). Radiation therapy was given to 47.4% of patients. Local recurrence rate was 68% (n=38), and four patients had recurrence twice. The average time between primary tumor and the first recurrence was 51.4 months (range 7-122, n=12), and 30.5 months between the first and the second recurrence (range 14-52, n=4). Four patients had metastasis (7.2%, n=55) (all to local/distant soft tissue and/or dermis). One patient had primary clivus tumor, then developed C2-3 lesion, and later, C5 lesion, which may be either metastasis or multifocal primary disease. Among all the clinical and histologic factors, the only statistically significant variable associated with local recurrence was the presence of tumor heterogeneity (p=0.03) (see Table 1). Margin status was difficult to evaluate since in many cases the specimen was received as aggregates (n=6 for non-recurrence group, n=15 for recurrence group). Patients without local recurrence had much better overall survival than patients with recurrence (124.2 vs. 65.6 months, p=0.012).

	No recurrence (n=12)	Recurrence (n=26)	<i>p</i>
Age (yrs) - mean	58	59.9	0.70
Male	7	17	0.73
Race (white)	12	20 (n=23)	0.69
Anatomic location			0.37
Clivus/skull base	5	9	
Cervical spine	0	6	
Thoracic/lumbar spine	4	6	
Sacrococcygeal bone	3	5	
Radiation therapy	4	11	0.73
Tumor type			0.40
Classic	12	19	
Chondroid	0	3	
De-differentiated	0	1	
Tumor heterogeneity	0	8 (n=22)	0.03
Cellularity (1-3)	1-10, 2-2, 3-0	1-14, 2-6, 3-1 (n=22)	0.35
Nuclear atypia (1-3)	1-8, 2-3, 3-1	1-12, 2-9, 3-2 (n=22)	0.47
Mitosis	5	13 (n=22)	0.48
Giant cells	5	13 (n=22)	0.48
Necrosis	1	7 (n=22)	0.21
Margin status -positive	1 (n=5)	1 (n=5)	1.0
Survival (months) - mean	124.2	65.6 (n=25)	0.012
Follow up time (months) - mean	78.9	50.8 (n=25)	0.23

Conclusions: Our study is one of the largest clinicopathologic series of chordoma from a single institution, with long-term follow up data. The high rate of local recurrence seemed to dictate the clinical outcome, and our finding of histologic heterogeneity associated with local recurrence was quite interesting. Larger studies are needed to validate the result, which may influence the clinical management.

74 Evaluation of Immunohistochemical Markers Smoothelin, DOG-1, Caldesmon and p16 in Leiomyosarcomas of Different Grades and Anatomical Sites of Origin

Kim Mayhall, Eleanor Lewin, Helena Lebeau, Tong Wu, Byron Crawford. Tulane University Medical School, New Orleans, LA.

Background: Leiomyosarcoma (LMS) is a malignant smooth muscle tumor. Expression of novel antibody smoothelin has previously been evaluated in gastrointestinal (GI) smooth muscle tumors but has yet to be studied in LMS of uterine and other soft tissue origin. DOG-1 expression is reported to be specific for GIST tumors. However, there is variable expression in LMS reported depending on site of origin. Overexpression of p16 is common in LMS of uterine and other types but has not been evaluated by tumor grade. This study explores the differential expression of these markers, in addition to caldesmon, in LMS cases to assess diagnostic utility.

Design: Using tissue microarrays, expression of smoothelin, DOG-1, caldesmon and p16 was evaluated by immunohistochemistry in 80 cases of LMS. The cases were subdivided by location of origin into uterine (N=30), non-uterine (N=50) and GI (N=10), as well as by grade into low grade (N=26) and intermediate and high grade (N=53). Differential expression among different grades and locations was evaluated. Smoothelin was also assessed in 20 benign uterine leiomyomas.

Results: The results of our study are shown.

	Smoothelin	DOG1	Caldesmon	p16
Uterine (N=9)	1/9 (11%)	0/9	4/9 (44%)	5/9 (56%)
Extra-uterine (N=17)	0/17	1/17 (6%)	7/17 (41%)	10/17 (60%)
Gastrointestinal (N=5)	0/5	0/5	4/5 (80%)	0/5
		Intermediate and High Grade		
	Smoothelin	DOG-1	Caldesmon	p16
Uterine (N=21)	0/21	0/21	12/21 (57%)	20/21 (95%)
Extra-uterine (N=32)	2/32 (6%)	1/32 (3%)	11/32 (34%)	24/32 (75%)
Gastrointestinal (N=5)	2/5 (40%)	0/5	3/5 (60%)	4/5 (80%)
		Smoothelin Expression		
Uterine Leiomyoma (N=20)		20/20 (100%)		
Uterine Leiomyosarcoma (N=30)		1/30 (3%)		
Extra-uterine Leiomyosarcoma (N=50)		2/50 (4%)		
GI Leiomyosarcoma (N=10)		2/10 (20%)		

Expression of markers in LMS has been broken down by tumor grade and site of origin. **Conclusions:** Smoothelin is a mature cytoskeletal protein in differentiated smooth muscle cells. Here we show its expression is lost mostly in LMS but retained in leiomyomas of uterine origin. Weak DOG1 expression is rare but possible in extra-uterine LMS. Expression of p16 is frequent in both uterine and extra-uterine types, but more common in higher grades. The use of smoothelin may be beneficial in differentiating atypical/symplastic leiomyomas and STUMPs from LMS. Additional results will be reported at the meeting.

75 Fibroma of Tendon Sheath With Fasciitis-Like Pattern Lacks USP6 Rearrangement and Is Genetically Distinct From Nodular Fasciitis: A Chromogenic In Situ Hybridization Study

Toru Motoi, Ikuma Kato, Akihiko Yoshida, Masachika Ikegami, Shinichiro Horiguchi, Takahiro Goto, Tsunekazu Hishima. Tokyo Metropolitan Cancer and Infectious Diseases Center Komagome Hospital, Tokyo, Japan; National Cancer Center Central Hospital, Tokyo, Japan.

Background: Fibroma of tendon sheath is a benign fibrous tumor typically involving the acral sites. In addition to its classic histology, it may occasionally display hypercellular fasciitis-like growth pattern (FTS-f), which closely resembles nodular fasciitis (NF). Similar histologic appearance and the association with antecedent trauma in a subset of both entities may suggest oncogenic relationship between NF and FTS-f. Because most NFs have recently been shown to have recurrent *MYH6-USP6* fusion genes, we seek to investigate FTS-f cases for the status of each of these partner gene by using chromogenic in situ hybridization (CISH) to determine the genetic relationship between NF and FTS-f. **Design:** Formalin-fixed paraffin-embedded specimens of 11 NFs, 1 intravascular fasciitis (IF) and 7 FTS-fs were retrieved. FTS-fs comprised fasciitis-like area in 5-80% of the tumor (mean, 40%). Three deep benign fibrous histiocytomas (BFH) were used as negative controls. All the specimens were subjected to CISH analysis using custom-designed dual-color break-apart *MYH9* and *USP6* probes and DAKO Duo CISH. Rearrangement-positive nuclei were scored by counting 100 lesional spindle cells.

Results: All NFs harbored *USP6* rearrangement in 6-30% (mean, 17%) of the cells. All but 1 (10/11, 91%) NF also showed *MYH9* rearrangement in 6-32% (mean, 16%) of the cells, indicating *MYH9-USP6*. As a negative control, the 3 BFHs lacked *MYH9* and *USP6* rearrangements with a positive-cell ratio of 1-2% (mean, 1.3%) and 0-2% (mean, 1.3%), respectively. All 7 FTS-fs and 1 IF lacked *MYH9* and *USP6* gene rearrangements with a positive-cell ratio being 0-2% (mean, 0.9%) and 0-3% (mean, 1.1%) in FTS-fs, respectively, and 1% and 0% in IF, respectively.

Conclusions: Despite histological similarity, FTS-f lacks *USP6* rearrangements and is cytogenetically distinct from NF. Consistent with prior reports, the *USP6* gene rearrangements were successfully demonstrated in all NFs. However, the rearrangements were found only in a subset of their lesional cells, which may reflect intratumoral heterogeneity of these "transient neoplasms". This modest positive-cell ratio in NFs may also represent a potential diagnostic pitfall, and it highlights the usefulness of CISH assays that enable bright-field visualization of cellular morphology.

76 Next-Generation Sequencing Analysis of Angiosarcomas Reveals Common MAPK Pathway Alterations and MYC Amplifications

Rajmohan Murali, Raghu Chandramohan, Inga Moller, Michael Berger, Kety Huberman, Agnes Viale, Mono Pirun, Nicholas Socci, Nancy Bouvier, Uwe Hillen, Sebastian Bauer, Jorg Schaller, Dirk Schadendorf, Thomas Mentzel, Donovan Cheng, Thomas Wiesner, Klaus Griewank. Memorial Sloan Kettering Cancer Center, New York, NY; University of Duisburg, Essen, Germany; Dermatopathology Duisburg, Duisburg, Germany; Dermatopathology Friedrichshafen, Friedrichshafen, Germany.

Background: Angiosarcomas (AS) are malignant endothelial neoplasms that may arise de novo or following radiation therapy (RT) for other tumors. Our aim was to characterize genomic alterations in AS using a targeted next-generation sequencing assay, to improve our understanding of their biology and to help guide future studies and clinical trials of appropriate targeted therapies.

Design: We identified patients with histologically-confirmed AS from institutional databases and retrieved clinico-pathologic data. DNA was extracted from paraffin-embedded tumor tissue, and subjected to MSK-IMPACT, a next-generation sequencing assay targeting all exons of 341 cancer genes. Variant calling was performed against a pooled normal control using MuTect (point mutations), SomaticIndelDetector (short insertions/deletions) and a custom pipeline for copy number aberrations. Mutations corresponding to common population polymorphisms were removed, as they were likely to be germline variants.

Results: The patients (24 women, 10 men) were aged 25-85 (median 69) years. AS arose on skin (n=22), liver (n=5), lung (n=2), adrenal, thyroid, nasal cavity, lymph node and heart (n=1 each), and developed following RT in 6 patients.

31 samples were sequenced with coverage exceeding 165x. (Median coverage was <100x in 3 samples, but hotspot mutations were identified in these tumors). 18 (53%) tumors harbored mutations involving the MAPK pathway: 9 AS contained hotspot mutations in *KRAS* (G12), *HRAS* (A59, Q61), *NRAS* (Q61), *BRAF* (V600) and *MAPK1* (E322), and 8 AS showed either focal amplifications in *MAPK1/CRKL* (chr22q11), *CRAF* (chr3p25) or broad chromosomal gains on chr7 including *BRAF*. MAPK activating hotspot mutations appeared to be mutually exclusive of amplifications of MAPK pathway genes. One AS showed *NFI* intragenic deletion as a mechanism for activating the MAPK pathway. *MYC* amplifications were seen in 8 (24%) AS, but only 4/8 (50%) *MYC*-amplified AS displayed MAPK activating mutations. Additionally, 4 AS were *VEGFR2* (*KDR*)-amplified, and 4 AS showed *ATRX* loss-of-function mutations. No convincing associations between genetic alterations and RT were identified.

Conclusions: Derangements of the MAPK pathway (53%) and *MYC* amplification (24%) are important in a substantial proportion of AS, and these two alterations may be independent of one another. Components of the MAPK pathway may therefore be viable therapeutic targets in AS patients.

77 Palisading in Synovial Sarcoma: A Diagnostic Pitfall

Rana Naous, John Goldblum, Steven Billings, Jesse McKenney, Abbas Agaimy, Brian Rubin. Robert J. Tomsich Pathology and Laboratory Medicine Institute, Cleveland Clinic, Cleveland, OH; Institute of Pathology, University Hospital, Erlangen, Germany.

Background: Nuclear palisading is a morphologic feature that is rarely mentioned in the context of synovial sarcoma (SS). Because palisading is often associated with nerve sheath tumors, and given that malignant peripheral nerve sheath tumor (MPNST) is difficult to distinguish from synovial sarcoma, we suspect that palisading may be used as evidence to support a diagnosis of MPNST. However, in our collective experience, this feature is an underappreciated histological feature of SS.

Design: The aim of this study is to characterize palisading in SS. 155 cases of SS were retrieved from our surgical pathology files from over a 16-year period and reviewed to identify areas of palisading, defined as parallel alignment of neoplastic nuclei in a typical "picket fence" configuration.

Results: Patient ages ranged from 7-84-years old (median 37.5 yrs) with a 1:1.2 F:M ratio (71F:84M). Anatomic locations included lower extremity (64), upper extremity (28), lung (15), chest wall (8), head and neck (9), pelvic girdle (6), heart (3), para-aortic region (1), kidney (4), retroperitoneum (1) and omentum (1). Tumors ranged from 0.3-36 cm (median 5 cm). 129 cases had monophasic and 26 had biphasic histology. Palisading was identified in 7 cases (4.5%) and involved the following anatomic sites: foot (2) buttock (1), hip (1), inguinal region (1), lung (1), and pleura (1). One of 7 cases was biphasic. Palisading was seen in 1% to 25% of the entire tumor area (median 5%) and was associated with excessive collagen deposition. Four of the 7 SS with palisading were tested for *SYT* gene rearrangement by FISH (2 positive; 2 negative).

Conclusions: Palisading is an uncommon finding in SS, present in only 4.5% of the cases in our series. Because it is not usually considered a feature of SS, its presence could cause diagnostic confusion with other tumors, especially MPNST. Awareness of this morphologic variation is important to avoid diagnostic confusion.

78 Detection of MYC Gene Amplification in Secondary Cutaneous Angiosarcomas By Fully Automated Dual Color Silver in Situ Hybridization Method

Kent Newsom, Karen Fritchie, John Reith, Elaine Dooley, Wonwoo Shon. University of Florida, Gainesville, FL; Mayo Clinic, Rochester, MN.

Background: *MYC* gene amplification and protein overexpression have been previously documented in secondary angiosarcomas (AS) and a small subset of primary AS. Both immunohistochemistry (IHC) and fluorescence *in situ* hybridization (FISH) analysis for *MYC* have been shown to be helpful in evaluating radiation-induced cutaneous vascular proliferations. However, FISH assay is labor intensive and cannot be stored for long term review, and anti-*MYC* IHC may lead to false positive/negative results. Relatively recently, a fully automated dual color silver *in situ* hybridization (DISH) has

been developed to overcome the practical limitations of FISH and IHC. In this study, we evaluate the diagnostic utility of this novel assay to distinguish secondary AS from other cutaneous vascular proliferations.

Design: Formalin-fixed, paraffin-embedded blocks from 12 secondary AS, 5 atypical vascular lesions (AVL), 3 primary AS, 2 chronic lymphedema, 2 angiomatosis/capillary hemangioma, and 1 congenital vascular malformation were retrieved from our surgical pathology archives and examined by DISH, using a commercially available probe. Appropriate controls were employed.

Results: 11/12 secondary AS showed *MYC* gene amplification (10 cases with > 8 *MYC*/CHR8 ratio and 1 case with ≥ 2 *MYC*/CHR8 ratio). Polysomy of chromosome 8 was present in one secondary AS (3 to 5 copies of *MYC* and CHR8). All cases of AVL, primary AS, chronic lymphedema, angiomatosis/hemangioma, and vascular malformation did not demonstrate *MYC* gene amplification or chromosomal aberration.

Conclusions: Based on our results, the determination of the *MYC* gene status using this fully automated DISH assay is a reliable technique and has many advantages. DISH could be a reasonable alternative to IHC and FISH in distinguishing secondary AS from AVL and other cutaneous vascular proliferations.

79 Diagnostic Utility of TGFBI To Distinguish Chondrosarcoma From Enchondroma

Hany Osman, Howard Wu, Shaoyong Chen. Indiana University School of Medicine, Indianapolis, IN.

Background: Low grade chondrosarcoma (CHS) and enchondroma pose a significant diagnostic challenge due to overlapping morphological features. To this date, there have not been reliable markers reported to distinguish chondrosarcoma from other cartilaginous tumors. Liquid chromatography - tandem mass spectrometry (LC-MS/MS) was carried out to identify possible diagnostic markers. In the present study, we evaluate the utility of TGFBI immunostaining in distinguishing CHS (grade I and II) from enchondroma.

Design: Protein extracts from formalin-fixed paraffin-embedded tissue blocks of low grade chondrosarcoma (5 cases) and enchondroma (5 cases) were analyzed using LC-MS/MS, and TGFBI was identified as a potential candidate marker for CHS. TGFBI was validated by studying its expression in 31 CHS (25 grade I and 6 grade II) and 36 enchondromas immunohistochemically. Only extracellular staining within the tumor matrix was considered positive. The immunostaining of TGFBI was scored according to percentage of staining in the whole tumor area (0, <5%; 1+, 5-25%; 2+, 26-50%; 3+, 51-100%) and intensity (weak, moderate, or strong).

Results: Among the 31 chondrosarcoma cases, 13 cases (9 grade I and 4 grade II) were positive for TGFBI (3+ in 6 cases, 2+ in 2 cases, 1+ in 5 cases), while only 4 out of the 36 enchondromas were positive (2+ in 1 cases, 1+ in 3 cases). Retrospective review of the H&E slides of 4 enchondroma cases with positive TGFBI staining showed one case displayed morphological features consistent with CHS. Majority of the positive cases showed strong intensity of staining.

Conclusions: TGFBI, a secreted extracellular matrix protein (ECM), is found increased in various tumors and can promote tumor metastasis. Immunostaining for TGFBI expression has a high specificity (89%) and moderate sensitivity (42%) for CHS and can be useful in differentiating chondrosarcoma from enchondroma. The impact of TGFBI on prognosis is yet to be studied.

80 Comprehensive Genomic Profiling of Bone Chordomas Reveals High Frequency of mTOR Pathway Alterations and Potential New Routes To Targeted Therapies

Janne Rand, Kai Wang, Christine Sheehan, Tipu Nazeer, Siraj Ali, Julia Elvin, Roman Yelensky, Doron Lipson, Juliann Chmielecki, Vincent Miller, Philip Stephens, Jeffrey Ross. Albany Medical College, Albany, NY; Foundation Medicine Inc, Cambridge, MA.

Background: Bone chordomas are rare slow-growing malignant bone tumors arising from fetal notochord, usually within vertebral bodies. Chordomas represent 1% of primary malignant bone tumors. Thirty-seven % of chordomas metastasize to other organs and 5% undergo dedifferentiation which may be present at the time of diagnosis. Aggressive surgery is generally needed to treat chordoma. The mean survival is approximately 7 years. We queried whether bone chordomas featured clinically relevant genomic alterations that could lead to targeted therapies for patients with either unresectable primary tumors or metastatic disease.

Design: DNA was extracted from 40 microns of FFPE sections from 38 samples of clinically advanced chordomas. Comprehensive genomic profiling was performed on hybridization-captured, adaptor ligation based libraries to a mean coverage depth of 618X for 3,230 exons of 182 cancer-related genes plus 37 introns from 14 genes frequently rearranged in cancer. The results were evaluated for all classes of genomic alterations (GA). Clinically relevant genomic alterations were defined as GA linked to drugs on the market or under evaluation in mechanism driven clinical trials.

Results: There were 18 male and 21 female patients with a mean age of 52.6. Three (7.9%) showed chondroid differentiation, two (5.3%) were dedifferentiated, thirty-three (86.8%) showed conventional histology. There were eight (21%) stage III, and thirty (79%) stage IV tumors at the time profiling. A total of 61 GA were identified (1.6 GA/chordoma) in 35 genes. Twenty (53%) of the chordomas featured at least 1 clinically relevant alteration. The most frequent altered genes were PI3K/mTOR pathway. Nine (24%) of the samples harbored alterations in this pathway, including *PTEN* (10.5%), *AKT3* (2.6%), *MTOR* (2.6%), *PIK3CA* (2.6%), *TSC2* (2.6%), and *STK11* (2.6%). Other clinically meaningful alterations were identified including alterations in *CCND1*, *CDK4*, *ERBB3*, *IGF1R* and *PTCH1*.

Conclusions: Bone chordomas are rare malignant neoplasms that require aggressive surgery for treatment. For patients with clinically advanced disease genomic profiling can uncover potential targets for systemic therapy. The resulting wide array of potential

targeted therapies both on the market and in clinical trials mandates that comprehensive diagnostic approaches be used to maximize treatment options for patients with this aggressive form of malignancy.

81 Cytogenomic Microarray Analysis of Dedifferentiated Liposarcoma: A Molecular Study in Search of Potential Biomarkers

Robert Ricciotti, George Jour, Benjamin Hoch, Yajuan Liu. University of Washington, Seattle, WA; Memorial Sloan Kettering Cancer Center, New York, NY.

Background: Molecular abnormalities underlying the pathogenesis and behavior of dedifferentiated liposarcoma (DDLs) are not well understood. Tumor location and FNCLCC grade of DDLs have been shown to have prognostic significance. *CDK4* amplification and copy number alterations (CNA) of other specific chromosomal loci have been proposed as having prognostic value; however, the significance of these and other potential biomarkers has not been fully elucidated.

Design: Thirty DDLs were retrieved and reviewed by a bone and soft tissue pathologist. Clinical information was obtained through electronic record review. DNA from FFPE tumor tissue was extracted and analyzed by cytogenomic microarray analysis. Data analysis was performed using Cytogenomics 2.7 to identify CNAs and level of amplification for *CDK4* and *MDM2*.

Results: CNAs in 6 regions of interest were compared with DDLs grade and disease status (mean follow-up 29 months). All cases with 19q13.11 loss (n=4) showed disease progression (DP) defined as local recurrence, metastasis, or death, and all with 19q13.11 gain (n=3) had no evidence of disease (NED) at last follow-up (Fisher's exact test $p=0.0286$). Three cases with 19q13.11 loss were grade 3 and all with gain were grade 1-2 tumors ($p=0.1429$). Five of 6 cases with CNAs of 3q29 (4 loss, 1 gain) had DP at last follow-up, including one with distant metastasis. This difference did not reach statistical significance. CNAs of 3q29 did not correlate with grade. Loss of 9p22.1 (n=11) and/or 11q24.2 (n=11) did not correlate with disease progression or grade. *CDK4* was amplified in 29 cases (range 10 to 72 copies). Level of *CDK4* amplification tended to be higher in cases with DP. All cases with very high levels of amplification (>39 copies, n=5), showed DP, but this trend did not achieve statistical significance (Wilcoxon rank-sum test $p=0.26$). *MDM2* amplification did not correlate with grade or disease progression.

Conclusions: The finding of 19q13.11 gain has not been previously described in DDLs. 19q13.11 loss and gain significantly correlate with worse and better outcome, respectively, but not with grade. In contrast to what has been previously reported CNAs at 3q29 may be more common in cases with DP, including metastasis, and 9p22.1 abnormality did not correlate with DP. High levels of *CDK4* amplification tend to be found in DDLs with DP as previously reported. Analysis of larger numbers of cases and identification of candidate genes are required to further define molecular biomarkers in DDLs.

82 TFE3 Expression and Rearrangement in Epithelioid Vascular Tumors

Cleofe Romagosa, Danielle de Jong, Marieke de Graaff, Karoly Szuhai, Piero Picci, Paolo Dei tos, Soeren Daugaard, Nick Athanasou, Enrique de Alava, Judith Bovee. Hospital Universitari Vall d'Hebrón, Barcelona, Spain; Leiden University Medical Center (LUMC), Leiden, Netherlands; Istituto Ortopedico Rizzoli, Bologna, Italy; General Hospital of Treviso, Treviso, Italy; Rigshospitalet, University of Copenhagen, Copenhagen, Denmark; Nuffield Orthopaedic Centre - Oxford University, Oxford, United Kingdom; Hospital Universitario Virgen del Rocío, Sevilla, Spain.

Background: The group of epithelioid vascular tumors includes a wide range of lesions. Nowadays the prognosis is mainly defined by the histological diagnosis. The morphological interpretation sometimes can be challenging due to overlapping features, especially between epithelioid haemangiomas (EH) and epithelioid haemangiioendotheliomas (EHE). Recently, translocations have been reported to occur in classic EHE (WWTR1-CAMTA1), EHE with vasoformative architecture and a better prognosis (YAP1-TFE3), and EH with atypical features (ZFP36-FOSB), but not yet in conventional EH. These translocations may provide tools to differentiate between these two types of tumors with different therapeutic and prognostic implications. The aim of this study was to evaluate the use of TFE3 immunohistochemistry and FISH in the differential diagnosis of epithelioid vascular lesions.

Design: TFE3 overexpression was evaluated by immunohistochemistry in 21 EH and 12 EHE from the archives of 6 bone and soft tissue tumour referral centers. In the subgroup of tumors with high TFE3 expression (4 EH + 2 EHE), FISH for TFE3 was performed.

Results: Seven out of 21 EH (33%) and five out of 12 EHE (41%) demonstrated strong positive TFE3 nuclear immunostaining. There were no clear histological differences between TFE3+ and TFE3- EH or EHE. Only 2 out of 4 TFE3+ EH and none out of 2 TFE3+ EHE showed rearrangement of the TFE3 gene by FISH. In retrospect, the 2 cases diagnosed as EH carrying TFE3 rearrangement demonstrated some hybrid features between EH and EHE. Both patients were free of disease with a follow up of 13 and 36 months respectively.

Conclusions: TFE3 positive immunostaining is not indicative of the presence of a TFE3 rearrangement in epithelioid vascular lesions. We here report on the occurrence of TFE3 rearrangement in 2 lesions previously diagnosed as EH, that had in retrospect some areas reminiscent of EHE, supporting previous claims that TFE3 rearranged epithelioid vascular tumors define a separate entity with a better outcome as compared to classic EHE.

83 Primary Synovial Sarcoma (SS) of the Digestive System: A Molecular and Clinicopathological Study of Fifteen Cases

Salvatore Romeo, Sabrina Rossi, Fabio Canal, Marta Sbaraglia, Licia Lawrino, Guido Mazzoleni, Maria Montesco, Laura Valori, Marta Campo Dell'Orto, Andrea Gianatti, Alexander Lazar, Angelo Dei Tos. Treviso General Hospital, Treviso, Italy; Bolzano Regional Hospital, Bolzano, Italy; Istituto Oncologico Veneto, Padova, Italy; Ospedali Riuniti di Bergamo, Bergamo, Italy; University of Texas MD Anderson Cancer Center, Houston, TX.

Background: Recently a few cases of synovial sarcoma (SS) of the abdominal viscera have been reported, raising awareness about the potential for confusion between this entity and KIT-negative gastrointestinal stromal tumors (GIST). We report the clinicopathological, immunophenotypical and molecular features of fifteen more SS occurring in the stomach (8 cases), epigastric region (one case), small intestine (one case), large intestine (three cases), involving both the terminal ileum and the caecum (one case) and liver (one case).

Design: Patients' clinical records were retrieved. Haematoxylin Eosin slides were reviewed and immunostains for SMA, DESMIN, CD34, CD117, S100, EMA, CK AE1/3, TLE1, CD56, CD99, BCL2, DOG1 were performed. Rearrangement of *SS18* gene region was screened in all cases: by conventional karyotype in one case and by either interphase FISH or Q-PCR or both in the remaining cases.

Results: Ten patients were male and five female, with an age range of 17-61 years (median 44). Tumour size ranged from 2 to 15 cm (median 8). Mitoses per 10 HPF ranged from 4 to 27 (median 9.5). Eleven tumours were monophasic fibrous SS, one biphasic SS and three poorly differentiated SS. SMA, Desmin, CD34, CD117 and S100 were negative in all cases, whereas EMA and/or CK AE1/AE3 were positive in all cases. TLE1, BCL2 and CD56 were positive in all tested cases. DOG1 was positive in one case. *SS18* gene region rearrangement was demonstrated in all cases. A fusion transcript was amplified in eight cases: either *sy-t-ssx1* or *sy-t-ssx2* respectively in four cases each. Follow-up information was available for 11 patients: range from 6 to 185 months (47 median).

Conclusions: SS is increasingly recognized at visceral sites. Molecular analyses play a key role when dealing with usual histotypes in unusual sites. Correct diagnosis is crucial for appropriate therapy.

84 Predictors of Recurrence in Giant Cell Tumor of Bone

Lauren Rosen, Diana Murro, Paolo Gattuso. Rush University Medical Center, Chicago, IL.

Background: Giant Cell Tumor of Bone (GCTB) is a benign but potentially aggressive tumor with a high rate of local recurrence and a low risk of distant metastases. Radiographic and histologic grading systems do not accurately predict clinical course. Our goal is to determine if a group of immunohistochemical (IHC) markers can serve as predictors of clinically aggressive behavior.

Design: Institutional surgical pathology records were searched from January 1993-June 2014 for cases of GCTB. Primary cases were stratified into recurrent (PR) and non-recurrent (PNR) groups. Clinical data including age, sex, tumor site, treatment and time to recurrence was collected. For cases in which paraffin blocks were available, IHC stains for Ki67, p63, p53, cyclin-D1, and c-myc were performed. Slides were reviewed blindly and independently by 2 pathologists. Ki67 was scored as low-intermediate (0-20%), and high ($\geq 21\%$). Of the remaining stains, $\geq 5\%$ tumor cell staining was considered positive, and intensity was scored as low (1-2+) or high (3+). Pearson chi-squared test was used for data analysis.

Results: 85 cases of GCTB were identified, including 22(25%) with recurrence and 3(4%) with lung metastases. Patients had a mean age of 37 years at diagnosis, with a male to female ratio of 1.4:1. Tumors were most commonly located in the distal femur and proximal tibia (42% of cases). Primary tumors were treated either by curettage (71%) or resection (29%). Among the recurrent cases, 15 had 1 recurrence, 6 had 2 recurrences, and 1 had 4. Mean time to first recurrence was 17 months. Recurrences occurred in 17/59 (28%) of patients treated with curettage and 5/30 (20%) of patients treated with resection. Paraffin blocks were available for staining in 9 PNR and 18 PR tumors. Cyclin D1 was preferentially expressed in the nuclei of giant cells, while the other stains were expressed predominately by mononuclear cells. There was no significant difference between clinical variables among the PR and PNR groups. The proportion of patients older than 45 was higher in the PNR group ($p=0.067$). P63 staining intensity was significantly higher in PR group ($p=0.044$).

Conclusions: Of the IHC stains studied, only p63 staining intensity was found to be of value in distinguishing recurrent from non-recurrent GCTB ($p=0.044$). Patients older than 45 are less likely to experience recurrence than younger patients ($p=0.067$). Interestingly, type of surgical procedure did not correlate with risk of recurrence. Expression of Cyclin D1 by giant cells may reflect the protein's role in giant cell formation.

85 Expression of the Neuroepithelial Marker INSM1 in Ewing Sarcoma and Other Small Round Cell Sarcomas

Jason Rosenbaum, Ali Chaudhri, Rebecca Baus, Ricardo Lloyd, Darya Buehler. University of Wisconsin Hospital and Clinics, Madison, WI.

Background: The significance of neural differentiation in Ewing sarcoma remains uncertain. INSM1 is a transcriptional repressor implicated in terminal differentiation of neural and neuroepithelial cells, and has emerged as a novel immunohistochemical (IHC) marker for neuroepithelial and neuroendocrine tumors. Expression of INSM1 in Ewing sarcoma (EWS) has not been investigated. To better understand the possible role of neural differentiation in this tumor, we tested a panel of genetically confirmed cases of EWS, with and without microscopic evidence of neural phenotype, and other small round cell sarcomas for expression of INSM1 by IHC.

Design: Cases included 23 EWS (14 bone, 9 extraskelatal), 3 desmoplastic small round cell tumors (DSRCTs), 7 alveolar rhabdomyosarcomas (ARMS), 4 embryonal rhabdomyosarcomas (ERMS), 10 poorly-differentiated synovial sarcomas (SS), 1 mesenchymal chondrosarcoma (MCS) and 11 medulloblastomas/central primitive neuroectodermal tumors (cPNETs). After confirmation of diagnosis, whole sections were analyzed for INSM1 expression by IHC. Nuclear staining was scored based on pattern as negative (<5%), focal (5-25%) or diffuse (>25%) and intensity from 1(+) to 3(+). Morphologic evidence of neural differentiation such as Homer Wright rosettes was noted. Genetic, clinical and outcome data were collected.

Results: All genetically confirmed Ewing sarcomas were negative for INSM1 expression, irrespective of the presence of Homer Wright rosettes (0/23). In contrast, INSM1 staining was strongly, diffusely positive in 10/11 (91%) of medulloblastomas/cPNETs. INSM1 expression was also noted in 3/7 ARMS (2 focal, 1 diffuse) and 1/3 DSRCT (focal). All other tumors including ERMS, SS, and MCS were negative for this marker.

Conclusions: INSM1 is not expressed in EWS, irrespective of microscopic evidence of neural phenotype, possibly because EWS cells do not reach terminal neural differentiation regulated by INSM1. INSM1 is highly expressed in medulloblastomas/cPNETs but its expression is rare in other translocation-associated round cell sarcomas. INSM1 expression in ARMS merits further investigation.

86 Impact of Mutation Status and Tumor Location on the Transcriptional Profile of Primary Sporadic Gastrointestinal Stromal Tumor: A RNAseq Approach on Archival FFPE Material

Sabrina Rossi, Daniela Gasparotto, Maurizio Polano, Elena Boscato, Luisa Toffolatti, Erica Lorenzetto, Francesco Sirocco, Marta Sbaraglia, Marta Campo Dell'Orto, Alessandra Mandolesi, Aurelio Sonzogni, Salvatore Romeo, Roberta Maestro, Angelo Dei Tos. General Hospital, Treviso, Italy; CRO National Cancer Institute, Aviano, Italy; University of Marche, Ancona, Italy; General Hospital, Bergamo, Italy.

Background: Gastrointestinal stromal tumor (GIST) is the most common sarcoma of the gastrointestinal tract. Sporadic GIST are characterized by activating mutations in the tyrosine kinase receptor *KIT* (~80%) or *PDGFRA* (~10%). The remaining fraction (10-15%), formerly defined as "wild-type" GIST, includes cases carrying either mutation in *BRAF* (~1%) or inactivation of the succinate dehydrogenase (SDH) pathway (~6%) and cases in which the underlined alteration is currently undetermined ("undetermined" GIST). Overall, the so called "wild-type" GIST, although heterogeneous, display a clinical course significantly different from *KIT*/*PDGFRA*-mutated cases, suggesting that the mutation status likely impinges on different signaling pathways.

Design: To shed light on this issue, we performed a RNAseq analysis on a preliminary series of 31 GIST cases representative of the different molecular patterns (18 *KIT*, 5 *PDGFRA*, 3 *BRAF*, 1 SDHB-deficient, 4 "undetermined GIST") and locations (16 stomach, 13 small intestine, 1 rectum, 1 esophagus). RNA was extracted from both formalin-fixed paraffin embedded (FFPE) (15) and frozen (17) samples. Libraries were constructed with Truseq Kit and paired-end sequenced on an HiSeq platform (Illumina) to obtain 30-40 millions aligned reads/sample. GATK workflow was used to analyze RNA-seq data and Cufflinks was used for differential expression analyses.

Results: FFPE and Frozen samples displayed a correlation greater than 0.95 in their RNAseq transcriptional profile. Unsupervised clustering highlighted a differential pattern for "undetermined" and *BRAF*-mutated GIST on one hand and *KIT*/*PDGFRA*-mutated cases on the other hand in both Frozen and FFPE specimens. The only SDH-deficient case included in the series clustered together with the "undetermined" and *BRAF*-mutated GIST. When the series was analyzed as a whole, unsupervised clustering identified two major groups distinct by location: small intestine versus stomach.

Conclusions: Our study indicates that FFPE and Frozen GIST samples provide similar results in RNAseq analyses, supporting the use of archival specimens for next generation sequencing studies. Our data, although preliminary, support the notion that GIST devoid of *KIT*/*PDGFRA* mutations display distinct molecular features and that tumor location affects GIST gene expression profiling, in line with previous studies.

87 The Wnt Receptor ROR2 Is a Novel Prognostic Marker and Potential Therapeutic Target in Dedifferentiated Liposarcoma

Navid Sadri, M Celeste Simon. Memorial Sloan Kettering Cancer Center, New York, NY; University of Pennsylvania School of Medicine, Philadelphia, PA.

Background: Genetically defined by chromosome 12q13-15 amplification, well-differentiated liposarcoma (WD-LPS) and dedifferentiated liposarcoma (DD-LPS) constitute a spectrum of disease, from an indolent low-grade, lipogenic tumor (WD-LPS) to a highly aggressive non-lipogenic (DD-LPS) tumor with metastatic potential. The molecular and cellular events underlying dedifferentiation are poorly understood. Wnt signaling is suggested to play an important role in both adipogenesis and sarcoma pathobiology.

Design: To determine the role of Wnt signaling in liposarcoma dedifferentiation, we compared the expression of Wnt receptors in WD-LPS and DD-LPS samples using available human datasets, which revealed an increase in ROR2 in DD-LPS. To explore the requirement of ROR2 in liposarcoma pathogenesis, we performed knockdown experiments using two independent shRNAs in DD-LPS cell lines. We examined the effects of ROR2 expression *in vivo* using a xenotransplantation model of DD-LPS. To identify downstream targets of ROR2 we used correlation expression studies using publicly available DD-LPS datasets and confirmed predicted correlations by qRT-PCR and western blot analysis.

Results: The expression of ROR2 strongly correlates with worse overall survival in patients with WD/DD-LPS. Silencing of ROR2 expression in WD-LPS and DD-LPS cell lines significantly inhibits tumor growth, induces PPAR γ expression (master regulator

of adipogenesis), and promotes adipogenic differentiation. Mechanistically, we propose that ROR2 expression inhibits adipogenic differentiation through repression of PPAR γ by modulating upstream AP-1 transcription factors, FosL2 and c-Fos.

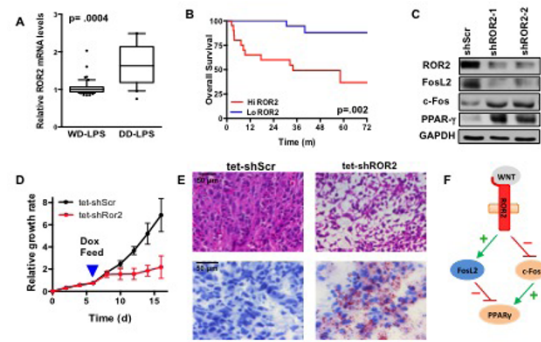


Figure 1. A. Increased ROR2 mRNA expression in human DD-LPS as compared to WD-LPS samples. B. ROR2 expression correlates with worse overall survival in patients with WD/DD-LPS. C. Knockdown of ROR2 results in reduction of FosL2 expression and increase in c-Fos and PPAR γ . D. Doxycycline (Dox) inducible knockdown of ROR2 expression in xenografted DD-LPS tumors results in significant tumor inhibition and E, adipogenic differentiation (H.E. and oil red O analysis). F. Proposed mechanism of action for ROR2 in DD-LPS

Conclusions: The up-regulation of ROR2 has previously been reported in osteosarcoma, leiomyosarcoma and GIST. Here we propose upregulation of ROR2 in DD-LPS represses PPAR γ expression and adipogenic differentiation through the differential regulation of AP-1 factors. ROR2 may serve as a prognostic and potential therapeutic target in DD-LPS.

88 Clear Cell Chondrosarcomas: A Clinicopathologic, Radiographic, and Immunohistochemical Analysis of 30 Cases

Alaa Salim, David Stockman. University of Texas MD Anderson Cancer Center, Houston, TX; University of South Carolina School of Medicine, Greenville, SC.

Background: Clear cell chondrosarcoma (CCC) is a rare, distinctive variant of chondrosarcoma, typically occurring in middle-aged adults. It possesses an indolent clinical course with a high rate of local recurrence, but infrequent metastases.

Design: Tumors with diagnoses of CCC were retrieved from the institutional archives from 1991 to 2014. The diagnosis of CCC was confirmed by histologic review. Tumors were further assessed by immunohistochemistry and clinical and radiological studies were reviewed. A control group of 40 chondrosarcomas were selected for comparison.

Results: CCC (n=30) occurred in 21M/9F (median, 45yrs, range 24-74yrs) and varied in size from 2.5-24.5cm (median, 7.8cm). Tumors involved the femur (n=13), chest wall (n=6), pelvic girdle (n=4), vertebrae (n=3), humerus (n=2), tibia (n=1), and fibula (n=1). Radiographic information and imaging was available in all cases. Of cases occurring in long bones, 70% were epiphyseal; 15% located at non-epiphyseal locations; and 15% were unable to be localized due to large tumor size and bone destruction. Tumors were typically circumscribed by a rim of sclerotic bone. Histologically, CCC consisted predominantly of round cells with clear to eosinophilic cytoplasm. Cases additionally possessed areas of metaplastic woven bone (90%), intralesional osteoid deposition (66%), and multinucleated osteoclast giant cells (33%). Cases of CCC expressed S-100 protein (66%), CD99 (66%), and pancytokeratin (50%). Patients often presented with pathologic fracture, localized to regionalized pain, and often of long duration. No patients had metastases at the time of diagnosis. Six patients died of disease after 15 to 201mo (median, 97mo); 7 patients were alive with disease and 13 without evidence of disease (median, 51mo). Metastases developed in 4 patients after periods of up to 64mo. Recurrences occurred in 11 patients. Histologic differences, mitotic activity, and tumor size were not related to CCC behavior or patient survival. Cases of CCC had better overall survival than Grade 2 and 3 chondrosarcoma control groups (p<0.05).

Conclusions: Clear cell chondrosarcoma is rare and can often be misdiagnosed; its range of morphologic, immunophenotypic, and behavioral differences separates it from its radiographic and histologic mimics. When compared to historical controls of conventional chondrosarcoma (Grade 2 and 3), CCC appeared to follow a less aggressive clinical course.

89 Diagnostic Utility of NCOA2 Labeling: A Survey of Bone and Soft Tissue Mesenchymal Neoplasia

Alaa Salim, Khalida Wani, Davis Ingram, Elizabeth Demicco, Alexander Lazar, Wei-lien Wang. University of Texas MD Anderson Cancer Center, Houston, TX; Mount Sinai Medical Center, New York, NY.

Background: *NCOA2* encodes a protein that assists nuclear hormone receptors in transcription activation. Recently, *NCOA2* was discovered to be involved in a recurrent translocation t(8;8)(q13.3;q21.1) in mesenchymal chondrosarcomas (MChs), which results in the fusion of *HEY1* with *NCOA2* and subsequent *NCOA2* overexpression. MChs is a rare malignant biphasic cartilaginous tumor composed of primitive mesenchymal cells and islands of well-differentiated hyaline cartilage, of which either component can be mistaken for other small round cell and cartilaginous tumors, especially on small biopsies. We examined the diagnostic utility of *NCOA2* immunohistochemical study in mesenchymal chondrosarcomas as well as its expression in other bone and soft tissue mesenchymal tumors, some of which may resemble MChs. **Design:** 100 whole and tissue microarray formalin-fixed paraffin-embedded sections were examined consisting of 26 MChs, 10 Ewing sarcoma (ES), 7 synovial sarcoma (SS),

22 solitary fibrous tumors(SFT), 15 leiomyosarcoma(LM), 8 chondrosarcomas(Chs), 8 osteosarcomas(OS), 2 enchondroma(En), 1 myxoid liposarcoma(Mlps) and 1 extraskelatal myxoid chondrosarcoma(EMC). Immunohistochemistry using an anti-NCOA2 antibody (AbCam, 1:200) was performed on 5mm-thick paraffin embedded sections. Labeling was assessed for both degree (weak, moderate, strong) and extent (0; 1+, <5%; 2+, 5-25%; 3+, 26-50%; 4+, 51-75%; 5+, >75%). 2+ nuclear labeling of any extent was considered to be positive.

Results: 24/26 MChs were positive for NCOA2 overexpression, with at least 2+ labeling, most with strong/moderate labeling. Other tumors also positive for NCOA2 included: 8/8 OS (majority 5+, strong), 10/10 SFT (5+, at least moderate), 13/15 LMS (5+, at least moderate), 7/8 Chs (majority 2-3+, moderate), 1/1 EMC, 1/1 MLPs. 6 of 10 ES (most with at least 4+, moderate) and 1/7 SS labeled for NCOA2. None of the En labeled for NCOA2.

Conclusions: NCOA2 nuclear expression is characteristic of mesenchymal chondrosarcoma. However, it is also expressed in other mesenchymal tumors, including mimickers of MChs and could play a role in tumorigenesis of these entities. Thus, molecular testing (on-going) is recommended to differentiate MChs from potential mimics.

90 Symplastic/Pseudoanaplastic Giant Cell Tumor of the Bone

Judy Sarungbam, Narasimhan Agaram, Sinchun Hwang, Chao Lu, John Healey, Meera Hameed. Memorial Sloan Kettering Cancer Center, New York, NY; Rockefeller University, New York, NY.

Background: Giant cell tumor of bone (GCTB) is a locally aggressive benign primary bone tumor comprising of mononuclear cells associated with evenly distributed numerous multinucleated osteoclast-like giant cells. The malignant counterpart of this tumor, primary malignant GCTB is quite rare and is characterized by sarcomatous transformation in a "de novo" GCTB or a secondary recurrent phenomenon from a previous conventional or radiated GCTB. Rarely conventional GCTB shows marked nuclear atypia referred to as symplastic/pseudoanaplastic change, which can mimic sarcomatous transformation. Herein we report a series of 8 cases of GCTB with symplastic /pseudoanaplastic change.

Design: A total of 181 cases of GCTB were identified from the pathology database of a tertiary care cancer center from 1993 to 2011. Eight cases of GCTB with symplastic change were identified and pathology slides of these cases were reviewed. Electronic medical records were reviewed for imaging features and clinical follow-ups. Ki 67 immunohistochemical analysis was performed on all 8 cases of GCTB with symplastic change. Sequencing of *H3F3A* gene is in process on all of the 8 cases.

Results: The 8 cases of GCTB with symplastic change included 6 females and 2 males, median age of 43.9years (range:28 - 64 years). Anatomic locations included distal femur (2), vertebra (3), proximal tibia (1), fibula (1) and ischium (1). Imaging features were concordant with GCTB including eccentrically located, expansile lytic lesions with cortical involvement. Histologic examination showed giant cells distributed in a uniform manner with interspersed mononuclear cells, whose nuclei have similar morphological appearance to the nuclei of giant cells. In all cases, mononuclear cells showed scattered foci of marked nuclear pleomorphism, with enlarged hyperchromatic nuclei, smudged nuclear chromatin and nuclear pseudoinclusions. Mitotic figures were not seen in these cells. While overall Ki-67 proliferative index ranged from 0-10%, these atypical and pleomorphic cells did not label with Ki-67. One patient (ischium) had radiation therapy and denosumab treatment and showed treatment associated exuberant new bone formation in curetted material. Clinical follow-up ranged from 10 to 196 months (median:70 months). Local recurrence was seen in 4 cases (50%).

Conclusions: GCTB with symplastic/pseudoanaplastic change is an uncommon variant of conventional GCTB which can mimic sarcomatous transformation. The relative absence of Ki-67 staining in these atypical cells can be useful in distinguishing it from malignant GCTB.

91 Malignant Peripheral Nerve Sheath Tumor (MPNST) Arising in Diffuse-Type Neurofibroma

Inga-Marie Schaefer, Christopher Fletcher. Brigham & Women's Hospital, Boston, MA.

Background: Diffuse-type neurofibroma is an uncommon variant of neurofibroma, associated with neurofibromatosis type 1 (NF-1) in ~60% of cases. Typically presenting in young adults as ill-defined plaque-like dermal/subcutaneous thickening, most cases are located on the trunk or head and neck region. Malignant transformation is extremely rare.

Design: Eight cases of MPNST arising in diffuse-type neurofibroma were identified in consult files between 1994 and 2014. H&E and immunohistochemical stains were examined. Clinical and follow-up information was obtained from referring pathologists and clinicians.

Results: Five patients were male and 3 female, aged between 31 and 59 years (median, 47.5 years). The diffuse-type neurofibromas were ill-defined subcutaneous lesions with diffuse growth pattern and infiltration between adnexal structures and adipose tissue, with tumor size ranging from 3.6 to 45 cm (median, 15 cm). All contained Meissner corpuscles. Four patients (#1-4) had a clinical history of NF-1, and one patient (#5) had Klippel-Trénaunay-Weber syndrome. 6/8 tumors arose on the trunk, and one tumor each on the leg and scalp, respectively. Areas of increased cellularity, nuclear atypia, increased nuclear-cytoplasmic ratio, and scattered mitoses (range, 1-63/50 HPF) were observed in all tumors, indicating transition to MPNST which was classified as low grade in 5 cases, intermediate to high grade in one case, and high grade in 2 cases, of which one showed heterologous angiosarcomatous differentiation. The neurofibroma components expressed S-100 quite strongly, whereas the areas of MPNST showed expression levels ranging from weak to moderate. Staining with neurofilament protein revealed scattered axons in one case (#6). Follow-up data, available for all cases (median, 80.5 months), revealed that one patient (#3) developed local recurrence after 9 months, treated with

re-excision. One patient (#5) had pulmonary metastases at initial diagnosis and died one month after tumor resection. All other patients were alive and without evidence of disease after 15-145 months (median, 83 months).

Conclusions: Diffuse-type neurofibroma may show transformation to MPNST in very rare instances, highlighted by focal hypercellularity, nuclear atypia, and mitoses. It is important to be aware of possible malignant transformation in diffuse-type neurofibroma, requiring thorough sampling of resection specimens and long-term clinical-follow-up of patients with unexcised lesions.

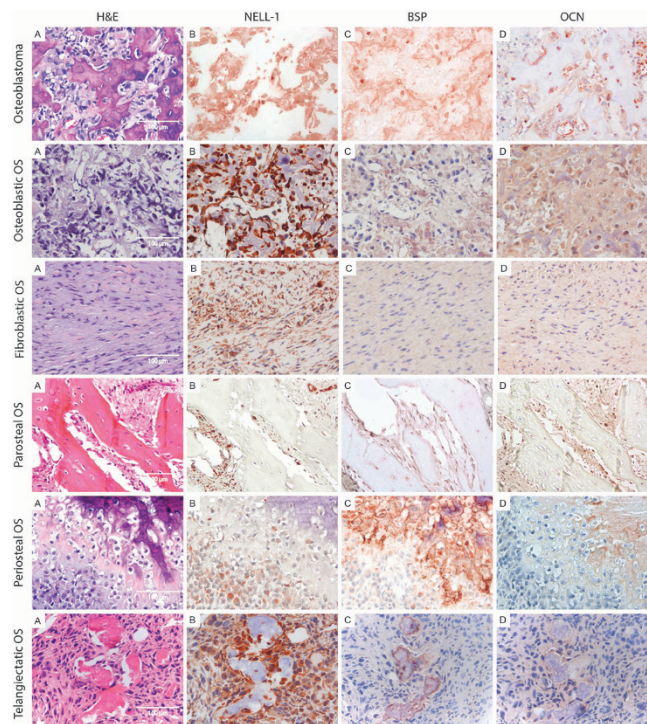
92 The Osteoinductive Protein NELL-1 Is Associated With Wnt/B-Catenin Signaling and Osteogenic Differentiation in Benign But Not Malignant Bone Tumors

Jia Shen, Gregory LaChaud, Swati Shrestha, Xinli Zhang, Greg Asatrian, Chia Soo, Kang Ting, Sarah Dry, Aaron James. University of California, Los Angeles, CA.

Background: NELL-1 is an osteoinductive protein first discovered in cranial sutures. Since that time, NELL-1 has been found to induce significant ossification in both small and large animal models of bone repair. With this, new molecular data suggests that NELL-1 induces bone formation by binding to IntegrinB1 and activating Wnt/B-catenin signaling. Despite this, expression of NELL-1 in benign and malignant bone tumors is entirely unknown.

Design: Human specimens were obtained from the UCLA pathology database (N=5-10 specimens per diagnosis). Tumor types included osteoid osteoma, osteoblastoma, osteosarcoma (OS) (osteoblastic, fibroblastic, and chondroblastic types), parosteal OS, periosteal OS, and telangiectatic OS. Demographics, history of chemotherapy and radiation, and clinical course were recorded. NELL-1 expression was documented via antibodies to either the C- or N-terminus. Semi-quantitative assessment of NELL-1 immunohistochemical staining was performed, documenting the presence, intensity, and distribution of immunostaining. Spatial correlation with osteogenic markers (Bone Sialoprotein, BSP; Osteocalcin, OCN) and Wnt signaling activity was performed (Axin2).

Results: NELL-1 expression was present in all bone tumors. Among benign bone tumors, strong and diffuse staining was observed across all tumors. This diffuse expression of NELL-1 correlated with osteogenic marker expression (OCN, BSP) and diffuse Wnt signaling activity (Axin2). In contrast, a relative reduction in NELL-1 staining and increased variability between tumor specimens was observed within OS. Surprisingly, among OS subtypes, fibroblastic osteosarcoma demonstrated the most reliable expression of NELL-1. Among OS, NELL-1 expression did not correlate with markers of osteogenesis (OCN, BSP) nor Wnt signaling activity.



Conclusions: Reliable and diffuse NELL-1 expression is a characteristic feature of osteoid osteoma and osteoblastoma. In contrast, NELL-1 expression is reduced in intensity and distribution in OS. NELL-1 expression in benign bone tumors is associated with osteogenic marker expression and Wnt signaling activity. Future studies will further examine the diagnostic, prognostic and basic biologic importance of NELL-1 in bone tumors.

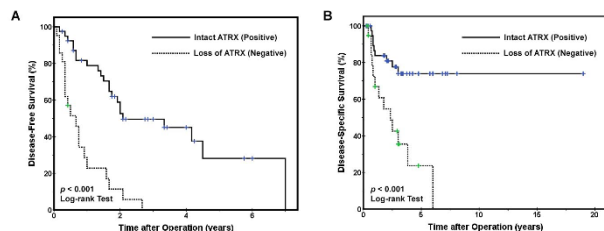
93 ATRX Loss Is a Poor Prognostic Factor in Extruterine Leiomyosarcomas

Aatur Singh, Rohit Bhargava, Miroslawa W Jones, Kristi Cressman, Raja Seethala. University of Pittsburgh Medical Center, Pittsburgh, PA.

Background: Leiomyosarcomas (LMS) are rare malignant tumors of smooth muscle origin and associated with a poor long-term prognosis. However, the clinical course of these tumors is not entirely predictable using conventional prognostic parameters, which do not take into account the biopsy of these neoplasms. Recent studies have identified activation of alternative lengthening of telomeres (ALT) in over 50% of LMS. ALT is a telomere maintenance mechanism and results in immortal growth of tumor cells. In addition, the ALT phenotype is associated with loss of ATRX protein expression, but the status of ATRX has not been fully characterized in LMS. Thus, immunohistochemical staining for ATRX was performed on a large cohort of LMS and correlated with various clinicopathologic factors.

Design: 108 surgically resected LMS (63 extrauterine and 45 uterine LMS) were immunolabeled for ATRX. Cases were scored as ATRX-negative in the absence of nuclear staining within neoplastic cells, while retained within surrounding non-neoplastic parenchyma. Results were correlated with patient demographics, pathologic features, disease-free survival (DFS) and disease-specific survival (DSS). The follow-up period ranged from 0.3 to 19 years (mean, 3.9 yrs; median, 3 yrs).

Results: ATRX loss was identified in 42 of 108 (39%) LMS with 5 cases demonstrating intratumoral heterogeneity. No significant differences between ATRX status and patient sex ($p = 0.50$), mean tumor size ($p = 0.46$), uterine vs extrauterine location ($p = 0.23$), tumor differentiation ($p = 0.06$), FNCLCC grade ($p = 0.39$) and vascular invasion ($p = 0.18$) were observed. However, ATRX-negative extrauterine LMS did correlate with shorter mean DFS (0.8 vs 3.6 yrs, $p < 0.001$) and shorter mean DSS (2.8 vs 14.8 yrs, $p < 0.001$); while, among uterine LMS, no differences in mean DFS or DSS were seen with regards to ATRX status ($p > 0.05$).



Conclusions: Loss of ATRX is a poor prognostic factor and associated with disease recurrence and decreased survival in patients with extrauterine LMS after surgical resection. In contrast, ATRX status seems to be irrelevant in uterine LMS, suggesting biologic differences between uterine and extrauterine LMS.

94 Evaluation of ETV1 Expression in Gastrointestinal Stromal Tumors (GIST) By Chromogenic RNA In Situ Hybridization

Steven Smith, Nallasivam Palanisamy, Jonathan McHugh, David Lucas, Brian Rubin, Rajiv Patel. Virginia Commonwealth University Health System, Richmond, VA; University of Michigan, Ann Arbor, MI; Cleveland Clinic, Cleveland, OH.

Background: Several lines of evidence implicate a key role for the ETS-family transcription factor, ETV1, in GIST, with computational studies implicating ETV1-dependent transcription as central to GIST molecular pathogenesis. However, due to the marked sequence homology between ETS family members and lack of specific antibodies for immunohistochemistry, evaluation of ETV1 expression *in situ* in archival tissues has proved very challenging, limiting interpretation (let alone, diagnostic utility) of ETV1 immunostains.

Design: A tissue microarray of 49 GISTs from varying primary sites in the gastrointestinal tract was stained by chromogenic RNA in situ hybridization (ISH) for ETV1. ETV1 expression was evaluated by intensity and proportion (0-4+) using a RNA ISH scoring system, recently validated in prostate cancer. Distributions of scores were compared with clinicopathologic and morphologic parameters by non-parametric correlation and chi square tests.

Results: All GISTs evaluated showed at least focal, low intensity expression of ETV1, including 29% with 1+, 50% 2+, and 21% 3+ expression; higher intensities such as seen in prostatic adenocarcinomas harboring ETV1 translocation were not observed. ETV1 ISH scores were not significantly associated with GIST tumor size, risk stratum, mutational status/type, or immunohistochemical expression of KIT. ETV1 ISH scores trended toward lesser intensity of expression in gastric versus non-gastric GISTs ($p=0.055$), reflective of the significantly lesser intensity of ETV1 ISH scores in epithelioid GISTs versus GISTs with spindle cytomorphology ($p=0.001$).

Conclusions: We provide the first specific demonstration of ETV1 expression in archival tissues of GISTs through use of chromogenic ISH. These findings establish a new, specific reagent for the study of ETV1 expression patterns *in situ* and identify an intriguing pattern of differential expression intensity between epithelioid and spindle cell GISTs.

95 Molecular Analysis of the Ras-Raf-MAPK Pathway in Langerhans Cell Histiocytosis

David Solomon, Nancy Joseph, James Grenert, Andrew Horvai. University of California, San Francisco, CA.

Background: Langerhans cell histiocytosis (LCH) is an aggressive neoplasm of Langerhans cells that commonly arises in the skeleton and hypothalamus of children and young adults. Approximately 50% of LCH cases harbor BRAF-V600E mutations,

and response to therapy with the BRAF inhibitor vemurafenib has been reported. Recent studies have identified other genetic alterations in the Ras-Raf-MAPK signaling pathway in LCH cases without BRAF mutation. Determination of the genetic alterations that drive LCH will improve diagnostic methods for histiocytic neoplasms and direct targeted therapy for this disease.

Design: Genomic DNA was purified from formalin-fixed, paraffin-embedded cases of LCH from 51 patients retrieved from the UCSF pathology archives. PCR-based melting curve analysis over exon 15 of the BRAF gene was performed. Sanger sequencing of KRAS, NRAS, and MAP2K1 genes and assessment for BRAF rearrangement by intronic next-generation sequencing is being performed. Molecular findings are being correlated with clinicopathologic data from the patient cohort.

Results: BRAF mutations were identified in 17/34 cases presenting with unifocal disease (50%), 8/14 cases presenting with multifocal disease (57%), and 1/3 cases of disease limited to pulmonary involvement (33%). No significant correlation of BRAF-V600 mutation status with patient age, sex, site of disease presentation, or disease recurrence after therapy was identified. The results of KRAS, NRAS, and MAP2K1 sequencing as well as testing for BRAF rearrangement in this cohort is underway and will be presented.

Conclusions: These studies are delineating the molecular pathways that define LCH and will direct future clinical trials of targeted therapeutics for LCH using BRAF and MEK inhibitors based on the unique molecular alterations present in each patient's tumor.

96 Novel BCOR-MAML3 and BCOR-ZC3H7B in Small Blue Round Cell Tumors (SBRCTs)

Katja Specht, Lei Zhang, Yun-Shao Sung, Sarah Dry, Sumathi Vaiyapuri, Christopher Fletcher, Cristina Antonescu. Technische Universität München, München, Germany; Memorial Sloan Kettering Cancer Center, New York, NY; University of California, Los Angeles, CA; Royal Orthopaedic Hospital, Birmingham, United Kingdom; Brigham & Women's Hospital, Boston, MA.

Background: The molecular characterization of SBRCTs is still evolving due to the rapid advancement of next generation sequencing, in particular paired-end RNA sequencing which is highly sensitive for novel translocation discovery. About two-thirds of *EWSR1*-negative SBRCTs are associated with *CIC-DUX4* related fusions, while another small subset with *BCOR-CCNB3* X-chromosomal paracentric inversions. In this study we sought to characterize further a large cohort of SBRCTs negative for previously reported gene abnormalities.

Design: We applied next generation paired-end RNA sequencing and FusionSeq algorithm to an intra-abdominal SBRCT index case from a 44 year-old man. The results identified the presence of a *BCOR-MAML3* fusion, in keeping with a t(x;4)(p11;q31) translocation, which was then confirmed by RT-PCR and was associated with marked up-regulation of *MAML3*. FISH using custom BAC probes for *BCOR*, *MAML3* and *ZC3H7B*, a previously reported partner of *BCOR*, was applied in a large cohort of 72 SBRCTs which were negative for *EWSR1*, *FUS*, and *CIC* rearrangements.

Results: FISH studies revealed the typical *BCOR-CCNB3* inversion in 6/72 (8%) cases tested, with an additional subset of 9/72 (13%) tumors showing a distinctive *BCOR* break-apart pattern, without *CCNB3* abnormalities. This last subset occurred all except one in males, with a mean age of 36 years (range 5-70), mostly in soft tissue (5/9) and 2 each in bone and lung. Among the *BCOR*-rearranged SBRCTs, 2 cases showed *MAML3* fusions (index case and iliac bone), with *ZC3H7B* in an additional soft tissue tumor.

Conclusions: This molecular study further expands the genetic signature of SBRCTs, with two additional novel fusions *BCOR-MAML3* and *BCOR-ZC3H7B* being identified in *EWSR1* and *CIC*-negative tumors. RT-PCR for *BCOR-CCNB3* fusions or *CCNB3* IHC will not be appropriate for detecting these alternative fusions, which will be identified instead by FISH technique. *MAML3* and *ZC3H7B* have been previously implicated in other translocation-associated mesenchymal lesions, such as biphenotypic sinonasal sarcoma and ossifying fibromyxoid tumor/endometrial stromal sarcoma, respectively.

97 Follicular Dendritic Cell (FDC) Sarcoma: Clinicopathologic, Immunohistochemical (IHC), and Ultrastructural Analysis of 98 Cases

David Stockman, Jason Chang, L Jeffery Medeiros. University of Texas MD Anderson Cancer Center, Houston, TX; University of South Carolina School of Medicine, Greenville, SC; Memorial Sloan Kettering Cancer Center, New York, NY.

Background: FDC sarcomas are rare neoplasms with a low to intermediate malignant potential that may be diagnostically challenging due to their rarity and variable histologic patterns. This study aims to further characterize the morphologic spectrum, IHC features, and biologic behavior of this tumor in the largest series of cases to date.

Design: Ninety-eight cases of FDC sarcomas were retrieved. The morphologic, IHC, and ultrastructural features and outcome data were analyzed.

Results: The patients were 54F and 44M ranging from 14-88 yrs (median 51 yrs). The tumors ranged in size from 1.0-30.0 cm (median 7.9 cm), and were primary nodal in 30/98 (30%) of cases. The anatomic distribution was as follows: head and neck (n=26), thorax (n=33), abdomen (n=37), and extremities (n=2). Fifty percent (50%) of patients had multicentric disease. Histologically, tumors were comprised of fascicles and storiform arrays of oval to spindle cells with vesicular chromatin, distinct nucleoli, and indistinct cytoplasmic borders forming frequent whorls. Electron microscopy performed on selected cases revealed the presence of abundant desmosomes and well-formed cellular junctions. By IHC, 55/56 (98%) cases were positive for clusterin, 28/32 (88%) for fascin, 12/14 (86%) for EGFR, 74/93 (80%) for CD21, 54/87 (62%) for CD35, and 37/63 (59%) for CD23. Follow-up data was available in 42/98 of patients; 31% of patients were found to have metastatic disease at time of presentation, and 42% of patients had disease recurrence after surgery. The median time to recurrence was 9 mo (range: 1-106 mo). Fifty-five percent (55%) died of disease 3 to 188 mo after diagnosis (median survival 21 mo). The 3- and 5-yr survival rates were 71% and 55%, respectively. Survival outcomes

did not correlate with patient age(p=0.41), tumor location(p=0.45), size(p=0.86), nodal vs. extranodal disease(p=0.95), multicentricity(p=0.83), mitotic activity(p=0.48), or presence of metastasis at presentation(p=0.92).

Conclusions: FDC sarcomas show a variable morphology and IHC reactivity. Clusterin and fascin immunostains appear to be the most reliable markers for this tumor, whereas traditional FDC markers such as CD21 and CD35 may be less sensitive. FDC sarcomas may exhibit a higher malignant potential and be associated with a more aggressive clinical course than previously thought (median surv. 21 mo).

98 Osteomyelitis: Can Strict Criteria Reliably Improve Diagnostic Concordance Among Pathologists?

Amelia Sybenga, Arundhati Rao. Scott & White Memorial Hospital/Texas A&M Health Science Center, Temple, TX.

Background: Histological exam of bone specimens is the gold standard of diagnosis for osteomyelitis; however, strict criteria are not widely recognized, and diagnostic concordance is as low as 30%. In a previous study reviewing 259 cases of suspected osteomyelitis, we demonstrated a 2 times increased risk of suffering a non-healing wound or further proximal amputation in patients originally diagnosed without osteomyelitis, but diagnosed with osteomyelitis utilizing our method (p=0.00001). We sought to validate this tool for both reproducibility and concordance among other pathologists.

Design: 6 pathologists, with experience ranging from 5 up to 45 years, were selected to perform slide reviews of 35 blinded, previously diagnosed cases of suspected osteomyelitis. Prior to beginning slide review, each pathologist was taught the 13 histological criteria, and given a tabulation sheet for each case to document each histological feature and his or her diagnosis. Diagnoses were limited to 1 of 5 options: acute, chronic, or acute and chronic osteomyelitis; no osteomyelitis; or other. Only slides of margins and biopsies were used, with a mixture of osteomyelitis and benign bone. 5 additional slides with non-osteomyelitis diagnoses were blindly inserted among the 35 cases as an additional control. The tabulation sheets were then collected, and a weighted score was applied to each histological criterion identified. A total score was calculated for each case. Finally, we compared concordance among pathologists, score and specific diagnosis, and an original diagnosis with the criteria based diagnosis and clinical outcomes.

Results: Concordance was significantly higher than previous studies had portended (p<0.05). Variability of histological findings among pathologists was minimal, with identification of sequestrum and involucrum being the most contentious. Additionally, diagnoses utilizing the criteria showed similar potential clinical outcomes as the previous study. Lastly, weighted criteria (score) demonstrated preference for the specific type of osteomyelitis: acute, chronic, or acute and chronic.

Conclusions: We have developed a histopathological tool that demonstrates clinical significance in the diagnosis of osteomyelitis in the foot and ankle, and may reduce rates of treatment failure. This tool improves diagnostic concordance among pathologists, and is reproducible.

99 Dedifferentiated Adamantinoma: Clinico-Pathological and Molecular Study on Four Cases

Roberto Tirabosco, Sam Behjati, Maria Amary, Hongtao Ye, Nischalan Pillay, Adrienne Flanagan. Royal National Orthopaedic Hospital – Stanmore, London, United Kingdom; Wellcome Trust Sanger Institute, Cambridge, United Kingdom; University College, London, United Kingdom.

Background: Adamantinoma (AD) is a rare primary malignant bone tumor showing epithelial differentiation, arising almost exclusively in tibia. AD may arise *de novo* or associated with osteofibrous dysplasia (OFD), and it is accepted that they form a morphological continuum, in which OFD and AD represent the benign and malignant ends of the spectrum, respectively. Dedifferentiation in AD (dAD) is an accepted entity, although its occurrence is exceptional. We retrieved from our archive four such cases, in which a high grade sarcoma, mostly an osteosarcoma, was associated with a conventional AD. Two cases were sited in the tibia, one in the ulna and one in a rib. Here we present the clinical, pathological and molecular features of these four cases.

Design: Ten cases of AD, four of which had a dedifferentiated component, and six cases of OFD were included in the study. Whole genome sequencing was undertaken on all OFD and AD, one of which had an osteoclast-rich dedifferentiated component. Targeted analysis of Histone H3.3 mutation hotspots was undertaken using next generation sequencing (NGS), in addition to FISH for *FGFR1* gene amplification in both the conventional and dedifferentiated component in all cases of dAD.

Results: Whole genome sequencing failed to demonstrate a recurrent specific molecular signature. However, a substitution in *H3F3A* mutation involving p.G34W, a mutation previously described in 95% of giant cell tumor of bone, was detected in the dAD with the osteoclast-rich component. No amplification of the *FGFR1* gene, previously described in ~20% of high grade osteosarcoma, was found.

A summary of clinical, pathological and molecular features is presented in Table 1

No.	Age / Sex	Site / Size (mm)	Recurrence (m)	Metastasis (m)	Follow up (m)	H3.3	FGFR1
1	40 / F	R Tibia / 65	No	Vertebrae (2)	DOD (7)	Yes	No
2	61 / M	L Ulna / 170	Yes (9)	Lungs (3)	DOD (15)	No	No
3	32 / F	L Tibia / 115	Yes (48)	Lungs (84)	DOD (135)	No	No
4	38 / F	L 1st Rib / 52	Yes (10)	No	AWD (38)	No	No

Conclusions: This is the largest series of dAD ever reported from a single Institution and includes two cases located in anatomical sites other than tibia. In line with other dedifferentiated bone sarcomas, dAD has a dismal prognosis, with high metastatic potential and high mortality, which can occur outside the conventional tibial location.

100 Clinicopathological Features and Prognostic Factors in Angiosarcoma: A Retrospective Analysis of 200 Patients From a Single Chinese Medical Institute

Lei Wang, Cong Tan, Jian Wang. Shanghai Cancer Center, Fudan University, Shanghai, China.

Background: Angiosarcoma is a rare soft tissue sarcoma, and the information about its clinicopathological features and prognostic factors are relatively limited. Nevertheless, it is of paramount importance for pathologists to make an accurate diagnosis, as misdiagnosis may lead to inappropriate administration and incorrect assessment of the prognosis. The purpose of this study is to report a large series of angiosarcoma based on the single-institute experience.

Design: We retrospectively analyzed 200 cases of angiosarcoma in a single Chinese medical institute from March 2006 to March 2014.

Results: Of the total 200 patients, 97 males and 103 females were included with ages at diagnosis ranging from 4 to 91 years (median, 53 years). The head and neck (64) was the most common primary site, followed by breast (33), bone (22), trunk (22), extremities (15), spleen (14), heart (10), lung (6) and liver (4). Other uncommon organs included the ovary, adrenal gland, ileum, colon, thyroid, brain and penis. According to the tumor location, 200 cases were divided into 4 groups: tumors involving (1) head and neck, (2) breast, (3) viscera (including internal organ and bone), (4) soft tissue (including trunk and extremities). One hundred and thirteen patients were followed up after angiosarcoma diagnosis. Forty-six patients of these 113 patients had died of angiosarcoma at a median interval of 10 months. The tumor recurrence/metastasis was identified in 66 patients at a median interval of 4 months. In all cases, the disease free survival (DFS) at 5-year was 19.3% and the overall survival (OS) at 5-year was 40.8%. Tumor location had significant effect on DFS (P=0.032) and OS (P<0.001). The patients with primary breast angiosarcoma had a significantly improved DFS and OS compared with the patients in the other three groups. While the patients with involvement of angiosarcoma in head and neck had relatively poor prognosis. Tumor size (≥5 cm) and differentiation also had effect on DFS (P=0.038, <0.001) and OS (P=0.008, <0.001). Both tumor differentiation and treatment modality (multidisciplinary treatment VS non-multimodal treatment) were the independent determinant of OS (P<0.001, 0.038). Tumor recurrence/metastasis was independent predictor of DFS (P<0.001).

Conclusions: Angiosarcomas are a family of sarcomas with distinct clinicopathological features. The clinical behavior depends considerably on the primary sites. Tumor differentiation, recurrence/metastasis, and treatment modality were independent prognostic factors.

101 Consistent Copy Number Changes and Recurrent PRKAR1A Mutations Distinguish Melanotic Schwannomas From Melanomas: SNP-Array and Next Generation Sequencing Analysis

Lu Wang, Ahmet Zehir, Justyna Sadowska, Nengyi Zhou, Marc Rosenblum, Klaus Busam, Narasimhan Agaram, William Travis, Maria Arcila, Snjezana Dogan, Michael Berger, Donovan Cheng, Marc Ladanyi, Khedoudja Nafa, Meera Hameed. Memorial Sloan Kettering Cancer Center, New York, NY.

Background: Melanotic Schwannomas (MS) are rare tumors derived from neuroectoderm that share histological features with melanocytic tumors and schwannomas. However, their genetics are poorly understood. To elucidate the genetic characteristics of melanotic schwannoma, we investigated DNA copy number and mutation profiling using SNP array and a next generation sequencing (NGS) platform in a series of cases.

Design: FFPE tumor tissues of 12 MS cases were available for the study. Matching normal tissues were available for 2 cases. Genomic DNAs extracted from tissue samples were subjected to copy number (CN) and allelic imbalance (AI) analysis by Affymetrix OncoScan SNP-array and screened for mutations in coding exons of 341 key cancer-associated genes using a hybrid capture-based NGS assay (MSK-IMPACT, MSKCC). Sanger sequencing was used to further verify recurrent mutations detected by MSK-IMPACT.

Results: SNP-array analysis revealed remarkably stereotypic chromosomal abnormalities in MS. Hypodiploidy was common, typically involving monosomies of chromosomes 1, 2, and 17. All 12 samples showed mutations in *PRKAR1A* gene by the MSK-IMPACT NGS assay. Other mutations were infrequent and predominantly non-recurrent. Two samples harbored two mutations in *PRKAR1A*, and the others had one mutation per sample. Total of 14 mutations detected in *PRKAR1A* were scattered across the gene, and most were inactivating mutations. *PRKAR1A* mutations were verified to be somatic in two cases in which matched normal was available. Interestingly, allelic imbalance on 17q, presenting as loss of heterozygosity (LOH) with or without CN losses, combined with a *PRKAR1A* mutation was observed in 9/12 MS cases. The remaining 3 cases included the two samples harboring two mutations in *PRKAR1A*.

Conclusions: *PRKAR1A* gene mutation is a recurrent genetic event in MS which also exhibits a stereotypic pattern of chromosomal losses. In contrast, melanomas are typically characterized by the presence of multiple CN aberrations, without demonstrable differences in the frequency of CN losses and gains. Inactivation of both alleles of *PRKAR1A* by “two hits”, i.e. either by one mutation coupled with LOH of 17q or by two mutations was observed in almost all cases (11/12), underscoring the central role of *PRKAR1A* in the pathogenesis of this neoplasm.

102 In-Situ Hybridization of MDM2 RNA Is a Useful Adjunct To Immunohistochemistry in the Diagnosis of Atypical Lipomatous Neoplasm/Well-Differentiated Liposarcoma

John Wojcik, Krishnan Mahadevan, G Petur Nielsen, Vikram Deshpande. Hospital of the University of Pennsylvania, Philadelphia, PA; Massachusetts General Hospital, Boston, MA.

Background: Atypical lipomatous neoplasm/well-differentiated liposarcoma (ALN/WDL) is the most common form of liposarcoma. Histologically, it may bear a strong resemblance to a number of benign mimics. Distinguishing ALN/WDL from its benign mimics is critical because of its greater likelihood of recurrence and its capacity to undergo dedifferentiation. Immunohistochemical (IHC) staining for MDM2 has become an extremely valuable tool in the diagnosis of ALN/WDL. In most cases, MDM2 shows strong nuclear expression due to the chromosome 12q13-15 amplification seen in these tumors. However, in other cases the staining may be weak, focal, or difficult to interpret due to the presence of MDM2 expression in histiocytes and other non-neoplastic cells. We sought to determine whether in-situ hybridization (ISH) for MDM2 mRNA could be a useful adjunct to IHC in the diagnosis of ALN/WDL.

Design: Fifteen lipomatous neoplasms were retrieved from the case files of our institution. Five of these were diagnosed as lipoma and ten were diagnosed as ALN/WDL. One of the lipomas and six of the ALN/WDL were selected for review based on equivocal IHC results. Representative sections of all cases were subjected to ISH QuantiGene® ViewRNA technology (Affymetrix, Santa Clara, CA) for MDM2 mRNA. H&E slides and MDM2 IHC stains of tissue from the same block were also examined in each case. The slides were reviewed by subspecialty bone and soft tissue pathologists blinded to the diagnosis and the initial interpretation of the staining.

Results: The patients included 9 males and 6 females, aged 42-74 (median 56) years. Tumors were located in the soft tissues of the proximal lower extremity (6), trunk (5), retroperitoneum (2), upper extremity (1) and groin (1). In all eight cases with an unambiguous IHC result (four lipomas and four ALN/WDL, negative and positive on IHC, respectively) ISH results were concordant. Of the seven cases with equivocal IHC results, all interpreted as weakly and focally positive on IHC, one was negative by ISH and six were positive. In all but one case where FISH or cytogenetics data were available, the ISH findings were concordant (6/7), and the ISH findings were in agreement with the final diagnosis in every instance.

Conclusions: ISH for MDM2 mRNA is a useful adjunct to IHC in distinguishing ALN/WDL from histologic mimics, and may be particularly useful in instances where the results of MDM2 staining are ambiguous.

103 "Trans"-Differentiation in Imatinib-Treated Gastrointestinal Stromal Tumor: A Report of Two Novel (Immunophenotypic)

Katie Wolters, Luis De Las Casas, Rajiv Patel, Andrew Folpe, Jodi Carter. Mayo Clinic, Rochester, MN; University of Toledo, Toledo, OH; University of Michigan, Ann Arbor, MI.

Background: Gastrointestinal stromal tumors (GIST) are the most common primary mesenchymal tumors of the gastrointestinal tract. Most GIST harbor activating mutations in *KIT*, encoding a receptor tyrosine kinase, or *PDGFRA*, encoding platelet-derived growth factor receptor alpha; thus, patients at high risk for disease progression are treated with imatinib mesylate or other tyrosine kinase inhibitors. "Trans"-differentiation of imatinib-treated GIST to anaplastic, rhabdomyoblastic, or undifferentiated phenotypes has rarely been described. To our knowledge, we report the first cases of imatinib-treated GIST acquiring carcinomatous and epithelial/myoepithelial morphologies and immunophenotypes.

Design: Our institutional and consultation archives were searched for cases coded as gastrointestinal stromal tumor, dedifferentiation, and imatinib, yielding two cases. The clinical history, histologic slides, and immunohistochemical studies were reviewed, and clinical follow-up was obtained.

Results: Case 1: 72M with a biopsy-proven, high-risk, spindle cell GIST (cKIT+/CD34+) of the rectum, treated with imatinib prior to surgical resection. The treated tumor had a distinctly bimorphic appearance: spindle cell GIST (cKIT+/CD34+) and a carcinomatous component containing gland-forming carcinomatous elements (CK7+/CK20+/cKIT-) and rhabdomyosarcomatous elements (desmin+/CK-cKIT-). The patient died of disease 15 years later. Case 2: 52F with a biopsy-proven, high-risk, spindle cell GIST (cKIT+/DOG-1+) of the small intestine, treated with imatinib. A pelvic metastasis, 24 months after diagnosis, showed a bimorphic appearance: spindle cell GIST (cKIT+/DOG-1+) admixed with foci showing epithelial/myoepithelial differentiation (CK+/patchy p63+ and S100+/cKIT-/DOG-1-). Currently, she is alive with no further disease progression. Molecular genetic testing for *KIT* and *PDGFRA* mutations is underway.

Conclusions: To the best of our knowledge, these represent the first reported cases of carcinomatous and epithelial/myoepithelial "trans"-differentiation in imatinib-treated GIST. These cases expand the histologic and immunophenotypic spectrum of treated GIST and promote awareness of this important diagnostic pitfall. Additional molecular genetic analysis may help to better understand the underlying molecular events and the clinical relevance of these unique cases.

104 ALK and ROS1 Expression in Inflammatory Myofibroblastic Tumor

Hidetaka Yamamoto, Kenichi Taguchi, Akihiko Yoshida, Kenichi Kohashi, Yoshinao Oda. Kyushu University, Fukuoka, Japan; Kyushu Cancer Center, Fukuoka, Japan; National Cancer Center Hospital, Tokyo, Japan.

Background: About half cases of inflammatory myofibroblastic tumor (IMT) have anaplastic lymphoma kinase (ALK) gene rearrangement and overexpress ALK fusion proteins. As IMT morphologically resembles various kinds of tumefactive lesions from

benign to malignancy, appropriate immunohistochemistry (IHC) for ALK is crucial for the pathological diagnosis. Recently, ROS1 fusion gene also has been reported in a few cases of ALK-negative IMT.

Design: In the present study, we compared two different methods of IHC for ALK in 35 cases of IMT; one is a conventional polymer method with ALK1 antibody, and another is a recently available, highly-sensitive polymer method with 5A4 antibody. ALK gene rearrangement was examined by fluorescence in-situ hybridization (FISH). ROS1 expression was also investigated by IHC.

Results: We found that ALK1 and 5A4 were positive in 20/35 (57%) and 22/35 (63%) cases, respectively. The staining intensity of 5A4 was stronger than that of ALK1, whereas there was no significant difference in staining pattern (intracellular localization) of ALK between the two antibodies. Two cases of ALK1-negative/5A4-positive IMT had ALK gene rearrangement by FISH. The results of 5A4 IHC and ALK FISH were essentially concordant. ROS1 was negative in all IMTs, irrespective of ALK expression.

Conclusions: Our data suggest that IHC with 5A4 may be more useful than IHC with ALK1 to accurately screen ALK-positive (ALK-rearranged) IMT for appropriate diagnosis and ALK-targeted therapy.

105 CDK8 Expression in Extruterine Leiomyosarcoma Correlates With Tumor Stage and Progression

Oleksandr Yergiyev, George Garib, Karen Schoedel, Alka Palekar, Mark Goodman, David Bartlett, Uma Rao. University of Pittsburgh Medical Center Shadyside Campus, Pittsburgh, PA.

Background: CDK8 subcomplex consists of four proteins - CDK8 kinase, Cyclin C, Med12 and Med13. It represses cell transcription by mechanisms that are not well understood. Recent studies demonstrate the role of recurrent Med12 mutations in the pathogenesis of uterine leiomyomas, but its role in the oncogenesis of extruterine smooth muscle tumors is not as clear. In addition, there is a paucity of literature on the role of CDK8 kinase in smooth muscle oncogenesis. In the current study we investigate the relationship between expression of both Med12 and CDK8 and clinical progression of extruterine leiomyosarcomas.

Design: Paraffin blocks of 20 primary and 17 recurrent soft tissue leiomyosarcomas, as well as two cases of metastatic uterine leiomyosarcomas were retrieved. Clinical and pathologic data were recorded where available, including tumor location, grade, stage, and time to first local recurrence and metastases. Follow up ranged from 5 to 129 months. Immunohistochemical stains for Med12 and CDK8 were performed utilizing appropriate controls. Nuclear staining was scored on a scale of 0 to 3 by the investigators blinded to the clinical information. Scores of 0 and 1 were interpreted as negative, while those of 2 and 3 were considered positive. Fisher exact test and t-test were utilized to correlate the results with the clinical information.

Results: Strong nuclear positivity for Med12 was found in 38 of 39 leiomyosarcomas while CDK8 was lost in 23 of 39 tumors including two uterine recurrences. Pathologic T stage was available on 16 patients. Six of these were staged as pT1 and 10 as pT2. Five out of six T1 tumors expressed CDK8, compared to only one out of ten T2 tumors (p=0.0076). When the second group was expanded to include those patients who did not have a recorded pathologic T stage but who had documented recurrence and/or metastatic disease (n=30), the difference in CDK8 expression was also significant (p=0.0102). CDK8 and Med12 expression did not correlate with tumor grade or time to recurrence.

Conclusions: Loss of CDK8 expression in soft tissue leiomyosarcomas as detected by immunohistochemistry is associated with tumors presenting at a more advanced stage and may be of value in predicting the tumor behavior. Loss of Med12 expression is not a feature of soft tissue leiomyosarcomas, regardless of stage or grade. CDK8 inactivation may represent the final common pathway in the Med12-CDK8 smooth muscle tumor oncogenesis mechanism.

106 Spectrum of Non-Synonymous Variants and Copy Number Alterations in Leiomyosarcomas Identified By Clinical Targeted Next-Generation Sequencing

Naomi Yoo, Catherine Cottrell, Haley Abel, Eric Duncavage. Washington University, St. Louis, MO.

Background: Leiomyosarcomas are rare soft tissue tumors with an aggressive clinical course that have not been well characterized at the genomic level. Using a next generation sequencing (NGS) based panel of common cancer-associated genes, we explored the genetic landscape of 25 leiomyosarcomas.

Design: DNA was extracted from formalin-fixed, paraffin-embedded (FFPE) tumor tissue identified histologically as leiomyosarcoma from a variety of anatomic sites. Library preparation was performed using liquid-phase cRNA capture probes targeting 151 cancer-associated genes. Libraries were sequenced to high depth of coverage using an Illumina Sequencer. In-house sequencing analysis pipelines were used to identify and characterize single nucleotide variants (SNV), indels, and copy number variation (CNV). SNV and indels were filtered to restrict to non-synonymous variants with a population minor allele frequency of <1% as reported in the NHLBI Exome Variant Server or 1000 Genomes databases.

Results: After filtering, analysis revealed 87 non-synonymous variants within 50 gene targets in 21 cases; 4 cases had no apparent mutations. The average platform depth across 151 gene targets was 1000x. Cases had 1 to 11 variants (mean 4.3, median 3). The most frequently altered genes were *TP53* (36%), *ATM* and *ATRX* (16%), and *NOTCH1*, *EGFR* and *RBI* (12%). Thirteen of the 87 variants had been previously identified in cancer (COSMIC database), including all *TP53* mutations. CNV was analyzed in 13 of the 25 cases, with 85% demonstrating copy number alteration. Losses were more prevalent than gains overall. The most frequent copy number losses were observed in chromosomes 10 and 13 (10 cases each), while the most frequent gains were seen in chromosome 17 (6 cases).

Conclusions: Our data further demonstrate the complex genetics associated with leiomyosarcomas. As a class, tumor suppressor genes were the most commonly mutated loci, including *TP53*, mutated in 36% of cases (9/25). The loss of key tumor suppressor genes is consistent with our observations that CNV was present in 85% of leiomyosarcomas. While no common therapeutically targetable gene was identified across these cases, future large cohort sequencing studies of leiomyosarcomas may provide a means for the molecular classification of these tumors and identify new treatment paradigms.

107 Identification of a Novel *FN1-FGFR1* Genetic Fusion as a Frequent Event in Phosphaturic Mesenchymal Tumor

Chang-Tsu Yuan, Yung-Ming Jeng, Sheng-Yao Su, Cher-Wei Liang, Chung-Yen Lin, Shu-Hwa Chen, Cheng-Han Lee, Jodi Carter, Chen-Tu Wu, Andrew Folpe, Jen-Chieh Lee. National Taiwan University Hospital and National Taiwan University College of Medicine, Taipei, Taiwan; Academia Sinica, Taipei, Taiwan; University of Alberta and Royal Alexandra Hospital, Edmonton, AB, Canada; Mayo Clinic, Rochester, MN.

Background: Phosphaturic mesenchymal tumors (PMT) are unusual soft tissue and bone tumors that typically cause hypophosphatemia and tumor-induced osteomalacia through secretion of phosphatonins such as fibroblast growth factor 23 (FGF23). PMT has recently been accepted by the World Health Organization as a formal tumor entity. The genetic basis and oncogenic pathways underlying its tumorigenesis remain obscure. **Design:** Four PMT samples were subjected to RNA sequencing in search of possible fusion transcripts, which would be confirmed by genomic DNA PCR, RT-PCR and western blotting. Fluorescence *in situ* hybridization (FISH) was performed on a total of 15 cases to check the presence of the fusion gene.

Results: Three of the four cases were found harboring a novel *FN1-FGFR1* fusion gene by RNA sequencing, which was confirmed by DNA PCR and RT-PCR. Western blotting corroborated the presence in two cases of the chimeric FGFR1 protein with increased sizes. FISH showed 6 cases with *FN1-FGFR1* fusion, out of an additional 11 PMTs. Overall, 60% (9/15) harbored this fusion.

Conclusions: We for the first time identified a highly recurrent genetic event in PMTs. The *FN1-FGFR1* fusion gene likely has an important role in tumorigenesis and may also have potential therapeutic implications. The *FN1* gene possibly provides its constitutively active promoter and the encoded protein's oligomerization domains to over-express and facilitate the activation of the FGFR1 kinase domain. Interestingly, the *FN1-FGFR1* chimeric protein, with various fusion points, was predicted to preserve its ligand-binding domains, suggesting an advantage of the presence of its ligands (such as FGF23) in the activation of the chimeric receptor tyrosine kinase, thus effecting an autocrine or paracrine mechanism of tumorigenesis. Further study is required to confirm these hypotheses.

108 A Subset of Spindle Cell Lipomas Harbors Rearrangements of the *HMGAI* Locus

Riyam Zreik, Xiaoke Wang, Jorge Torres-Mora, Karen Fritchie, Andre Oliveira. Mayo Clinic, Rochester, MN.

Background: Spindle cell lipomas are benign adipocytic neoplasms composed of varying amounts of mature adipose tissue, bland spindle cells, and collagen fibers. A single case of spindle cell lipoma with t(2;6)(p16-21;p21) expressing *HMGAI* protein was reported by Dumollard JM et al in 2001. We have encountered a second case with classic histologic features and t(1;6)(p32;p21.3). This finding led us to hypothesize that, similar to ordinary lipomas, a subset of spindle cell/pleomorphic lipomas could also harbor rearrangements of the chromatin remodeling gene *HMGAI*.

Design: Twenty-four spindle cell lipomas and 8 pleomorphic lipomas with classic histologic features were retrieved from our institutional archives and screened for rearrangements of the *HMGAI* and *HMGAI2* loci using custom-designed break apart FISH probes. The spindle cell lipomas were seen in 20 males and 4 females with a mean age of 59 years (range 40-86 years) and involved most frequently the neck (7), back (7), face/ear (3), arm/shoulder (2), thigh (2), buttock (2), and labia (1). The pleomorphic lipomas were seen in 7 males and 1 female with a mean age of 56 years (range 37-72 years) and involved the shoulder/neck (4), ear/scalp (3) and back (1).

Results: Balanced rearrangements of the *HMGAI* locus were found in 3 (of 24; 13%) spindle cell lipomas but in no pleomorphic lipoma. All tumors were negative for *HMGAI2* rearrangements.

Conclusions: Similar to ordinary lipomas, a small subset of spindle cell lipomas harbors rearrangements of the *HMGAI* locus. This finding suggests that these two subtypes of lipoma may share common oncogenic pathways, at least in a subset of cases. Further studies are needed to better understand the biologic implication of this novel finding in spindle lipoma pathogenesis.

109 Morphologic Diversity in Desmoid-Type Fibromatosis: Clinicopathologic Correlation and Potential Diagnostic Pitfalls on Core Biopsy Specimens

Riyam Zreik, Karen Fritchie. Mayo Clinic, Rochester, MN.

Background: Desmoid-type fibromatosis is a locally aggressive neoplasm characteristically composed of long sweeping fascicles of bland fibroblasts and myofibroblasts that may occur at a variety of abdominal, intra-abdominal and extra-abdominal sites. Occasionally alternative morphologic patterns are identified, and this may lead to diagnostic difficulty on small biopsy specimens, especially for pathologists who do not routinely examine soft tissue specimens. Additionally, little data is available as to the distribution and frequency of these patterns.

Design: 165 resection specimens of desmoid-type fibromatosis were retrieved from our institutional archives. All available H&E slides from each case (ranging from 1-14 slides) were reviewed, and the diagnosis was confirmed. The morphologic patterns were catalogued and compared by site, age and sex.

Results: Patterns identified included: conventional (165 cases, range 10-100%), hypocellular/hyalinized (46 cases, range 5-80%), staghorn vessels (35 cases, range 5-30%), myxoid (27 cases, range 5-40%), keloid (24 cases, range 5-50%), nodular fasciitis-like (15 cases, range 5-40%), and hypercellular (6 cases, range 5-20%). Tumors with keloid areas, as well as those with prominent staghorn blood vessels, mimicked entities such as solitary fibrous tumor. Those cases with nodular fasciitis-like areas raised the possibility of nodular fasciitis and reactive processes. Hypercellular foci led to the consideration of spindle cell sarcoma, while the differential diagnosis of hypocellular/hyalinized areas was broad. By site, the greatest variation of patterns was observed in intra-abdominal lesions, and men showed more morphologic variability than females. Adults (>18 years) exhibited more histologic diversity than adolescent and pediatric patients (≤18 years).

Conclusions: The morphologic spectrum of desmoid-type fibromatosis is diverse and often underappreciated. Intra-abdominal lesions tend to show the greatest morphologic diversity, and awareness of the histologic patterns that may occur is necessary to prevent misdiagnosis, especially on small biopsy specimens.

110 Myxoinflammatory Fibroblastic Sarcoma (MIFS) and Hybrid Hemosiderotic Fibrolipomatous Tumor (HFLT)/MIFS: Related or Not? A Clinicopathological and Molecular Cytogenetic Study of 34 Cases

Riyam Zreik, Jodi Carter, William Sukov, William Ahrens, Karen Fritchie, Elizabeth Montgomery, Sharon Weiss, Andrew Folpe. Mayo Clinic, Rochester, MN; Carolinas Medical Center, Charlotte, NC; Johns Hopkins, Baltimore, MD; Emory University, Atlanta, GA.

Background: MIFS, a locally aggressive, rarely metastasizing fibroblastic tumor that typically involves the distal extremities, has been reported to show t(1;10)(*TGFB3-MGEA5*) in some instances. This genetic event has also been reported in HFLT, and in rare tumors showing hybrid features of HFLT and MIFS. These findings have led to speculation that HFLT and MIFS are closely related. However, areas resembling HFLT have been present in only a very small minority (~1%) of previously reported MIFS, and we recently found *TGFB3* or *MGEA5* rearrangements in only 1 of 6 studied cases. Thus the relationship between MIFS and HFLT is still unclear. We studied the clinicopathological and molecular cytogenetic features of 34 cases of MIFS and hybrid HFLT/MIFS with the goal of clarifying these issues.

Design: Available slides from 38 cases diagnosed as "MIFS" or "hybrid HFLT/MIFS" were retrieved from our archives. Following re-view by 2 experienced soft tissue pathologists, 4 cases were excluded, leaving a final group of 27 MIFS and 7 hybrid HFLT/MIFS. Cases were tested for *TGFB3* and *MGEA5* gene rearrangements using previously published methods.

Results: MIFS occurred in 10F and 17M, with a mean age of 45 years (range 15-82 years) and involved the hand/arm (N=12), foot/leg (N=14), and cheek (N=1). Hybrid HFLT/MIFS occurred in 6F and 1M, with a mean age of 60 years (range 49-78 years) and involved the foot (N=4) and leg (N=3). All MIFS conformed strictly to the current WHO definition; no case showed areas resembling HFLT. Hybrid HFLT/MIFS showed zones of classical HFLT juxtaposed to areas of myxoid sarcoma, showing some but not all features of classical MIFS. By FISH, 11 informative MIFS were negative for *TGFB3* or *MGEA5* rearrangements. In contrast, 2 of 4 tested hybrid HFLT/MIFS showed *TGFB3* or *MGEA5* rearrangement.

Conclusions: Our morphological and FISH findings suggest that MIFS and hybrid HFLT/MIFS may be unrelated, with the latter entity representing a form of morphological progression within HFLT. We speculate that not all studies may have utilized the same diagnostic criteria for MIFS. On-going FISH study of the remaining cases should help to clarify these issues.

Breast Pathology

111 Multicentre Genomic and Protein Expression Analysis Reveals SPAG5 as a Key Oncogene and Biomarker and a Target for Personalized Therapy in Breast Cancer (BC)

Tarek Abdel-Fatah, Dongxu Iu, Devika Agarwal, Paul Moseley, Andrew Green, Ian Ellis, Graham Ball, Steven Chan. Nottingham City Hospital NHS Trust, Nottingham, United Kingdom.

Background: Recently our neural network analysis of Breast Cancer gene expression array (GEA) data has revealed SPAG5 as a major hub in the proliferation pathway. In this study pre-clinical, molecular and clinicopathological functions of SPAG5 was investigated in patient cohorts from multi-centres.

Design: 1. The expression and functionality of *SPAG5*, its relationships to the p53 network and the response to different therapies, have been evaluated pre-clinically in a panel of BC cells.

2. Gene expression analysis of mRNA *SPAG5* and its clinicopathological significance have been analysed in two large cohorts (METABRIC cohort; n=1950 and Uppsala cohort; n=249), and then validated in a 3400 case dataset derived from global multi-centre resource. Neural network and functional pathway analysis have been carried out in 2000 BC cohort.

3. The relationships between *SPAG5* protein expression and clinicopathological outcomes and response to systemic therapies have been analysed in 2500 BC patients derived from four cohorts including: 1) a series of 1650 primary early BC cohort, 2) 350 ER negative BC cohort treated with adjuvant anthracycline combination therapy, 3) 250 locally advanced BC treated with neoadjuvant anthracycline with/without taxane, and 4) 250 of HER2 positive BC treated with trastuzumab based adjuvant CT. 4. A series of 171 BC was used for integrative analysis of *SPAG5* gene copy number (using aCGH), mRNA expression (using GEA) and protein expression.